LIQUID CRYSTALS FOR MOBILITY CONTROL

by

Francis Stephen Sommer, B.S. in Physics

THESIS

Presented to the Faculty of the Graduate School of

The University of Texas at Austin

in Partial Fulfillment

of the Requirements

for the Degree of

Master of Science in Petroleum Engineering

THE UNIVERSITY OF TEXAS AT AUSTIN

May, 1986

ACKNOWLEDGEMENTS

The author would like to gratefully acknowledge Dr. Robert S. Schechter for his technical guidance and inspiration. Dr. William H. Wade is also recognized for his time and suggestions which greatly enhanced the final product.

The CEOGRR provided financial support for this project and much is owed to the sponsoring companies for their continued assistance.

Moral support was provided by the authors friends and family and many thanks are given to my wife, Deborah, for her patience and friendship.

TABLE OF CONTENTS

LIST OF FIGURES

LIST OF TABLES

CHAPTER I

Introduction

1.1 Overview

The development of chemical flooding as an enhanced oil recovery process has sparked a concerted effort to understand the physio-chemical properties which describe micellar solutions. There has been particular emphasis placed on the development of compounds (i.e. surfactants) that can reduce oil-water interfacial tensions. These molecules permit the mobilization of large quantities of oil which can not be moved by conventional water flooding techniques. Strictly speaking, the term chemical flooding usually refers to micellar-polymer flooding, thereby distinguishing it from other EOR processes which might involve chemicals such as alkaline flooding.

An outline of the principal components employed in a micellar-polymer flood can be illustrated as a block sequence of injected chemical slugs. Figure 1.1 shows such a diagram. With reference to this figure and the summary given by Lake[1], the recovery process may be explained as follows:

a) Initially, there is injection of an aqueous preflush. The purpose of the preflush is to adjust the reservoir salinity to optimize surfactant interfacial partitioning. If the natural reservoir salinity is too high or too low, the surfactant which follows the preflush will not form the desired optimum middle phase and recovery will be impaired. It is the critical dependence of surfactant phase behavior on salinity which necessitates the use of a preflush.

b) Following the preflush is an aqueous surfactant-rich slug. Its function is to form a stable middle phase microemulsion with the remaining oil. This is the surface-active component of the flood; its ability to reduce oil-water interfacial tension is the primary recovery mechanism.

c) Behind the microemulsion is a mobility control agent. It is used to force a controlled push of the oil-water-surfactant mixture to the production wells. This slug is usually a polymer-thickened aqueous solution and its viscosity should be approximately 40cp insitu.

d) After the mobility control agent is a mobility taper. The taper is designed to gradually change the viscosity from the mobility control slug to the chase water which will follow the taper. Use of a taper ameliorates the effects of an adverse mobility ratio which would exist if the viscous mobility control agent were injected directly in front of the non-viscous chase water.

e) The last slug is a volume of chase water. Since the chase water need not contain any sacrificial chemicals, it provides the least expensive method of completing the push of the oil bank to production.

With some modifications the micellar-polymer flooding process as outlined has been used in pilot tests with varied results.[2] The technique relies heavily on the integrity of polymer-thickened water to act as a mobility control agent, and while development of the surface active slug has been widely pursued, the mobility control component of chemical flooding has only recently received the same degree of attention. Traditional wisdom has dictated that because polymers have the ability to produce high viscosities at dilute concentrations, they should be used as the control drive chemical. However, the problems encountered with the use of these long chain molecules, such as their susceptability to permanent shear degradation, dependence

on bacterial additives, inability to work at reservoir temperatures above 375K, and high cost, motivativates one to consider alternative compounds which do not share these disadvantages. Surfactants represent such a class of molecules; therefore, the principal aim of this work will be to determine the feasibility of replacing the polymer used for mobility control in a chemical flood with surfactant.

1.2 Scope of Investigation

In order for surfactants to replace polymers as a drive control fluid, it is vital on economic grounds that they be able to demonstrate viscous behavior at low concentrations (i.e. approximately 0.5 wt.%). Of course, one must insist that the surfactants' rheological properties be viable at reservoir conditions. This means that the presence of oil should not destroy solution viscosity, and the presence of salt should not cause precipitation of surfactant from solution. The ideal surfactant then, would be one which shows high viscosities at dilute concentrations, is indifferent to hydrocarbon, and has an acceptable one phase working region in temperature-salinity space.

With these explicit goals, it may seem that the determination of whether or not surfactants can function as mobility control agents is a straight forward task, one subject to a simple experimental analysis. In reality the problem becomes a complex optimization assignment since the best surfactant molecule for mobility control purposes is unknown. One must have a link between surfactant structure and viscosity in order to design and subsequently test those molecules which could most successfully achieve the desired goals. Unfortunately, current theoretical limitations simply do not permit one to relate the structural features of surfactant molecules, directly and quantitatively, to a physical parameter such as viscosity.

Inspired by the apparent intractability of the problem, Chapter 2 of this text represents an effort to bridge the gap between surfactant molecular characteristics and solution viscosity. A model will be presented which can at least give qualitative predictions of how changes in surfactant structure affect solution viscosity. Chapter 3 provides a test of the theory against experiment. The effect of surfactant structure on viscosity is measured. In addition, the phase boundaries in temperature-salinity space are determined, and the rheological response of surfactants in the presence of oil will be examined. These results yield the necessary information to complete a feasibility study and a comparison of experimental vs. theoretical trends. The results aer discussed in Chapter 5. Conclusions can be found in Chapter 6.

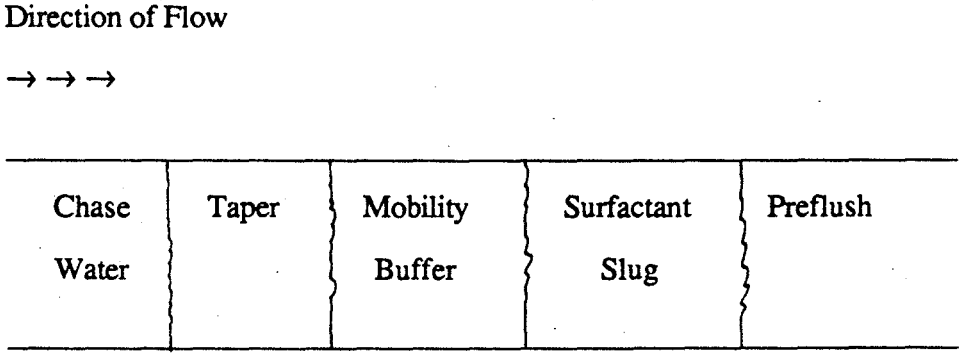

Figure 1.1 Idealized cross-section of a micellar-polymer flood.

From Lake[1], November 1983.

CHAPTER 2

Micellization and Viscosity

2.1 Purpose

This chapter presents a physico-chemical model which will lend some predictability to the physical character (i.e. viscosity) of surfactant solutions.

2.2 Viscosity Formulas for Particle Solutions

Attempts to predict solution viscosities have proven to be a formidable problem. Beginning with Einstein's fundamental analysis of the viscosity of dilute suspensions of rigid spherical particles, many equations have since been proposed in an effort to extend his work to non-spherical and non-rigid particles at higher concentrations.[1,2] In his seminal study, Einstein was able to show that for a system of spherically shaped, suspended particles, sufficiently far apart so that one may neglect interactions between them, the following viscosity relation is valid,

$$\eta' = \eta(1 + 2.5\varphi) \qquad (2.2.1)$$

where

η' = viscosity of solution

η = viscosity of solution without particles

φ = volume fraction of particles

As a progression of Equation (2.2.1), if velocity gradients are kept small, then even when the particles are not spherical, Simha[3] has shown that Einstein's equation can be applied to ellipsoids of revolution, in which case

$$\eta' = \eta (1 + v\varphi) \qquad (2.2.2)$$

The v in this expression represents a shape factor. It is designed to account for the deviation of the particle shape from that of a true sphere. By definition, one would expect the shape factor to depend on the dimensions of the particle. This is in fact true and Figure 2.1 shows a plot of Simha's shape factors for ellipsoids of revolution as a function of particle axial ratio.

In a strict sense, a cylindrical structure is not an ellipsoid of revolution, however, a prolate ellipsoid may be used as its hydrodynamic equivalent.[3] This allows one to assume expressions for the axial ratio, J, and shape factor, v, of a cylinder in terms of a prolate ellipsoid. Considering a prolate ellipsoid of equal rodlike dimensions, the following relation for the axial ratio may be written,[4]

$$J = [\, 2L^3 / (3D^2L - D^3) \,]^{1/2} \qquad (2.2.3)$$

in which

L = length of rod

D = diameter of rod

Likewise, the dependence of v on J for prolate ellipsoids, as noted in Figure 2.1, can be assumed for cylinders. The curve shown in that figure is closely approximated by the following functions:[3]

$$v = 2.5 + 0.407\,(J - 1)^{1.508} \qquad 1 < J < 15 \tag{2.2.4}$$

and

$$v = 1.6 + (J^2 / 15)\,[(\ln 2J - 1.5)^{-1} + 3(\ln 2J - 0.5)^{-1}] \quad J > 15 \tag{2.2.5}$$

Thus, for a dilute, rigid rod-like solution of particles one may make a good estimate of viscosity using Equations (2.2.2) and (2.2.4 or 2.2.5) provided the axial ratio is known. Of course, using Equation (2.2.3) to evaluate J requires knowledge or an estimate of the particles length , L, to its diameter, D.

2.3 Micellar Viscosity Equations

While the preceeding section was concerned with particles, one may make analogous arguments for dilute micellar solutions. For the reader unfamilar with the general concept of a micelle, see Wennerstrom.[5] The following equations will therefore have many similarities to those used in describing rigid particle systems. Some important differences exist, however, most notably the presence of an additional hydrodynamic term and a viscosity dependence on the weighted average micellar aggregation number, ϖ.[4]

Imagining a dilute solution of sphero-cylindrical micelles with a shape as illustrated in Figure 2.2, one may write the following general expression for the relative viscosity,[4,6]

$$\eta_r = (\eta / \eta_{cmc}) = 1 + v_c\varphi + k_1(v_c\varphi)^2 + k_2(v_c\varphi)^3 \tag{2.3.1}$$

where

η = relative solution viscosity

η_{cmc} = viscosity of solution at the cmc

v_c = volume fraction of micelles

φ = volume fraction of micelles

The squared term in Equation (2.3.1) is a measure of hydrodynamic interactions, and the constant k_1 is approximated to be 0.75. The cubic-ordered contribution, $k_2(v_c\varphi)^3$, accounts for intermicellar interactions and with the assumption of a dilute solution it may be neglected.[4] The volume fraction of micelles may be determined from the following expression,

$$\varphi = (S - S_{cmc})\, v_s / v_w \qquad (2.3.2)$$

where

v_s = volume of surfactant

v_w = volume of water molecule

S = total surfactant concentration as a mole fraction

S_{cmc} = critical micelle concentration as a mole fraction

Equation (2.3.1) closely resembles the viscosity expression developed for rigid particles. Unlike Equation (2.2.1), however, the subscript of v_c denotes that in the micellar case, this parameter will be a function of surfactant concentration, and more directly the average aggregation number. This can be seen more clearly by considering the expression for the axial ratio of the cylindrical micelle in Figure 2.2,[4]

$$J = (L / w) = 1 + 2/3 \{ R / (R + \delta)\} [\varpi / N_o - 1] \qquad (2.3.3)$$

where

R = effective surfactant tail length (the distance measured from the center of the micelle to the micellar surface)

N_o = maxium aggregation number for a spherical micelle

δ = effective length of surfactant head group, (including bound counterions and hydrated water molecules)

Since viscosity depends on v_c which is a function of axial ratio, the relation between J and ϖ of Equation (2.3.3) demands that viscosity vary with average aggregation number.

For straight chain molecules calculation of the R and N_o in Equation (2.3.3) is straight forward. One can say for these surfactants:[5]

$$R = (1.265n_c + 1.5) \text{ in angstroms (Å)} \qquad (2.3.4)$$

and

v_o = the surfactant tail volume

$$= (26.9n_c + 27.4) \text{ in Å}^3 \qquad (2.3.5)$$

where

n_c = number of carbon atoms in surfactant tail

Therefore, N_o is simply the volume of a sphere with radius R, divided by the volume of one surfactant tail, v_o. These relations hold only for straight tailed molecules, with other geometries requiring different calculations of R and v_o. In such cases it might be necessary to estimate these parameters based upon information about the bond angles between atoms within the surfactant.

If the forgoing arguments are accepted, then a review of the parameters in Equation (2.3.1) reveals that all variables, except ϖ and δ, can be easily estimated. Yet, by its definition, δ can be expected to change by a small amount since most surfactant head group lengths and counterion hydration numbers span a relatively narrow range.[7,8] In addition, given that δ will not vary greatly, if one considers surfactants where $n_c \geq 12$, R will generally be sufficiently large compared to δ so that J will be insensitive to this parameter. Hence, without great loss, δ may be assumed a constant and as a first estimate, $\delta \cong 6$ Å.[4]

This means that ϖ is the only unknown in the viscosity Equation, (2.3.1). Assuming this parameter to be calculable, Equation (2.3.3) can be used to obtain an axial ratio and subsequently a shape factor from Equations (2.2.4 or 2.2.5). Since the volume fraction of micelles can be estimated from (2.3.2), all of the necessary information to calculate the viscosity of a dilute micellar solution would be available. Thus, it is apparent that for surfactant solutions, an estimate of viscosity relies ultimately on the determination of ϖ. In fact, calculation of the average aggregation number is the central task when predicting dilute micellar solution viscosities; therefore, the remainder of this chapter will concern itself with a model which can facilitate a prediction of this variable.

2.4 Thermodynamics of Micellization

The development of any model which will predict surfactant aggregation numbers and viscosities must begin by considering the mechanics of self-assembly, a process known to be critically governed by thermodynamic considerations. Currently, two popular thermodynamic models, the phase seperation model and the kinetic model, best describe micellization.

The phase separation model regards micelles as a separate phase. If μ_N and μ_1 represent the chemical potentials per mole of amphiphile incorporated into micelles of aggregation number N, and unassociated amphiphile in aqueous solution, respectively, then equilibrium between the two phases demands

$$\mu_N = \mu_1 \tag{2.4.1}$$

Assuming dilute solution theory to be valid, activity coefficients can be set equal to unity. One can then write for the free amphiphile chemical potential,

$$\mu_1 = \mu_1^{\theta} + kT \ln X_1 \tag{2.4.2}$$

where

k = Boltzman's Constant

X_1 = mole fraction of free amphiphile

μ_1^{θ} = standard chemical potential of monomeric state

Since the micelles form a unique phase in this model, one may choose the micelle state itself as the standard state without loss of generality, thus,

$$\mu_N = \mu_N^{\theta} \tag{2.4.3}$$

Combining the above yields,

$$\mu_N^{\theta} = \mu_1^{\theta} + kT \ln X_1 \tag{2.4.4}$$

Tanford[9] notes that equations like Equation (2.4.4) neglect the cratic contribution to μ_N that occurs as a result of micelles mixing with solvent. This approximation should not be made and the phase separation model renders an incorrect expression for the treatment of μ_N.

In the mass action model, monomer and micelles are considered to be in association/disassociation equilibrium. The development with which we will follow here is that of Israelachvili, Mitchell, and Ninham.[10] In this case, one writes for the chemical potential of free and aggregated amphiphile,

$$\mu_1 = \mu_1^\theta + kT \ln X_1 \tag{2.4.5}$$

and

$$\mu_N = \mu_N^\theta + kT \ln (X_N / N) \tag{2.4.6}$$

where

(X_N / N) is the mole fraction of micelles of size N

Equilibrium between the monomeric and micellar states demands that,

$$\mu_1^\theta + kT \ln X_1 = \mu_N^\theta + (kT / N) \ln (X_N / N) \tag{2.4.7}$$

This equation shows that in the limit of large N the phase separation and mass action models are identical since the R.H.S. of Equation (2.4.7) will approach μ_N^θ. Solving Equation (2.4.7) for X_N gives,

$$X_N = N X_1^N \exp\{N (\mu_1^\theta - \mu_N^\theta) / kT\} \tag{2.4.8}$$

Equation (2.2.8) describes the distribution of aggregates or micelles. Assuming that one knows $(\mu_1^\theta - \mu_N^\theta)$ as a function of temperature and aggregation number, use of Equation (2.4.8) also requires knowledge of X_1. Since the parameter most likely known is the total mole fraction of surfactant, S, a mass conservation formula for this quantity may be written which can be used with Equation (2.4.8) to determine the distribution function,

$$S = \sum X_N \tag{2.4.9}$$

It is clear from Equation (2.4.8) that when $(\mu_1^\theta - \mu_N^\theta)$ is positive, aggregation is favored. In fact, the tendency for micellization is maximized when μ_N^θ is minimized. This concept proves to be important when the size of aggregates is compared. In addition, if $(\mu_1^\theta - \mu_N^\theta)$ can be determined then one may calculate the needed parameter for viscosity estimation, ϖ. This becomes clearly evident if one considers the definition of ϖ,

$$\varpi \equiv \sum NX_N / \sum X_N \tag{2.4.10}$$

Thus, the dependence of ϖ on X_N is explicit, and it is realized that Equation (2.4.8) must be solved before ϖ, and subsequently the viscosity, can be estimated.

2.5 Free Energy Considerations

Equation (2.4.8) is of little practical use in its present form. It is not generally known how $(\mu_1^\theta - \mu_N^\theta)$ varies as a function of aggregation number and

temperature. It is advantageous, therefore, to separate this free energy difference into components and model the respective parts individually. Combining the various contributions to μ_N^θ and μ_1^θ provides a method of quantitatively determining (μ_1^θ - μ_N^θ). It also allows one to see the relative significance of the terms which comprise the free energies.

(μ_1^θ - μ_N^θ) may be written as the sum of three terms: (1) a hydrophobic interaction energy, (2) an interfacial energy due to hydrocarbon/water contact area, and (3) an electrostatic repulsive energy. Of these three contributions to the total free energy, it is only the hydrophobic part which drives micellization while the remaining two energies actually work to inhibit it. The hydrophobic term will be discussed first, as it plays a key role in the formation of aggregates.

Hydrophobic Contribution

When micelles were first observed, there was considerable controversy as to the mechanisim of their formation. Tanford[9] has summarized the available scientific evidence relevant to this question with the surprising conclusion being that systems in which surfactant aggregates form are at higher entropy states than those in which the surfactant molecules are distributed randomly throughout the system. Apparently, water molecules are able to form a more ordered structure about a surfactant tail than they can about each other. This concept was first suggested by Frank[11] and proposes that the presence of the lipophilic portion of the amphiphile requires water molecules to decrease their random orientation. Such reordering of water molecules in the presence of surfactants has been termed the "iceberg effect".[11,12] While it is true that micellization may increase the local ordering of amphiphilic molecules which decreases entropy, this is more than offset by the increasing entropy of the water.

The restriction of water movement by the presence of a hydrocarbon or any apolar compound has been called the hydrophobic effect or hydrophobic interaction. It is responsible for the small solubilities of apolar compounds in water.

Because the exact structure of water in the presence of hydrocarbon is not known, it is impossible to assess from theoretical considerations alone, the magnitude of hydrophobic interaction. Therefore, the hydrophobic effect is best described by using the concepts of classical thermodynamics. If $\Delta\mu^\circ_{HF}$ is the difference between the standard free energies of a hydrocarbon at infinite dilution in a hydrocarbon solvent (μ°_{HC}) and that in water (μ°_{AQ}), then one may write,

$$\Delta\mu^\circ_{HF} = \mu^\circ_{HC} - \mu^\circ_{AQ} \qquad (2.5.1)$$

For-straight tailed molecules, this free energy of transfer includes a contribution of -2100 cal/mole per CH_3 group and a contribution of -850 cal/mole per CH_2 group. A more general formulation which describes cyclic and branched chains, as well as linear ones, relates the free energy of transfer to the surface area of contact between water and hydrocarbon in the aqueous phase. The free energy of transfer is 25 ± 5 cal/mole per $Å^2$ of surface measured at the distance of closest approach of water molecules to hydrocarbon.[13,14] Since the motion of hydrocarbon in a micelle is less free than it would be in a true bulk hydrocarbon phase, the free energy of transfer to a micelle should be somewhat less than for a bulk phase. Thus, the observed values of -2000 cal/mole of CH_3 and -700 cal/mole of CH_2 group are accepted.[9]

It is this free energy change which represents the driving force to form micelles. Clearly, the molecular mechanisms are complex involving the detailed structure of water. Such processes are most difficult to model; starting with, for

example, statistical mechanics. In all thermodynamic considerations, the free energy related to the transfer of the lypophilic from water to the interior of a micelle is regarded, like it has been here, as a given quanity. Any other approach is impractical.

Electrostatic Contribution

Having characterized the hydrophobic component of the free energy, we now seek to model the electrostatic contribution to $(\mu_1^\theta - \mu_N^\theta)$. It is important to understand the general character of a micelle for this development. A micelle made up of ionic amphiphiles is a highly charged entity, and ions of opposite charge are drawn into the vicinity of the micellar surface by the electrical field created by the surface charge. These oppositely charged ions, called counterions, are distributed in a diffuse layer around the micelle but their concentration in excess of the counterion concentration, is a function of the distance from the center of the micelle. This separation of charge between amphiphile and counterion gives the micelle a number of interesting properties; and in addition, it represents an important factor in the thermodynamics of micellization. In this regard, there are two principal issues to be addressed in this section. The first concerns the distribution of counterions about a micelle. This entails calculation of the concentration of counterion as a function of position. Both spherical and cylindrical micelles will need to be considered. The second is to develop the relationship between the electrical potential at the interface relative to the surface charge of the micelle. Given these relationships, the electrical free energy of a micelle can be calculated.

1. The Poisson-Boltzman Equation

The variation of the electrical potential with distance from an interface is a classical electrostatic problem, and the equation which describes it is the Poisson equation,[15]

$$\nabla \cdot \nabla \Psi = -\rho_{ex} / \varepsilon \qquad (2.5.2)$$

where

∇ = the Gradient operator

Ψ = electrostatic potential

ρ_{ex} = charge density which is a function of position

ε = dielectric constant of the medium

To specify the boundary conditions, convention dictates that one should measure all potentials from the interface where the potential has the value Ψ_o. As the distance from an isolated surface increases to infinity, the value of Ψ approaches zero. In the discussion to follow, an isolated surface will mean that only one micelle at a time is being considered. More concentrated solutions would necessitate the consideration of intermicellar interactions not examined here.

The primary difficulty is expressing the charge density as a function of the potential so that Equation (2.5.2) can be solved. The usual procedure is to describe the ion concentration in terms of the potential by means of a Boltzmann factor in which the work required to bring an ion to a position where the potential is given by $Z_i e\Psi$, where Z_i is the ion valence and e is the unit charge. The probability of finding an ion at this position is given by,[16]

$$n_i = n_i^{(\infty)} \exp\{ -Z_i e\Psi / kT\} \qquad (2.5.3)$$

where

n_i = concentration of ion i at a point near the surface where the potential is Ψ

$n_i^{(\infty)}$ = concentration far from the surface or the bulk ionic concentration

The charge density may be related to the ion concentration by making use of Equation (2.5.3) as follows,

$$\rho_{ex} = \sum Z_i e\, n_i = \sum Z_i e\, n_i^{(\infty)} \exp\{ -Z_i e\Psi / kT\} \qquad (2.5.4)$$

Combining Equations (2.5.4) and (2.5.2) yields the Poisson-Boltzmann equation,

$$\nabla \cdot \nabla\Psi = (-1/\varepsilon) \sum Z_i e\, n_i^{(\infty)} \exp\{ -Z_i e\Psi / kT\} \qquad (2.5.5)$$

The derivation of the Poisson equation assumes that the potentials combine in an additive manner. By contrast, the Poisson-Boltzmann equation expresses the variation of the potential as an exponential function. Hence, a fundamental inconsistency is introduced when Equations (2.5.4) and (2.5.2) are brought together. The incompatibility of these equations is insignificant in the special case where ($Z_i e\Psi$ / kT) < 1. With this restriction, generally known as the Debye-Huckel approximation, the exponential terms can be expanded, and to a good approximation, only the linear terms in Ψ retained.[16,17] Thus, expanding the exponential of Equation (2.5.5), and keeping only linear terms, one can write,

$$\nabla \cdot \nabla \Psi = (-1/\varepsilon) \sum Z_i e\, n_i^{(\infty)} \{ 1 - (Z_i e \Psi / kT) \} \qquad (2.5.6)$$

Because of electrical neutrality, the net ionic charge must be equal to zero,

$$\sum Z_i\, n_i^{(\infty)} = 0 \qquad (2.5.7)$$

and so,

$$\nabla \cdot \nabla \Psi = \Psi / \lambda^2 \qquad (2.5.8)$$

where λ is the Debye length defined by,

$$\lambda^2 = \varepsilon kT / e^2 \sum Z_i^2\, n_i^{(\infty)} \qquad (2.5.9)$$

2. The Spherical Micelle

Using Equation (2.5.8), one can determine the variation of the potential with position, provided the geometry of the system is specified. The simplest model and one being adopted for use here, considers the ionic charge of the amphiphilic molecules to be confined to a spherical surface of fixed radius. The surface charge density is assumed to be small enough so that the Debye-Huckel approximation is valid, the counterions are considered point charges and the dielectric constant for water is taken as constant. Although this is a highly idealized model, the essential features of the diffuse portion of the double layer are seen, and the observed trends are qualitatively predicted. Other more comprehensive models are in the literature, but these complex formulations are not necessary for the purpose of this work.[18,19]

For the simplest case, Equation (2.5.8), written for a spherical micelle, is

$$\Psi/\lambda^2 = r^{-2}\, d[r^2\, (d\Psi/dr)] / dr \qquad (2.5.10)$$

The solution is,

$$\Psi = (A / r) \exp\{-r / \lambda\} \qquad (2.5.11)$$

where

A = a constant of integration

For this simple model, the constant can be evaluated from the condition that $\Psi \rightarrow \Psi_\circ$ as $r \rightarrow a$, the radius of the micelle. Using this boundary condition the final solution becomes,

$$\Psi = (\Psi_\circ a / r) \exp\{(a - r) / \lambda\} \qquad (2.5.12)$$

The potential is therefore seen to decrease rapidly as r increases. Within a distance of three or four times the Debye length, the potential has almost decayed to zero. The charge density also decreases rapidly, and with the approximation being used here, one may say,

$$\rho_{ex} = -\varepsilon\Psi / \lambda^2 = (-a\, \varepsilon\Psi_\circ / \lambda^2 r) \exp\{(a - r) / \lambda\} \qquad (2.5.13)$$

This equation shows that the charge in the diffuse layer is opposite to that of $\Psi_\circ$, and that much of the counterion charge is located near the surface of the micelle.

A relationship between N, the aggregation number, and the potential can easily be developed since the counterion charge must be equal, but opposite in sign to, the micellar charge,

$$\sigma_s = e Z_i N = - {}_a\int \rho_{ex} 4\pi r^2 dr \qquad (2.5.14)$$

where

σ_s = total micellar surface charge

Substituting the differential Equation, (2.5.2), for ρ_{ex} into Equation (2.5.14) yields

$$\sigma_s = \varepsilon {}_a\int \nabla \cdot \nabla \Psi \, 4\pi r^2 dr \qquad (2.5.15)$$

so

$$\sigma_s = 4\pi\varepsilon {}_a\int (d/dr)\, r^2 d\Psi/dr \; dr \qquad (2.5.16)$$

Performing the integration of Equation (2.5.16) gives the desired expression relating the surface charge to the surface potential,

$$\sigma_s = 4\pi\varepsilon a \Psi_\circ (1 + a / \lambda) \qquad (2.5.17)$$

The relationship between σ_s and $\Psi_\circ$ is seen to be a linear one as dictated by Equation (2.5.17). This, however, is not generally the case. If other more comprehensive and complex treatments of the spherical micelle are considered, the solutions to the Poisson-Boltzmann equation will not yield a linear relation betweeen the surface potential and the surface charge.[17]

3. The Cylindrical Micelle

The second application of Equation (2.5.8), which will be of importance here, considers a cylindrical micelle. For micelles composed of a large number of amphiphiles, the aggregated structure can no longer be considered spherical and for very large micelles rod-like shapes, such as the one illustrated earlier in Figure 2.2, are generally envisioned.[20] The distribution of counterions in the diffuse layer about a rod-like micelle can be readily ascertained if essentially the same idealized concepts which were applied to the spherical micelle are maintained. Thus, the Poisson-Boltzmann equation for a long cylinder is

$$\Psi/\lambda^2 = r^{-1}\, d[r\,(d\Psi/dr)]\,/\,dr \qquad (2.5.18)$$

With boundary conditions analogous to the spherical case, namely, $\Psi = \Psi_\circ$ at $r = d$, and $\Psi \rightarrow 0$ as $r \rightarrow \infty$, Equation (2.5.18) can be solved to yield,

$$\Psi = \Psi_\circ K_\circ (r / \lambda) / K_\circ (d / \lambda) \qquad (2.5.19)$$

where

$K_\circ$ = modified Bessel function of the second kind order 0

d = the radius of the rod

For large values of (r / λ), the Bessel function of Equation (2.5.19) may be expanded as the series,

$$K_\circ (r / \lambda) \cong (\pi \lambda / 2r)^{1/2} \exp\{-r / \lambda\} [\, 1 - 8\lambda / r + ...] \qquad (2.5.20)$$

so that just like the spherical case, the potential is again seen to fall off rapidly to zero within a few Debye lengths from the surface.

Following the procedure used to calculate the surface charge for the spherical micelle, one finds in the cylindrical case,

$$\sigma_s = 2\pi\epsilon d \Psi_\circ [K_1 (d / \lambda) / \lambda K_\circ (d / \lambda)] \qquad (2.5.21)$$

where

K_1 = modified Bessel function of the second kind order 1

In Equation (2.5.21), σ_s is the charge per unit length of cylinder. This is different from the spherical case where σ_s represented the total micellar charge.

The significance of cylindrical aggregates for viscosity modification cannot be overstated. It is the presence of these micelles which are believed to give rise to high viscosities at dilute concentrations.[20,21] For this reason, after completing the current discussion of free eneregy calculations, Section 2.6 will show a particular thermodynamic model for rod-like aggregates.

4. Electrostatic Free Energy

Thus far, expressions for the electrical potential as a function of position for cylindrical and spherical micelles has been presented. With these quantities now calculable, attention can be directed toward determining the real variable of interest, the electrostatic free energy. Stigter [22] has devoted extensive analysis to calculation of the free energy necessary to charge a micelle. This free energy (isothermal work)

is not obtainable from an elementary integration of the potential as it is in the case of a capacitor. The main difficulty arises from the complex relation between the potential and the surface charge.[16] However, with the Debye-Huckel approximation retained, the problem is made easier since the relation between Ψ and σ is linear.

In Stigter's[22] model, the micelle is imagined to be initially formed under neutral conditions. At this point the charge, both positive and negative, is brought in from infinity in small steps, $\sigma_s\, d\xi$, where ξ is a charging parameter varying between 0 and 1 during the charging process. When an amphiphile is charged, a counterion in the diffuse region of the double layer is simultaneously charged so that electrical neutrality is maintained at every point in the buildup of the charges. Expressed mathematically, one writes,

$$0 = \sigma_s \xi + \int \rho'_{ex}\, dV \qquad (2.5.22)$$

where

ρ'_{ex} = is the charge density at a point in the diffuse layer when a fraction of the surface, ξ, is charged

The electrical free energy can be found by incorporating the values of the potential at the surface, Ψ'_o, and in the double layer, Ψ', where the primes indicate an arbitrary stage in the charging process. Using these in Equation (2.5.22) gives an integral expression for the electrical free energy,[22]

$$\Delta F_{electical} = \sigma_s \int \Psi'_o\, d\xi + \int d\xi/\xi \int \Psi' \rho'_{ex}\, dV \qquad (2.5.23)$$

which after application of the divergence theorem can be written as,

$$\Delta F_{electical} = \varepsilon \int d\xi/\xi \int \nabla\Psi' \cdot \nabla\Psi' \, dV \qquad (2.5.24)$$

The first term on the right of Equation (2.5.23) represents the work necessary to charge the amphiphiles while the second is the work gained by positioning the counterions in the diffuse layer. The first term is positive and always larger than the second term which is negative, and therefore, the electrical free energy is a positive quanity.

Neither Equation (2.5.23) or (2.5.24) necessitates the use of the Debye-Huckel approximation, but as remarked eariler, unless this condition is imposed, the integration is greatly complicated and different approaches for calculating the free energy will yield different results with no sure way of ascertaining which is better. In this work, the format is to assume the linearization of the Poisson-Boltzmann equation throughout the development of the electrical free energy. Applying Equation (2.5.24) to the spherical micelle developed here previously, one finds that

$$\Delta F_{el} = (\sigma_s^2 / 2\varepsilon a) [1 + a / \lambda] \qquad (2.5.25)$$

Doing the same for the cylindrical case leads to the following expression,

$$\Delta F_{el} = (\sigma_s^2 \lambda / \varepsilon dL)[K_o (d / \lambda) / K_1 (d / \lambda)] \qquad (2.5.26)$$

The sphero-cylindrical micelle as depicted in Figure 2.2 is an idealized and simplified illustration. A small modification of this micellar geometry, which has profound consequences, allows for the presence of an excluded radius. Such a

micelle is shown in Figure 2.3. We give physical significance to the excluded radius as providing a volume in which the surfactant head groups reside. Recall that previously the micellar radius only considered the surfactant tail length.

We can denote the excluded distance (b-R) as $\Delta\alpha$-carbon since by definition this parameter represents the distance between the α-carbon atom of the surfactant tail and the center of the charge distribution. The mutual electrostatic repulsion between head groups means that the larger the ratio of the distance to the micellar surface, denoted by R in Figure 2.3, to the excluded radius b, the more stable the micelle. This is because as R/b increases the charge is effectively spread over a larger area. So for larger (b-R) one expects a micelle to accomodate more monomers in a spherical state and require higher salinities for a transition to a cylindrical geometry. These predictions can be examined later, for now it is important to write the appropriate modifications to Equations (2.5.25) and (2.5.26) for the electrostatic free energy of a spherical and cylindrical micelle, respectively. For micelles with radius of exclusion b and surface radius R, the work of Hill[23] allows one to write for the electrostatic free energy of a sphere,

$$\Delta F_{el} = (\sigma_s^2 / 2\varepsilon R) [1 - \kappa R / (1+ \kappa b)] \qquad (2.5.27)$$

and for a long cylinder of length L

$$\Delta F_{el} = (\sigma_s^2 / \varepsilon L)[(K_o (\kappa b) / \kappa b K_1 (\kappa b)) + \ln b/R] \qquad (2.5.28)$$

where

$$\kappa = 1 / \lambda$$

and the σ_s^2 in both expressions represents the total micellar surface charge. If R is set equal to b, that is the surface radius and radius of exclusion are the same, then as expected Equations (2.5.27) and (2.5.28) reduce to Equations (2.5.25) and (2.5.26), respectively.

In order to successfully use both Equations (2.5.27) and (2.5.28), one must include an empirical constant, β, which corrects the Debye-Huckel approximation for its over estimation of ΔF_{el}. Incorporation of this constant is well noted in the literature.[13,22,24] The Debye-Huckel theory, without correction, does not adequately assess the electrostatic interaction energy between head groups of the micelle. Much of the inadequacey arises because the theory treats counterions as point charges. Failure to consider the finite size of the counterions allows for unrealistic counterion charge densities about the micelle. As suggested by Tanford, a correction factor of about 0.5 provides quantitative agreement with experiment.[24] Thus, Equations (2.5.27) and (2.5.28) are written as

$$\Delta F_{el} = (\beta \sigma_s^2 / 2\varepsilon R) [1 - \kappa R / (1+ \kappa b)] \qquad (2.5.29)$$

and

$$\Delta F_{el} = (\beta \sigma_s^2 / \varepsilon L)[(K_o (\kappa b) / \kappa b K_1 (\kappa b)) + \ln b/R] \qquad (2.5.30)$$

respectively, and it is understood that β has the value of 0.5.

This completes the formulation of the equations necessary to calculate the electrostatic contribution to the free energy. The remaining quanity necessary for an evaluation of $(\mu_1^\theta - \mu_N^\theta)$ is the surface term. It is discussed next.

Surface Contribution

Because it is assumed that amphiphilic head groups do not cover sufficient micellar surface area to prevent the aqueous phase from contacting the micelle's hydrocarbon-like core, a surface term is generally included in the total free energy expression. The free energy of this contact between hydrocarbon and water can be represented by γA (per amphiphile), where A is the area per amphiphile at the micellar surface and γ is the energy per unit of area between hydrocarbon and water. Padday and Uffindell [25] have calculated γ for n-hexane and water as 53.3 ergs / cm^2 and found this value to be practically invariant as the oil was changed from hexane to n_c = 30.

This completes the development of the terms which contribute to the free energy of micellization. One can now combine components to formulate an equivalent expression for $(\mu_1^\theta - \mu_N^\theta)$. In a general fashion this yields,

$$(\mu_1^\theta - \mu_N^\theta) = -\Delta\mu^\circ_{HF} - \Delta F_{electrical} - \gamma A \qquad (2.5.31)$$

where, as expected, we identify the hydrophobic, electrical, and surface contributions to the free energy, respectively. Note also that the hydrophobic term in this expression is the only positive contribution to the indicated free energy difference, (i.e. recall that $\Delta\mu^\circ_{HF}$ had previously been defined for the reverse process $(\mu_N^\theta - \mu_1^\theta)$ and it was negative, hence the negative sign in (2.5.29) makes this already negative expression positive, while the other two terms, $(-\Delta F_{electrical})$ and $(-\gamma A)$ are now negative quantities). So, as anticipated, the hydrophobic effect favors the aggregated, or micellar, state; the electrical and surface terms do not.

2.6 Thermodynamics and Geometry

The free energy model which was developed in Section 2.5 allows one to determine the relative preference of a given surfactant molecule for the monomeric vs. aggregated states. It provides for the necessary and important calculation of (μ_N^θ - μ_1^θ). However, in its current form, it has two distinct disadvantages, both of which retard our goal of determining the relationship between surfactant structure and viscosity.

The first problem with the present model is that it creates substantial complexity when one tries to make a quantitative calculation of the free energy at temperatures other than room temperature. This complication occurs as a result of the hydrophobic term. While one may calculate the effect of temperature on the electrostatic contribution to the free energy, and the surface term may be considered a constant with respect to this variable, the hydrophobic term has a complex temperature dependence which is not easy to assess. Good solubility data of liquid hydrocarbons in water, as a function of temperature at normal pressures, is not abundant, and the linear trends which are found at 298K are not apparent at higher temperatures. Thus, due to the presence of the hydrophobic term, temperature effects are not easily estimated with the current thermodynamic model.

The second inadequacy with the previous free energy development is that it does not specifically consider the key role which aggregate shape plays in determining solution viscosities. It is insufficient to have merely estabilished that the aggregated or micellar state is favored over the monomeric state. The overwhelming evidence supporting the belief that rod-like aggregates are responsible for high viscosities necessitates that one must also be concerned with micellar geometry. In other words, for the purposes of viscosity modification, it is vital to know which micellar structure

is preferred (i.e. spherical or cylindrical). The deficiency of the current model, as it has been developed thus far, is that it tells only when micellization will occur and not which aggregate geometry is favored.

The two difficulties with the current model suggests that a thermodynamic theory which effectively removes consideration of the hydropholic term and predicts micellar geomety as well as average aggregation number is needed in order to advance our goal of predicting solution viscosities. Fortunately, such a model has been developed by Missel, Benedek, Young, and Carey.[26] The salient features of their thermodynamic treatment are reviewed here.

The theory is formulated by considering a thermodynamic analysis of a rod-like micelle such as the one which was illustrated in Figure 2.2. It is assumed that the smallest possible micellar size is N_o. When the rod-like micelle has minimum aggregation number N_o, it reduces to a sphere since there are $N_o/2$ molecules in each hemispherical end cap. For a rod-like micelle containing N molecules, $N-N_o$ are in the cylindrical region.

In a system for which $N < N_o$, this theory assumes that there are no micelles or that only the free amphiphile state exists. When $N > N_o$, a spectrum of chemical potentials exists and is given by

$$(\mu_N^\theta / N) - \mu_1^\theta = [\, \mu_{No}^\theta - N_o\mu_1^\theta + (\mu^\theta - \mu_1^\theta)(N - N_o)\,] / N \qquad (2.6.1)$$

where μ^θ is the chemical potential of a molecule in the cylindrical portion of the micelle, and μ_{No}^θ is the standard chemical potential to form a spherical micelle. This equation makes no distinction between μ^θ in very large micelle and μ^θ in a much smaller, almost spherical aggregate. Thus, the chemical potential necessary to add a

single molecule to the cylindrical region is independent of the number of such molecules already present in that region, and so the local environment "seen" by an amphiphile incorporated in the cylindrical part of the micelle is independent of the length of the rod. Once $N-N_o$ is sufficiently large, this is clearly an excellent approximation. Equation (2.6.1) can be rewritten as

$$N\mu_1^\theta - \mu_N^\theta = N_o\mu_1^\theta - \mu_{No}^\theta + (N-N_o)(\mu_1^\theta - \mu^\theta) \qquad (2.6.2)$$

We seek to combine Equation (2.6.2) with the general equation describing the distribution of aggregates, Equation (2.4.8). Rewriting Equation (2.4.8) as X_N / N yields,

$$X_N/N = X_1^N \exp\{(N\mu_1^\theta - \mu_N^\theta) / kT\} \qquad (2.6.3)$$

To simplifiy one defines the following

$$\Phi = \mu_{No}^\theta - \mu_1^\theta N_o \qquad (2.6.4)$$

and

$$\Gamma = \mu^\theta - \mu_1^\theta \qquad (2.6.5)$$

The quantity Φ is the gap spacing or free energy difference between the smallest possible micelle and the monomer chemical potential of N_o molecules. The second parameter, Γ, is the ladder spacing. It represents the increment of free energy associated with the addition of a surfactant monomer to the cylindrical region. It is

also advantageous to define two characteristic mole fractions X_A and X_B whose magnitudes are related to the energy gap spacing per monomer $\Phi / (N_o - 1)$ and the ladder spacing as follows

$$X_A = \exp\{ \Phi / (N_o - 1)kT \} \tag{2.6.6}$$

and

$$X_B = \exp\{ \Gamma / kT \} \tag{2.6.7}$$

It is now possible to express X_N, Equation (2.6.3) in a number of different forms

$$X_N = N X_1^N \exp\{ (-\Phi - (N-N_o)\Gamma) / kT \} \tag{2.6.8}$$

or

$$X_N = N X_B^{No} (X_1 / X_B)^N \exp\{ - \Phi / kT \} \tag{2.6.9}$$

and equivalently as

$$X_N = N X_A (X_1 / X_A)^{No} (X_1 / X_B)^{N-No} \tag{2.6.10}$$

Equation (2.6.9) shows that X_N is a decreasing function of N since X_B is less than unity. The distribution of aggregates must satisfiy the material balance equation which can be written as

$$S = X_1 + \Sigma X_N \tag{2.6.11}$$

where X_1 is the mole fraction of monomer in the solution. Substituting Equation (2.6.10) into Equation (2.6.11) gives

$$S = X_1 + \Sigma N X_A (X_1 / X_A)^{No} (X_1 / X_B)^{N-No} \qquad (2.6.12)$$

This summation is expressed more easily if one makes the following definition

$$\begin{aligned} K &= (1 / X_A) (X_A / X_B)^{No} = \exp\{+ (\Phi - N_o\Gamma) / kT \} \\ &= \exp\{ \mu_{No}{}^{\theta} - \mu^{\theta} N_o) / kT \} \end{aligned} \qquad (2.6.13)$$

Using Equation (2.6.13) in Equation (2.6.12) and summing yields

$$S = X_1 + K^{-1} (X_1/X_B)^{No+1} \{ N_o/[1-(X_1/X_B)] + 1/[1-(X_1/X_B)]^2 \} \qquad (2.6.14)$$

From this equation, it can be noted that as S becomes large, $X_1 \rightarrow X_B$. In this case Equation (2.6.14) can be rewriten with X_B approximately equal to X_1

$$K(S-X_B) \cong (X_1/X_B)^{No+1} \{ N_o/[1-(X_1/X_B)] + 1/[1-(X_1/X_B)]^2 \} \qquad (2.6.15)$$

This equation reveals that $K(S-X_B)$ fixes (X_1/X_B) and thereby determines the decay rate of the X_N in Equation (2.6.10).

Assuming that $K(S-X_B)$ is large, that is $K(S-X_B) >> N_o^2$ then one may approximate (X_1/X_B) as

$$X_1 / X_B \cong 1 - 1 / [K (S - X_B)]^{1/2} \qquad (2.6.16)$$

and to a further approximation one can write for X_N

$$X_N = NK^{-1} \exp\{ -N / [K (S - X_B)]^{1/2} \} \qquad (2.6.17)$$

Thus, the distribution of micelles decreases monotonically with increasing N, and the width of the exponential decay expands in direct proportion to $K (S - X_B)^{1/2}$.

Equation (2.6.17) is an important result, and several conclusions may be drawn from this expression for X_N. To increase $K(S-X_B)$, one can increase the surfactant concentration S. Since higher values of $K(S-X_B)$ will produce a broader distribution of aggregates, it follows that increases in S will also produce a wider distribution of aggregates. This means that more micelles will have a cylindrical-like shape. So, increasing surfactant concentration should move the average aggregate shape away from spheres toward cylinders and thereby increase solution viscosity. This result is not unexpected, and increases in detergent concentration have been related to rod-like micelle formation and subsequently higher solution viscosities.[21]

One can also increase $K(S-X_B)$ by decreasing X_B. Recalling the definition of X_B Equation (2.6.7) it is seen that this may be accomplished by making μ^θ a more negative number. The additon of salt, which effectively shields the micellar surface, or the addition of a polar compound, such as alcohol, both lower μ^θ, and therefore increase the width of the aggregate distribution, X_N. Another way to increase the distribution of micelles is to increase X_A. Since Φ is a negative number (${\mu_N}^\theta_o$ is a larger negative number than ${\mu_1}^\theta$) X_A is increased by increasing Φ.

2.7. Calculation of K

Early in the previous section, it was explained why the general thermodynamic model developed in Section 2.4 was inadequate to achieve the goal of relating surfactant structure to viscosity. The more specialized thermodynamic model which was outlined in Section 2.6 attains the desired result. This is seen more clearly by investigating the relationships between the variables of the equations developed in Section 2.6 and the average aggregation number.

To begin, one may recall the definition of the weighted average aggregation number, Equation (2.4.10), which may be written as

$$\begin{aligned} \varpi &= \Sigma N X_N / (S - X_1) \\ &= \Sigma N^2 (X_N / N) / (S - X_1) \end{aligned} \qquad (2.7.1)$$

The R.H.S. of Equation (2.7.1) is simply the total number of aggregates weighted by N^2 and divided by the molecules of amphiphile associated into aggregates of any size.

With the assumption that $K(X-X_B) >> N_o^2$, Equation (2.6.17) may be used in Equation (2.7.1) to give the approximation

$$\varpi = N_o + 2[K(X-X_B)]^{1/2} \qquad (2.7.2)$$

Equation (2.7.2) is a simple expression describing the variation of ϖ with surfactant concentration. This result is the most important aspect of the Missel, Benedek, Young, and Carey theory. For the purposes of viscosity modification, it is essential. It provides a method of calculating ϖ without the need to estimate the complex temperature dependence implicit in the hydrophobic term. It also has the advantage of

predicting surfactant geometry so that even if the theory fails to predict quantitative viscosities, qualitative trends relating surfactant structure to viscosity can still be established. These important characteristics of Equation (2.7.2) are somewhat hidden in the factor K, and it is instructive, therefore, to consider this term in more detail.

The physical meaning of the parameter K is actually quite simple. If one takes the logarithim of Equation (2.6.13), the result is

$$\ln K = [\mu_{No}^{\theta} - \mu^{\theta} N_o] / kT \qquad (2.7.3)$$

Thus, K is essentially the difference in the chemical potential between N_o molecules in the cylindrical portion of the micelle compared with N_o in the hemispherical regions of the micelle. When cylindrical micelles are the favored state, $\mu^{\theta} N_o$ will be more negative than μ_{No}^{θ} and K will be positive. This of course means that the free energy per monomer in the cylindrical region of the micelle must be less than the free energy per monomer in the hemispherical region. The hydrophobic term, however, should be approximately the same, regardless as to whether the amphiphile is incorporated in the hemispherical or cylindrical regions, respectively. Therefore, the free energy difference per amphiphile can be expressed as

$$(\mu_{No}^{\theta} - \mu^{\theta} N_o) / N_o = [(\mu_{No}^{el} - N_o \mu_o^{el}) + \gamma(A_{sphere} - A_{cylinder})] / N \qquad (2.7.4)$$

where

$N_o \mu_o^{el}$ = the electrostatic free energy necessary to form a cylindrical micelle of N_o molecules

μ_{No}^{el} = the electrostatic contribution to the free energy of a spherical

micelle defined by Equation (2.5.27)

and (A_{sphere} - $A_{cylinder}$) is the difference between the area of a sphere and cylinder with N_o monomers. With this equation one can now easily identify the two desired aspects of this thermodynamic model with regard to viscosity predictions,

1) the absence of the hydrophobic term
2) specific considerations of micellar geometry

2.8 Explicit Procedure For Use of Equations

All of the relevant terms necessary to calculate viscosity are now available. It is appropriate to review the procedure which will be used. We desire first to calculate ϖ, Equation (2.7.2). We assume that S, the total surfactant concentration of the system, is known. The N_o which appears in Equation (2.7.2) may be calculated from geometric considerations of surfactant tail volume and tail length or with Equations (2.3.4) and (2.3.5) for straight chain molecules. This leaves K as the only unknown in Equation (2.7.2), and to estimate this parameter, Equation (2.7.3), and hence the free energy difference, $(\mu_{No}^{\theta} - \mu^{\theta}N_o)$, must be solved. It is instructive to rewrite Equation (2.7.4) for this purpose.

$$\begin{aligned}(\mu_{No}^{\theta} - \mu^{\theta}N_o) &= (\mu_{No}^{el} - N_o\mu_o^{el}) + \gamma(A_{sphere} - A_{cylinder}) \\ &= \Delta F_{el}^{sphere} - \Delta F_{el}^{cylinder} + \gamma(A_{sphere} - A_{cylinder}) \qquad (2.8.1)\end{aligned}$$

For calculations, a more explicit form of Equation (2.8.1) is necessary. Considering first the electrostatic terms, one can employ the expressions derived

earlier for ΔF_{el}^{sphere} and $\Delta F_{el}^{cylinder}$. Recalling Equations (2.5.29) and (2.5.30) which can be written as

$$\Delta F_{el}^{sphere} = (\beta (N_o e)^2/4\pi\varepsilon 2R) [(1 + \kappa(b-R)) / (1+ \kappa b)] \quad (2.8.2)$$

and

$$\Delta F_{el}^{cylinder} = (\beta (N_o e)^2/4\pi\varepsilon L) [(K_o(\kappa b) / \kappa b\, K_1(\kappa b)) + \ln b/R] \quad (2.8.3)$$

where

κ = $56.79 \times 10^9 (I / T)^{1/2}$ $(Meters)^{-1}$

I = salt concentration (Molar)

T = Temperature (K)

ε = 8.854×10^{-12} $(Meters)^{-3}\, Kg^{-1}\, (Seconds)^4\, (Amperes)^2$

R = micellar surface radius (Meters)

b = excluded micellar radius (Meters)

β = 0.5

and the electrostatic energies are in joules.

The L which occurs in Equation (2.8.2) can be expressed in terms of the surface radius R. This is possible because we have considered a cylindrical micelle of equal aggregation number to that of a sphere. Hence, demanding that the density in the interior of both cylindrical and spherical aggregates must be the same, one can write

$$4\pi R^3 / 3 = \pi R^2 L \quad (2.8.3)$$

Therefore, the simple relation for L is

$$L = 4R / 3 \qquad (2.8.4)$$

Equation (2.8.4) can be used in Equation (2.8.2). With this substitution equations (2.8.1) and (2.8.2) can be combined to give

$$\Delta(\Delta F_{el}) = \beta\,(2.31 \times 10^{-28}\, N_o^2 / R\varepsilon)\,[\,0.5\,(1 + \kappa(b-R)) / (1+ \kappa b)) - 0.75\,((K_o(\kappa b) / \kappa b K_1(\kappa b)) + \ln b/R)] \qquad (2.8.5)$$

We can simplify Equation (2.8.5) by making the following substitutions

$$Z0 = K_o(\kappa b) \qquad (2.8.6)$$

$$Z1 = K_1(\kappa b) \qquad (2.8.7)$$

$$Z3 = (Z0 / \kappa b\, Z1) + \ln b/R \qquad (2.8.8)$$

$$Z4 = (1 + \kappa(b-R)) / (1+ \kappa b) \qquad (2.8.9)$$

and

$$Z5 = 0.5\,(Z4) - 0.75\,(Z3) \qquad (2.8.10)$$

Using substitutions in (2.8.5) yields

$$\Delta(\Delta F_{el}) = \beta\,(2.31 \times 10^{-28}\, N_o^2 / R\varepsilon)\, Z5 \quad \text{(joules)} \qquad (2.8.11)$$

Equation (2.8.11) is the working expression for the calculation of the electrostatic free energy difference which is needed in the evaluation of K, Equation (2.8.1). When all

the parameters in this equation have the units as specified previously, the resulting energy will be in joules. Multiplying by 1.0×10^7 gives ergs.

The second term which must be estimated in order to use Equation (2.8.1) is the surface contribution to the indicated free energy difference. As it was advantageous to substitute for L in the calculation of $\Delta(\Delta F_{el})$, this substitution will be useful in the evaluation of $\gamma(A_{sphere} - A_{cylinder})$. Expressing the surface term with the respective areas included shows that

$$\begin{aligned} \Delta\text{Surface} &= \gamma(A_{sphere} - A_{cylinder}) \\ &= \gamma(4\pi R^2 - 2\pi RL) \end{aligned} \qquad (2.8.12)$$

Upon substitution for L

$$\begin{aligned} \Delta\text{Surface} &= \gamma(4\pi R^2 - 2\pi R\, 4R / 3) \\ &= 4\gamma\pi R^2 / 3 \end{aligned} \qquad (2.8.13)$$

Using for the value of γ, 5.2×10^{-15} ergs / Å^2, this expression can be written as,

$$\Delta\text{Surface} = 4\pi\, (5.2 \times 10^5) R^2 / 3 \quad \text{(ergs)} \qquad (2.8.14)$$

where R must be in meters.

Making use of Equations (2.8.11) and (2.8.14) we can now write the more desirable and explicit form of Equation (2.8.1),

$$(\mu_{No}{}^{\theta} - \mu^{\theta} N_o) = \Delta(\Delta F_{el}) + \Delta\text{Surface}$$

$$= \beta\,(2.31 \times 10^{-28} N_o^2 / R\varepsilon)\, Z5 \times 10^7 + 4\pi\,(5.2 \times 10^5) R^2 / 3 \quad \text{(ergs)} \qquad (2.8.15)$$

Using Equation (2.8.15) in Equation (2.7.3), K can be determined. A simple computer program greatly facilitates the calculations. Appendix C shows a Fortran program which evaluates K by first calculating the free energy difference of Equation (2.8.15). With the value of K known, it is easy to determine from Equation (2.7.2) the average aggregation number, ϖ. The calculation of this variable is included in the computer program.

To obtain viscosities, one first substitutes the values of ϖ into Equation (2.3.3) which determines the micellar axial ratio, J. Knowledge of J permits the use of Equations (2.2.4) or (2.2.5) and provides a micellar shape factor, v_c. With an approximation of v_c, Equation (2.3.1), and subsequently the relative viscosity of the micellar solution, can be solved.

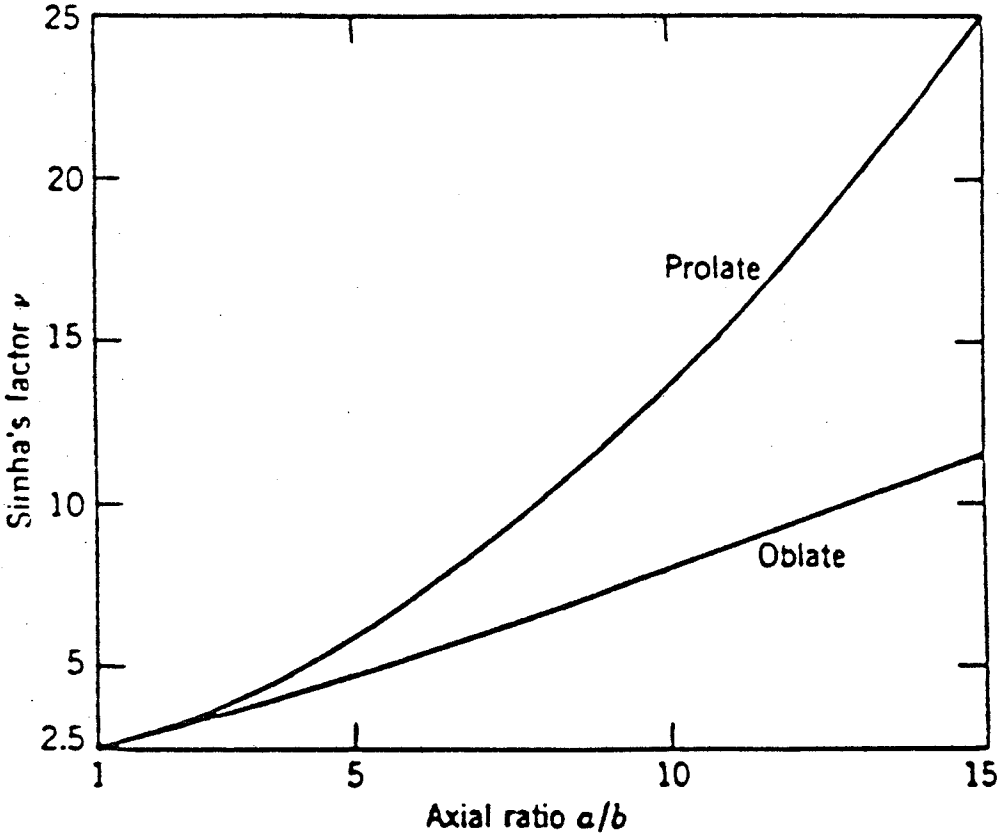

Figure 2.1 Shape Factor as a Function of Axial Ratio

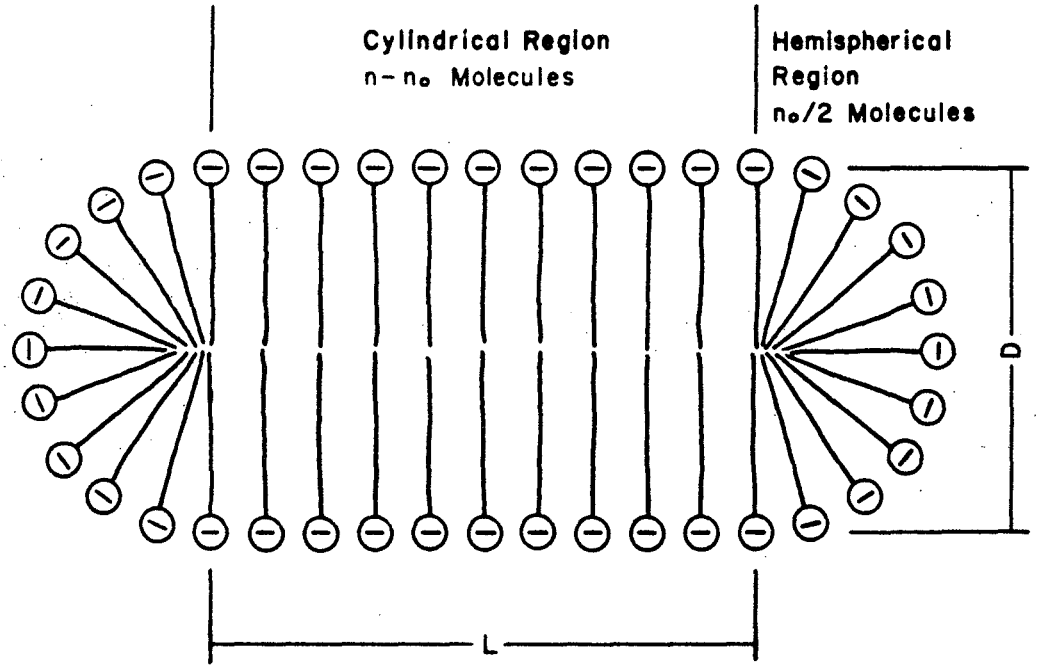

Figure 2.2 Schematic representation of a spherocylindrical micelle with characteristic length, L, and diameter, D.

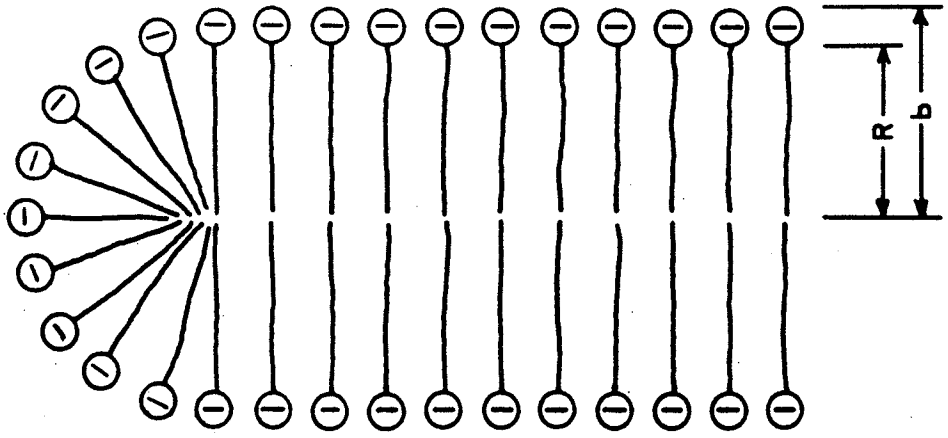

Figure 2.3 Drawing of a rod-like micelle showing the micellar surface radius, R, and the excluded radius, b.

CHAPTER 3

Model Results

3.1 Purpose

The goal of this chapter is to illustrate and analyze numerical values obtained from the theoretical equations given in the previous chapter.

3.2 Clarifications

We desire now to investigate the qualitative and quantitative predictions of the viscosity model which has been developed. Our interest lies in creating rod-like micelles so as to achieve significant viscosities using dilute surfactant solutions rather than polymers. As explained in the introduction, such surfactant solutions may offer several advantages when used as mobility control agents in a chemical flood. The qualitative trends which we observe will help decide which surfactant structure is best suited for achieving our goal. However, before actually considering any theoretical results, two comments are warranted to ensure that the findings will be accurately interpreted.

First, it must be observed that the equation given in the literature and used here for the calculation of surfactant tail length, Equation (2.3.4), includes 1/2 the bond length between the α-carbon atom of a sulfate surfactant tail and the oxygen atom of attachment in the head group. A more general formula for calculating of the micellar core radius has been given by Tartar[1] as

$$R = [\,(n_c - 1)\,1.27 + 2 + w/2\,] \quad \text{Å} \qquad (3.2.1)$$

where

w = the distance bettween the alpha carbon atom of the surfactant tail and the atom in the polar head to which it is bonded

When w takes on the value 1.42 Å, which equals the carbon-oxygen bond length, Tartar's expression yields the same results as Equation (2.3.4). Thus, the equation noted earlier for tail length calculations actually includes an allowance of w/2 or 0.71 Å for the surfactant head group. To calculate the excluded radius of a molecule, one simply adds the effective tail length R to the $\Delta\alpha$-carbon value of that specific surfactant. Hence, for all subsequent calculations of tail length Equation 3.2.1 will be used.

Secondly, it should be understood that the general analysis being considered here addresses dilute surfactant systems. The thermodynamic equations which have been developed are expressly intended for such solutions. For example, it has been noted that when the free energy change given by Equation (2.7.3) is negative, spheres are preferred, aggregation numbers will be small, and hence viscosities should be low. While this contention is maintained to be true, it must be realized that with very high surfactant concentrations, almost any detergent solution can be made viscous. However, it is not the intention of this work to describe such systems, since the levels of surfactant required would be impractical for our goal of achieving high viscosities with low detergent concentrations.

3.3 Qualitative Viscosity Relationships

A formal review of the model is now initiated. The theoretical results from the equations in Chapter 2 will be examined first for qualitative consistency and then for quantitative accuracy. We distinguish between these two tests of the theory in the following manner. The qualitative discussion will address the sign of the free energy difference ($\mu_{No}^{o} - N_o\mu^{o}$). When the sign is negative, spheres and low viscosities should be observed, and when it is positive, rods and high viscosities should be possible. Thus, in a sense, the qualitative test is an examination for failure only. Examining the absolute magnitude of ($\mu_{No}^{o} - N_o\mu^{o}$) leads very naturally to a quantitative review of the theory. In this aspect of the analysis, one seeks to look at predicted aggregation numbers. Are they feasible, too large or too small? The combination of qualitative and quantitative performance tests should underline clearly the strengths and weaknesses of the theory.

a) Viscosity - Effective Tail Length and and Δα-Carbon Distance

The first variables to be examined qualitatively are effective surfactant tail length and Δα-carbon distance. Increasing the micellar surface radius while holding all other parameters constant can be accomplished by extending the length of the surfactant tail. Of course, changes in either R or Δα-carbon will affect other parameters such as N_o, v_o, K, etc. The associated changes in these variables are accounted for in the computer program. We test the effect of varying the hydrocarbon tail length from $n_c = 12$ to $n_c = 16$. This corresponds to a change in R of 16.68 Å to 21.74 Å. For each value of R we increment in steps of 0.5 Å a change in the Δα-carbon distance from 0.71 Å to 3.2 Å. Table 3.3a shows the results of the computer

run. Listed are the surfactant tail volume v_o, surfactant tail length, (equivalently for straight chain molecules this is R), excluded micellar radius b, maximum spherical aggregation number N_o, $\Delta\alpha$-carbon distance, free energy change ($\mu_{No}^o - \mu^o N_o$), K, and aggregation number ϖ. The salt concentration, temperature, and value of the dielectric constant are also indicated.

The trends illustrated in Table 3.3a are interesting. There are several important features to be realized. First, it is instructive to compare values of constant surfactant tail length with an increasing $\Delta\alpha$-carbon distance. Unmistakably, for a given choice of R, a larger $\Delta\alpha$-carbon value is seen to decrease the free energy change ($\mu_{No}^o - \mu^o N_o$). This means that an increased $\Delta\alpha$-carbon distance moves away from the formation of large rod-like aggregates and toward the creation of small sphere-like ones. In fact, it may be recalled that whenever the free energy change is negative, spheres are the preferred aggregate geometry. Therefore, looking at Table 3.3a, one can say that in those cases when $\Delta\alpha$-carbon $\geq$ 3.2 Å, and the effective surfactant tail length is less than 14 carbon atoms, rods will not be the preferred micellar shape.

In this work, we will associate the sulfate head group with a $\Delta\alpha$-carbon distance of 3.2 Å. This differs slightly from the value listed by Stigter[2] of 3.6 Å which was obtained from an interpretation of x-ray data. Accepting then, that 3.2 Å is at least a reasonable approximation of the $\Delta\alpha$-carbon distance in a sulfate molecule, at the temperature and salinity specified in Table 3.3a, rodlike aggregates, and thus high viscosities, would not be expected from sodium dodecyl sulfate solutions. However, for this same value of $\Delta\alpha$-carbon, when the tail length is increased to 14 carbon atoms, the sign of ($\mu_{No}^o - \mu^o N_o$) changes from negative to positive. So we anticipate that for equal molar surfactant concentrations and the conditions of Table

3.3a, a tetradecyl sulfate solution could exhibit viscous behavior while sodium dodecyl sulfate would not.

Futhermore, the positive increase in the free energy difference with longer effective surfactant tail lengths is shown in Table 3.3a to be continuous and this implies that even greater aggregation numbers, and consequently higher viscosities, should be realized with a molecule having a C_{16} tail. It is not possible, though, to make experimental viscosity measurements with hexadecyl sulfate at the conditions of Table 3.3a. This molecule is below its Kraft temperature in a 313 K, 0.8 molar salt solution and therefore it precipitates. Yet, this does not preclude a real comparison because at a higher temperature it is possible to examine the viscosities of equal molar C_{12}, C_{14}, and C_{16} sodium sulfate solutions. The fact that increases in the free energy lead to higher aggregation numbers should, in the limit of surfactant solubility, reveal the maximun micellar size for a particular surfactant at specified conditions of temperature and salinity. As ϖ increases, it must eventually approach a value where micelles become so large they become visible to the naked eye. This, of course, characterizes the precipitation point.

Table 3.2b shows the output of a second computer run with the temperature raised to 333 K and the salt concentration kept at 0.80 molar. The data now shows that for $\Delta\alpha$-carbon values $\geq$ 3.2 Å, C_{12} and C_{14} molecules will prefer a spherical aggregate, while it is possible for a surfactant with a C_{16} tail to form rod-like micelles. Therefore, at the conditions of Table 3.3b, sodium dodecyl and tetradecyl sulfate solutions should not yield high viscosities, unlike sodium hexadecyl which has the potential to be viscous.

Having studied and isolated the effect of increasing efffective surfactant tail length, it is now progressive to look more closely at the relationship between $\Delta\alpha$-

carbon and (μ_{No}^{o} - $\mu^{o}N_{o}$). Table 3.3a shows a clear trend: for a given value of R, as $\Delta\alpha$-carbon is increased, (μ_{No}^{o} - $\mu^{o}N_{o}$) is decreased. For all values of R the effect is profound but it becomes particularly important at shorter tail lengths. Looking at R = 16.68 Å which corresponds to a C_{12} surfactant tail length, the free energy difference becomes negative when the $\Delta\alpha$-carbon distance has reached 3.2 Å. Yet, for the same value of R, if the $\Delta\alpha$-carbon distance is 1.7Å the free energy difference is clearly positive. The ammonium chloride head group is reported to have a $\Delta\alpha$-carbon distance of 1.8 Å, or about 1/2 the value of the sulfate head group.[2] Thus, Table 3.3a implies that equal molar solutions of dodecyl ammonium chloride and sodium dodecyl sulfate will be very different in character. The former should have a preferred rod-like micellar geometry and be viscous, while the latter should form spherical aggregates and not show any appreciable viscosity. Experimentally, it is not possible to compare SDS and DAC at the conditions of Table 3.3a because at 313 K, the latter precipitates at salinities well below 0.8 M. It is possible, however, to lower the salt concentration to 0.35 M and make a comparison. The theoretical results are illustrated in Table 3.3c, and as expected, the smaller $\Delta\alpha$-carbon distance of DAC allows this molecule to form rod-like micelles, while SDS aggregates are notably spherical.

To summarize the findings of the model thus far, we find the following statements can be made:

1) Increasing surfactant tail length should increase viscosity. A comparison of sodium dodecyl, tetradecyl and hexadecyl sulfate can provide an experimental check.

2) Increasing the Δα-carbon distance should decrease viscosity. Dodecyl ammonium chloride, sodium dodecyl sulfonate and sodium dodecyl sulfate can be compared.

b) Viscosity-Surfactant Tail Volume and Tail Branching

We seek here to see the effect of increased surfactant tail volume. It must remembered that increased tail volume does not necessarily mean increased tail branching. Branching is a seperate matter, and is really just another case of changing the effective surfactant tail length. Increased branching moves the head group further down the tail, and thus, decreases the effective tail length. Having already determined that there is a direct relationship between tail length and viscosity, it follows that the model predicts increased tail-branching should result in lower viscosities.

The most dramatic example of a difference in tail volumes exists between a single-tailed molecule and its analogous twin tailed species. Hexadecyldimethylammonium acetate and dihexadecyldimethylammonium acetate are examples of molecules which illustrate such a difference. The theoretical effect of doubling the surfactant tail volume can be easily examined. Table 3.3d shows a computer run for the prescribed conditions of salt and temperature with single-tailed surfactants. The conditions of Table 3.3d, very low salinity and low detergent concentration, force all micelles to be spherical. The fact that larger Δα-carbon values permit the formation of slightly larger spherical micelles in no way represents a departure from the observation that an increase in this variable moves away from the formation of rod-like aggregates. It is expected that molecules with larger Δα-carbon values will sustain a spherical shape beyond that of molecules with smaller Δα-

carbon distances. In fact, the ability to accomodate more molecules in the spherical state is precisely why surfactants with large $\Delta\alpha$-carbon values do not form rod-like micelles as capably as those with smaller values of this parameter. Table 3.3e shows for the same conditions as Table 3.3d, the result of doubling the surfactant tail volume. Comparison of the outputs indicates that with twin-tailed surfactants, there is a substantial positive increase in the magnitude of the free energy difference (μ_{No}^{o} - $\mu^{o}N_{o}$). The small negative numbers characteristic of the single-tailed surfactants in Table 3.3d are notably replaced with large positive values when the tail volume has been doubled. Theoretically then, an increased surfactant tail volume is assured of causing a movement toward larger rod-like micelles and consequently higher viscosities. We summarize the results of this section as follows:

1) Increased tail branching decreases the effective surfactant tail length and therefore should lead to lower viscosities.
2) Increased surfactant tail volume is seen to increase the preference for rod-like micelle formation and thus should promote higher viscosities.

c) Temperature and Salt Effects

A qualitative look at the influence of temperature and salt is straight forward. Considering the data of Table 3.3a, one may run the same inputs with the exception of raising the salinity to 1.1 M concentration. The results of these computer calculations are listed in Table 3.3f. It can be immediately noticed that all values of (μ_{No}^{o} - $N_{o}\mu^{o}$) have increased positively at this higher salinity. The most important transition appears to be that, in this particular case, even a molecule with a C_{12} tail and a $\Delta\alpha$-carbon value of 3.2 Å is capable of forming rods. Thus, unlike the

preferred spherical micelles which $C_{12}SO_4Na$ should form at the conditions of Table 3.3a, rods are possible and viscous behavior may be observed with this surfactant at the salinity of Table 3.3f.

In a similar fashion, the data of Table 3.3a may be compared with that of Table 3.3b which shows the effect of increasing the temperature from 313 K to 333 K. Greater temperatures are clearly unfavorable toward the formation of rod-like micelles. The significant decrease in values of (μ_{No}^o - $N_o\mu^o$) at 333 K illustrates this relationship.

Summarizing the observed relations between temperature, salt, and free energy change indicates that

a) Increased salt concentrations favor the formation of rod-like micelles. This should increase viscosities.

b) Temperature increases favor the formation of spherical aggregates. The result should be a decrease in viscosity.

d) Ethylene Oxide Addition

The model does not specifically lend consideration to the addition of ethylene oxide units. However, if we assume that the addition of (EO) groups increases the effective $\Delta\alpha$-carbon length, then, based on earlier results it would be anticipated that increased number of EO groups will cause a decrease in viscosity and an improvement in phase stability. This prediciton may easily be examined by comparing three surfactants with different (EO) numbers.

3.4 Quantitative Predictions

If the absolute magnitude of the free energy calculation (μ_{No}^{o} - $N_o\mu^o$) is correct, it should be possible to find a correlation between predicted aggregation numbers and viscosities. Looking again at Tables (3.3a - 3.3f) with emphasis this time on ϖ, reveals that the general trends estabilished qualitatively remain intact. Aggregation number, like the free energy difference, increases with any of the following: increased effective tail length, decreased $\Delta\alpha$-carbon distance, increased surfactant tail volume, increased salinity, and/or decreased temperature. However, the specific values of ϖ are questionable and in most cases are not practical. The predicted aggregation numbers are too small when $\Delta\alpha$-carbon is large and are too large for smaller values of this parameter. In general, ϖ appears to be disproportionately sensitive to the value of $\Delta\alpha$-carbon.

It is implied here that perhaps an alternative description of the excluded micellar radius is needed. The definition of $\Delta\alpha$-carbon dictates that this parameter is a constant, however, the meaning which is given to $\Delta\alpha$-carbon here may necessitate a functional dependence on other variables such as temperature, salinity, and even aggregate geometry. In other words, if $\Delta\alpha$-carbon is to give a measure of the distance of closest approach between counter ions and the micellar surface, thereby determining the excluded micellar radius, it is probably incorrect to assume that this parameter is a constant with respect to changes in temperature, salinity, or aggregate shape. Given a more accurate relationship between excluded micellar radius and aggregation number, one that is consistent with the observed qualitative trends, a more complete picture of viscosity and surfactant structure would be possible.

It is possible, however, to select at least one instance a case where the predicted aggregation number seems to be reasonable. Referring again to Table 3.3a,

the predicted value of ϖ for a C_{16} surfactant with an alpha carbon distance of 3.2 Å is shown to be 18,800. This number being reasonable, one could calculate the number of rods in solution and the length of one rod-like micelle. Solving the following equation for the length of a rod, L,

$$\varpi v_o = \pi R^2 L \qquad (3.4.1)$$

shows that L equals approximately 5851 Å or about 0.585 μ.

3.5 Design Implications

Having considered the theoretical implications of the model in some detail, it is possible to now combine all the individual trends and characterize an "ideal" surfactant. We begin by considering the "ideal" head group. The theory shows that high viscosities are consistent with small Δα-carbon values. We anticipate, however, that phase transitions which are not explicitly predicted by the theory must also be taken into consideration. For instance, we know from experimentation that carboxylates having a very small Δα-carbon distance are salt sensitive and precipitate easily. We therefore choose a small Δα-carbon distance, but one somewhat larger than that of a carboxylate. A sulfonate head group seems a good choice. Its Δα-carbon value of 2.4 Å is much less than that of a sulfate, but not as small as that of a carboxylate where Δα-carbon equals 2.1 Å. Of course, cationic head groups are precluded from consideration apriori since they would experience unacceptable adsorption.

With respect to surfactant tail length, the theory indicates that long-tailed molecules experience a significantly greater tendency toward the formation of rod-like

micelles than do shorter tail lengths. However, one may not use tail lengths of arbitrary length, because as the number of methylene groups increases, so does insolubility. In addition, the choice of hydrophobic tail length must be made with consideration of the head group structure. That is, once a $\Delta\alpha$-carbon distance is selected, the maxium acceptable tail length is restricted by the solubility properties of the head group. In this respect, a sulfonate head group again appears optimum since it permits one to work with surfactant tail lengths of 18 carbon atoms. Head group configurations with smaller $\Delta\alpha$-carbon values would not be compatible with such long tail lengths. The strong relationship that is theoretically observed between surfactant tail length and aggregation number suggests that a long tail length is a necessary characteristic of a molecule exhibiting viscous behavior at dilute concentrations. Hence we imagine that 18 carbon atoms in the surfactant tail may be an optimum choice.

Thus far, it has been reasoned that the ideal surfactant molecule should have a sulfonate head group and a long, 18 carbon atom, tail length. Yet, there is reason to expect some difficulty with this arrangement since very long surfactant tail lengths are known to be salt sensitive. The obvious solution is to reduce the tail length, but this is not desirable given the relationship between tail length and aggregate size. It becomes clear that we must slightly reduce the surfactant tail length in a manner not adverse to the molecule's aggregation properties. Working from the theory, it is known that increases in surfactant tail volume are beneficial toward the formation of extended structures. Thus, one possible solution might be to place a "kink", or bend, in the surfactant tail. This would serve to reduce the effective surfactant tail length, and therefore, enhance phase stability while simultaneously mitigating the adverse viscosity effects of a shortened tail length by increasing the tail volume. In

consideration of all this, one approach might be insertion of a carbon-carbon double bond within the surfactant tail. These bonds are characterized by a smaller bond angle and have less freedom of movement than single bonds. If placed in the tail, they should act as "kinks", increasing the effective surfactant tail volume by introducing curvature to what was a straight-chained arrangement, while marginally decreasing the surfactant tail length since a curved tail containing an equal number of atoms as a straight tail must be effectively shorter. The result should be increased phase stability, with no loss and possibly a gain in viscosiy.

The precise balance of tail length to tail volume which will provide the highest viscosities, and yet maintain acceptable phase behavior, can not be exactly predicted since the theory does not yield quantitative answers. Qualitatively though, a double bond placed at the middle of the surfactant tail would seem to be a good choice, both maximizing the increase of tail volume and the proportionate decrease in tail length. In summary then, taking together all the predictions of the theory and the previous discussion, one molecule which satisifies the optimum conditions is oleyl sulfonate. This molecule has an 18 carbon atom tail length, a double bond in the middle, and a sulfonate head group. The experimental studies of Chapter 4 will reveal if this structure does indeed have an optimum behavior ,and if it does, whether or not such a molecule can be used for mobility control purposes.

Table 3.3a

Computer Calculations for 313 K and 0.8 M Salt

Surfactant concentration is 0.035 Molar

Assumed value of cmc is 0.002 Molar

Salt Concentration 0.8 Molar

Temperature is 313 K

Dielectric Constant is 73.19

v_o Å^3	R Å	b Å	N_o	Δα-carbon Å	$(\mu_{No}^o - N_o\mu^o)$ ergs	K	ϖ
350	16.7	17.2	60.7	1.2	3.82E-12	2.55E+39	7.79E+17
		17.7	66.1	1.7	3.05E-12	4.88E+30	1.08E+14
		18.2	71.9	2.2	2.09E-12	1.11E+21	1.63E+09
		18.7	78.0	2.7	9.07E-13	1.33E+09	1.86E+03
		19.2	84.4	3.2	negative	3.29E -05	8.44E+01
404	19.2	19.7	79.4	1.2	5.16E-12	7.91E+51	4.34E+24
		20.2	85.6	1.7	4.26E-12	6.58E+42	1.25E+20
		20.7	92.1	2.2	3.15E-12	5.18E+31	3.51E+14
		21.2	98.9	2.7	1.82E-12	1.80E+18	6.55E+07
		21.7	106.1	3.2	2.06E-13	1.18E+02	1.07E+02
458	21.7	22.2	100.7	1.2	6.70E-12	2.55E+67	2.46E+32
		22.7	107.6	1.7	5.66E-12	7.30E+56	1.32E+27
		23.2	114.9	2.2	4.39E-12	1.55E+44	6.08E+20
		23.7	122.4	2.7	2.89E-12	1.19E+29	1.68E+13
		24.2	130.3	3.2	1.11E-12	1.47E+11	1.88E+04

Table 3.3b

Computer Calculations for 333 K and 0.8 M Salt

Surfactant concentration is 0.035 Molar

Assumed value of cmc is 0.002 Molar

Salt Concentration 0.8 Molar

Temperature is 333 K

Dielectric Constant is 66.80

v_o Å^3	R Å	b Å	N_o	Δα-carbon Å	$(\mu_{No}^o - N_o\mu^o)$ ergs	K	ϖ
350	16.7	17.2	60.7	1.2	3.53E-12	2.56E+33	2.47E+15
		17.7	66.1	1.7	2.68E-12	2.15E+25	2.26E+11
		18.2	71.9	2.2	1.61E-12	1.81E+15	2.07E+06
		18.7	78.0	2.7	2.98E-13	6.49E+02	7.92E+01
		19.2	84.4	3.2	negative	3.81E -13	8.44E+01
404	19.2	19.7	79.4	1.2	4.80E-12	2.11E+45	2.24E+21
		20.2	85.6	1.7	3.79E-12	6.78E+35	4.02E+16
		20.7	92.1	2.2	2.57E-12	1.72E+24	6.40E+10
		21.2	98.9	2.7	1.08E-12	1.57E+10	6.21E+03
		21.7	106.1	3.2	negative	2.11E -07	1.06E+02
458	21.7	22.2	100.7	1.2	6.24E-12	1.11E+59	1.62E+28
		22.7	107.6	1.7	5.08E-12	1.17E+48	5.04E+22
		23.2	114.9	2.2	3.68E-12	6.35E+34	1.23E+16
		23.7	122.4	2.7	2.06E-12	1.10E+19	1.68E+08
		24.2	130.3	3.2	4.05E-14	2.42E+00	1.30E+02

Table 3.3c

Computer Calculations for 313 K and 0.35 M Salt

Surfactant concentration is 0.035 Molar

Assumed value of cmc is 0.002 Molar

Salt Concentration 0.35 Molar

Temperature is 313 K

Dielectric Constant is 73.19

v_o Å^3	R Å	b Å	N_o	Δα-carbon Å	$(\mu_{No}^o - N_o\mu^o)$ ergs	K	ϖ
350	16.7	17.2	60.7	1.2	2.77E-12	6.44E+27	3.91E+12
		17.7	66.1	1.7	1.80E-12	1.24E+18	5.43E+07
		18.2	71.9	2.2	6.13E-13	1.46E+06	1.31E+02
		18.7	78.0	2.7	negative	4.34E -09	7.79E+01
		19.2	84.4	3.2	negative	1.18E -25	8.44E+01
404	19.2	19.7	79.4	1.2	3.81E-12	1.85E+38	6.66E+17
		20.2	85.6	1.7	2.68E-12	8.82E+26	1.45E+12
		20.7	92.1	2.2	1.33E-12	2.08E+13	2.22E+05
		21.2	98.9	2.7	negative	1.06E -02	9.89E+01
		21.7	106.1	3.2	negative	4.66E -22	1.06E+02
458	21.7	22.2	100.7	1.2	5.01E-12	2.42E+50	7.59E+23
		22.7	107.6	1.7	3.72E-12	2.30E+37	2.32E+17
		23.2	114.9	2.2	2.18E-12	8.30E+21	4.44E+09
		23.7	122.4	2.7	3.72E-13	5.46E+03	1.26E+02
		24.2	130.3	3.2	negative	2.74E -18	1.30E+02

Table 3.3d

Computer Calculations for 308 K and 0.005 M Salt

Surfactant concentration is 0.018 Molar

Assumed value of cmc is 0.002 Molar

Salt Concentration 0.005 Molar

Temperature is 308 K

Dielectric Constant is 73.19

v_o Å^3	R Å	b Å	N_o	Δα-carbon Å	$(\mu_{No}^o - N_o\mu^o)$ ergs	K	ϖ
350	16.7	17.2	60.7	1.2	negative	≈ 0	6.07E+01
		17.7	66.1	1.7	negative	≈ 0	6.61E+01
		18.2	71.9	2.2	negative	≈ 0	7.19E+01
		18.7	78.0	2.7	negative	≈ 0	7.80E+01
		19.2	84.4	3.2	negative	≈ 0	8.44E+01
404	19.2	19.7	79.4	1.2	negative	≈ 0	7.94E+01
		20.2	85.6	1.7	negative	≈ 0	8.56E+01
		20.7	92.1	2.2	negative	≈ 0	9.21E+01
		21.2	98.9	2.7	negative	≈ 0	9.89E+01
		21.7	106.1	3.2	negative	≈ 0	1.06E+02
458	21.7	22.2	100.7	1.2	negative	≈ 0	1.01E+02
		22.7	107.6	1.7	negative	≈ 0	1.08E+02
		23.2	114.9	2.2	negative	≈ 0	1.15E+02
		23.7	122.4	2.7	negative	≈ 0	1.22E+02
		24.2	130.3	3.2	negative	≈ 0	1.30E+02

Table 3.3e

Computer Calculations for 308 K and 0.005 M Salt

with the Surfactant Tail Volume Doubled

Surfactant concentration is 0.018 Molar

Assumed value of cmc is 0.002 Molar

Salt Concentration 0.005 Molar

Temperature is 308 K

Dielectric Constant is 73.19

v_o Å^3	R Å	b Å	N_o	Δα-carbon Å	$(\mu_{No}^o - N_o\mu^o)$ ergs	K	ϖ
700	16.7	17.2	30.3	1.2	3.01E-12	6.12E+30	8.78E+13
		17.7	33.1	1.7	2.37E-12	1.82E+24	4.79E+10
		18.2	35.9	2.2	1.63E-12	4.04E+16	7.13E+06
		18.7	39.0	2.7	7.50E-13	4.61E+07	2.80E+02
		19.2	42.2	3.2	negative	1.82E -02	4.22E+01
808	19.2	19.7	39.7	1.2	4.05E-12	2.17E+41	1.65E+19
		20.2	42.8	1.7	3.31E-12	6.56E+33	2.88E+15
		20.7	46.1	2.2	2.46E-12	1.40E+25	1.33E+11
		21.2	49.5	2.7	1.49E-12	1.53E+15	1.39E+06
		21.7	53.1	3.2	3.69E-13	5.94E+03	5.58E+01
916	21.7	22.2	50.3	1.2	5.24E-12	3.21E+53	2.01E+25
		22.7	54.0	1.7	4.40E-12	9.34E+44	1.09E+21
		23.2	57.4	2.2	3.45E-12	1.82E+35	1.52E+16
		23.7	61.2	2.7	2.37E-12	1.76E+24	4.71E+10
		24.2	65.2	3.2	1.15E-12	6.08E+11	2.78E+04

Table 3.3f

Computer Calculations for 313 K and 1.1 M Salt

Surfactant concentration is 0.035 Molar

Assumed value of cmc is 0.002 Molar

Salt Concentration 1.1 Molar

Temperature is 313 K

Dielectric Constant is 73.19

v_o Å^3	R Å	b Å	N_o	Δα-carbon Å	$(\mu_{No}^o - N_o\mu^o)$ ergs	K	ϖ
350	16.7	17.2	60.7	1.2	4.12E-12	2.67E+41	2.52E+19
		17.7	66.1	1.7	3.41E-12	1.94E+34	6.79E+15
		18.2	71.9	2.2	2.52E-12	2.04E+25	2.22E+11
		18.7	78.0	2.7	1.41E-12	1.40E+14	5.76E+05
		19.2	84.4	3.2	4.00E-14	2.53E+00	8.44E+01
404	19.2	19.7	79.4	1.2	5.55E-12	5.93E+55	3.75E+26
		20.2	85.6	1.7	4.71E-12	2.20E+47	2.23E+22
		20.7	92.1	2.2	3.68E-12	9.37E+36	1.49E+17
		21.2	98.9	2.7	2.42E-12	2.17E+24	7.18E+10
		21.7	106.1	3.2	9.02E-13	1.18E+09	1.78E+03
458	21.7	22.2	100.7	1.2	7.19E-12	1.73E+72	6.41E+34
		22.7	107.6	1.7	6.21E-12	2.60E+62	7.86E+29
		23.2	114.9	2.2	5.03E-12	3.50E+50	9.12E+23
		23.7	122.4	2.7	3.61E-12	2.07E+36	7.02E+16
		24.2	130.3	3.2	1.93E-12	2.47E+19	2.42E+08

CHAPTER 4

Experimental

4.1 Purpose

This chapter will provide an experimental check of the theoretical trends indicated in Chapter 3. It will also provide the tests necessary to determine the net feasibility of using surfactants for mobility control.

4.2 Introduction

The first experimental objective of this work was to make measurements of viscosity and determine whether or not the theoretical predictions given by the equations in Chapter 2 could be supported. The results from these tests, even if they did not completely agree with theory, would still provide a framework from which one could design an "ideal" surfactant molecule for mobility control purposes. This leads quite naturally to the second experimental objective, which was to determine the feasibility of using an "ideal" surfactant as a mobility control agent.

It must be realized that there is an important limiting distinction betweeen the principal aims of these two different experimental goals. The first seeks essentially to determine the relationship between viscosity and the following variables:

a) surfactant tail length (l_c)

b) distance between the surfactant alpha carbon atom and the center of the head group charge ($\Delta\alpha$-carbon)

c) surfactant tail volume (v_o)

d) position of tail branching

e) temperature of solution

f) salinity of solution

g) number of ethylene oxide groups (EO)$_x$

These test results may be compared directly with the predictions of Chapter 3. Since in this study we are only interested in general trends, all classes of surfactants, (i.e. nonionics, anionics, and cationics), can be considered as acceptable molecules for these experiments.

This is not the case for the second experiment. Here, one must work from the results of the first analysis and look more practically at the problem. This implies the that one consider a more restricted group of molecules. For example, the strong adsorption of positively charged molecules on negatively charged reservoir surfaces precludes the use of any cationic surfactant as a viable mobility control agent. Thus, while cationic molecules may be used to establish trends, they would not be considered as acceptable candidates in the feasibility study.

4.3 Considerations for Success

The considerations for success in the first analysis may be judged as to how well the theory predicts the observed viscosity trends. Although quantitative comparisons are desired in this regard, even a qualitatively exact theory would be of value and so experimental results will be compared with theory for qualatative purposes.

Considering the feasibility study, one may recall that the conditions for success were mentioned in the introductory chapter where it was noted that one must demand the following from an "ideal" surfactant :

a) high viscosities at dilute concentrations
(approximately 40 cp at 0.5 wt. %)

b) phase stability in temperature salinity space
(large 1Ø working region)

c) indifference to oil
(maintenance of viscosity in the presence of hydrocarbon)

A surfactant molecule which can accommodate the requirements listed above may be viewed as an acceptable candidate for use as a mobility control agent in a surfactant-micellar flood. Experimentation is performed which tests these necessities.

4.4 Chemicals

Surfactants were obtained from a variety of sources and companies. Appendix A lists all the molecules which were important in the analysis of this work. It also illustrates the respective manufacturers of these chemicals. Some of the detergents used were synthesized in our laboratory at UT - Austin, and as indicated in the Appendix, they are denoted by a UT source code.

All surfactants, with the exception of oleyl sulfonate, were at least 99% pure isomeric compounds. While it is true that the column separation technique employed here to make oleyl sulfonate is not an exact method, it is also known that any reasonable procedure for isolating such double bonded molecules will not yield purities as high as those realized with simpler compounds. The difficulty arises because one can not be certain that the position of the double bond is consistent. While on the average, the location of the double bond may be at the desired carbon number, there will undoubtedly be some molecules present with double bonds at other positions. Thus, the oleyl sulfonate compound may be assumed less than 99%

pure, and although an exact measurement of this molecule's purity was not conducted, melting point and phase behavior studies indicate a relatively isomeric compound.

Appendix B shows drawings of the various surfactant structures. It serves as an illustrative tool for discussion purposes. The geometries are not drawn to scale nor do the bond angles represent exact configurations, however, the salient features of head group location and structure are exhibited.

4.5 Phase Behavior

For all surfactants, it was determined that a first priority should be the evaluation of a phase boundary in temperature-salinity space. The phase curve in many ways serves as a template for the design of all other surfactant experiments. It enables one to decide which molecules can be compared to determine the effect on viscosity which results from differences in the various surfactant structual features. These tests need to be conducted at constant temperatures and salinities in order to isolate the molecular variable of interest. For such experiments, it is important to ensure that both surfactants are in a one phase region during the comparison; the phase curve provides this information. In addition, it shows which surfactants do not have a reasonable 1Ø region over practical temperatures and salinities, and as a result, they would not uphold an essential requirement for field use as a mobility control agent.

The phase study begins with the preparation of surfactant solutions. For each surfactant, a stock solution of 5 g/dl was made. Using a Mettler H80 balance ± 0.00005 g, 1.25 g of surfactant was weighed and transferred to a Kimax flask to

which distilled water was then added until a total volume of 25 ml was recorded. A similar procedure was used to make stock solutions of NaCl.

Sample preparations of various concentrations were made by the addition of these stock solutions, and when necessary, distilled water. The various volumes were collected using a Corex 2ml pipette ± 0.005 ml and then transferred to 5 ml Corning disposable pipettes. Stock solutions were heated to approximately 70° C in order to ensure complete dissolution of surfactant before transfer. The pipettes were sealed at the open end by an oxygen torch and placed in a 90° C Forma Scientific model 2564 shaker bath ± 0.2° C.

Phase studies were conducted by visual observation. The pipettes were shaken vigorously by hand and allowed to rest for not less than three days in the shaker bath. Visual inspection was then made to determine if cloudiness, precipitation, or liquid crystal formation had occurred. The presence of liquid crystals was determined by noting the birefringence of plane polarized light. After such observation, the temperature of the bath was reduced, allowed to equilibrate for one day, and then the foregoing procedure was repeated until the phase curve was obtained.

Figure 4.1 shows an example of a completed phase diagram. Plotted there are the transition boundaries from one to two phases for sodium dodecyl, tetradecyl, and hexadecyl sulfate, respectively. Points which lie to the right or below a given phase curve denote a 1Ø region while all points which lie above or to the left indicate a 2Ø region. Similar plots have been determined for a number of other surfactants and these are illustrated in Figures 4.2 to 4.7. The significance of the various phase diagrams is explained in the discussion section, of Chapter 5.

For non-ionic surfactants, it was impractical to construct a phase diagram using the same procedure which delineated transition boundaries for ionic surfactants. The primary reason for this is the indifference of most non-ionics to the presence of salt. Over the salinities of interest here, and in fact even over much larger salt concentrations, salt has a negligible effect on non-ionic phase behavior. Non-ionics do, however, exhibit a marked phase behavior dependence on temperature. As the temperature of these molecules is increased, they all show movement toward the formation of a cloudy solution. If the temperature is increased enough, surfactant will precipitate from solution. This results in the formation of a two-phase system. The temperature at which a solution of a given non-ionic shows cloudiness is generally referred to as that molecules colud point temperature. This temperature is a complicated function of surfactant structure, although some general trends have been noted.[1] For the purpose of this work, it is only necessary to note the respective cloud points of the molecules used for experiments. Table 4.1 shows a list of the non-ionics used in this work and their respective cloud point temperatures.

4.6 The Viscometer

All viscosities reported in this work were obtained from measurements with a Contraves Low Shear 30 viscometer. The Contraves is a Covette-Hatschek type viscometer in which the inner cylinder is stationary and the outer cylinder rotates with a constant, but adjustable, speed ω.[2] Figure 4.8 shows the velocity profile of the fluid between the two cylinders as it would appear if one were looking down the axis of rotation.

The data obtained from the Contraves is viscosity as a function of shear rate. For non-newtonian fluids, this is of course, an apparent viscosity. The

viscosity is calculated from the shear stress which is obtained from the torque required to keep the inner cylinder from rotating. The rotational force arises from the frictional drag of the moving fluid between cylinders.

The defining equation of interest for the Contraves is Newton's law which relates the shear stress to the rate of shear. Newton's law may be expressed as

$$\tau = \mu \omega \qquad (4.6.1)$$

where

τ = shear stress

μ = viscosity

ω = shear rate

4.7 Experimentation

1) Structural Relationships

Viscosity studies were performed to accomplish the objectives outlined at the begining of this Chapter. Consistent with the first goal, experiments were designed which would illustrate the relationship between viscosity, the various surfactant strucual parameters, solution salinity, and solution temperature. Table 4.2 provides a summary of the surfactant structural variables which were tested and the corresponding molecules employed in those evaluations. It should be noted that the choice of these molecules for the indicated studies was not random. Except for the variable of interest, experiments were needed which would compare nearly identical molecules. This, and the uniqueness of surfactant phase behavior, placed a constraint on the selection of molecules for viscosity tests. All experiments designed here had to

work within these considerations. The results from the experiments listed in Table 4.2 are plotted in Figures 4.9 to 4.15, respectively. Figure 4.16 illustrates the relationship between (EO) addition and solution viscosity. A complete discussion of these results is reserved until Chapter 5, where these experiments are compared with the predictions given in Chapter 3.

2) Ideal Relationships

The second experimental goal was to test the practicality of using surfactants for mobility control. This is the feasibility study mentioned at the beginning of this Chapter. Tests were conducted to evaluate if one "ideal" sufactant molecule, namely oleyl sulfonate, could indeed function as a mobility control agent. The anlaysis consisted of the following:

a) a viscosity scan over surfactant concentration at constant temperature and salinity

b) a phase behavior study in temperature salinity space (noted previously in Figure 4.4)

c) a viscosity scan in the presence of increasing oil

The effect of surfactant concentration on viscosity is defined in Figures 4.17 and 4.18 which together show viscosity as a function of shear rate for five different surfactant molarities. Figure 4.19 shows for two constant shear rates the relation between surfactant concentration and viscosity. The non-newtonian character of the viscosity plots made it interesting to graph the break point shear rate (i.e. that shear rate at which the viscosity breaks toward lower values) against surfactant concentration. This information is shown in Figure 4.20 which plots break point shear rate vs. concentration. The oleyl sulfonate oil test, (Experiment c), examined the effect of n-

decane addition on solution viscosity. Five 3 ml samples of 0.5 wt% (0.0141 Molar) surfactant and 2% (0.345 Molar) NaCl were prepared. In these, between 0 and 40 ml of n-decane was added in increments of 10 ml. Viscosity measurements of the resulting mixtures were made at 49° C and the results recorded on a plot of grams of added decane/grams of surfactant vs. viscosity as noted in Figure 4.21.

Because oil solubility is a function of many variables, it was reasoned that one must consider an optimum salinity in order to gain better insight into the implications of Figure 4.21. One needs to look at many oils and at significantly higher oil concentrations to determine the range of oil solubilities, thereby developing a more complete picture of the viscosity-oil relationship.

This gave impetus to perform a similar, but more extensive, oil experiment which considered the effect of adding various oils to viscous sodium hexadecyl sulfate solutions. In this study, seven 3 ml solutions of 0.035 M sodium hexadecyl sulfate and 0.80 M NaCl were made. To each of these, 2 ml of one of the following oils was added: n-heptane, n-octane, n-nonane, n-decane, undecane, dodecane or tetradecane. Adding 2 ml of oil ensured that there would be an excess oil phase present. After shaking vigorously, these surfactant mixtures were allowed to equilibrate for seven days in a 60° C oil bath. In all tubes, a gel-like phase appeared between an upper oil-rich phase and a lower aqueous-rich phase.

The gel-like phase varied in volume as one would expect since surfactant partioning between oil and water is a function of oil chain length or ACN number.[3] In the n-heptane and tetradecane mixtures, it occupied more than half the total solution volume and the oil-rich phase seemed almost absent. The primary phase of interest in this work is the aqueous or lower one since it would presumably represent the mobility control phase. Hence, this phase was extracted by means of a 10 cc syringe

and its viscosity was measured at the equilibrium temperature, 60° C. The viscosities were all approximately the same, and so to preserve readability in presenting the results, only three of the seven viscosity measurements are plotted in Figure 4.22. Including the remaining four viscosities would not offer any new information. As with all other experiments, an interpretation of the results is made in the next chapter.

4.8 Difficulties

During the collection of data several problems were encountered. Comments about them are given to provide for a critical evaluation of the techniques employed, and to present this material more coherently.

The exact phase analysis of diamylsodiumsulphosuccinate was complicated by the criteria used to determine phase separation. This surfactant showed slightly cloudy behavior even as a stock liquid. The cloudiness prevailed in solution but was noticeably enhanced at points which were regarded as evidence of a phase transition. The initial cloudiness may have been the result of impurities. The same problem was observed with alkyl benzene compounds, and therefore, it is was difficult to determine exact phase boundaries for these molecules. All other surfactants produced very clear solutions and even small deviations from this character were considered as a move toward the formation of extended structures or precipitation. Even with this procedure, it was occasionally difficult to decide when a particular solution was cloudy enough to warrant the determination of a phase transition.

Viscosity values obtained with the Contraves 30 were recorded about every 20 seconds unless an obvious fluctuation of the output was noticed. At high concentrations (high viscosities), the Contraves had a tendency to show variation of output with time. This was particularly true at moderate shears. In these cases, a

visual average was recorded. The readings at lower concentrations were generally more stable. Special care was needed to prevent the trapping of air bubbles in solution before, or during, transfer of the samples to the measuring cup. When a few bubbles were observed, they were removed with a capillary tube. Observation of many air bubbles resulted in discarding the sample and begining a new experiment.

TABLE 4.1

Non-Ionic Cloud Point Temperatures

Surfactant	Cloud Point Temperature
nonylphenol-$(EO)_8$ (CO-610)	26 ° C
nonylphenol-$(EO)_{10}$ (CO-660)	63 ° C
nonylphenol-$(EO)_{12}$ (CO-720)	81 ° C

TABLE 4.2

Structural Parameters and Surfactants

Structural Parameter Examined	Molecules Used
surfactant tail length (R)	sodium dodecyl sulfate
	sodium tetradecyl sulfate
	sodium hexadecyl sulfate
surfactant alpha carbon distance ($\Delta\alpha$-carbon)	sodium dodecyl sulfate
	dodecylammonium chloride
	sodium dodecyl sulfonate
surfactant tail volume (v_o)	hexadecyldimethylammonium acetate
	dihexadecyldimethylammonium acetate
	$1\text{Ø}C_{12}$ sulfonate
	$6\text{Ø}C_{16}$ sulfonate
ethylene oxide addition $(EO)_x$	CO-660
	CO-710
	CO-720

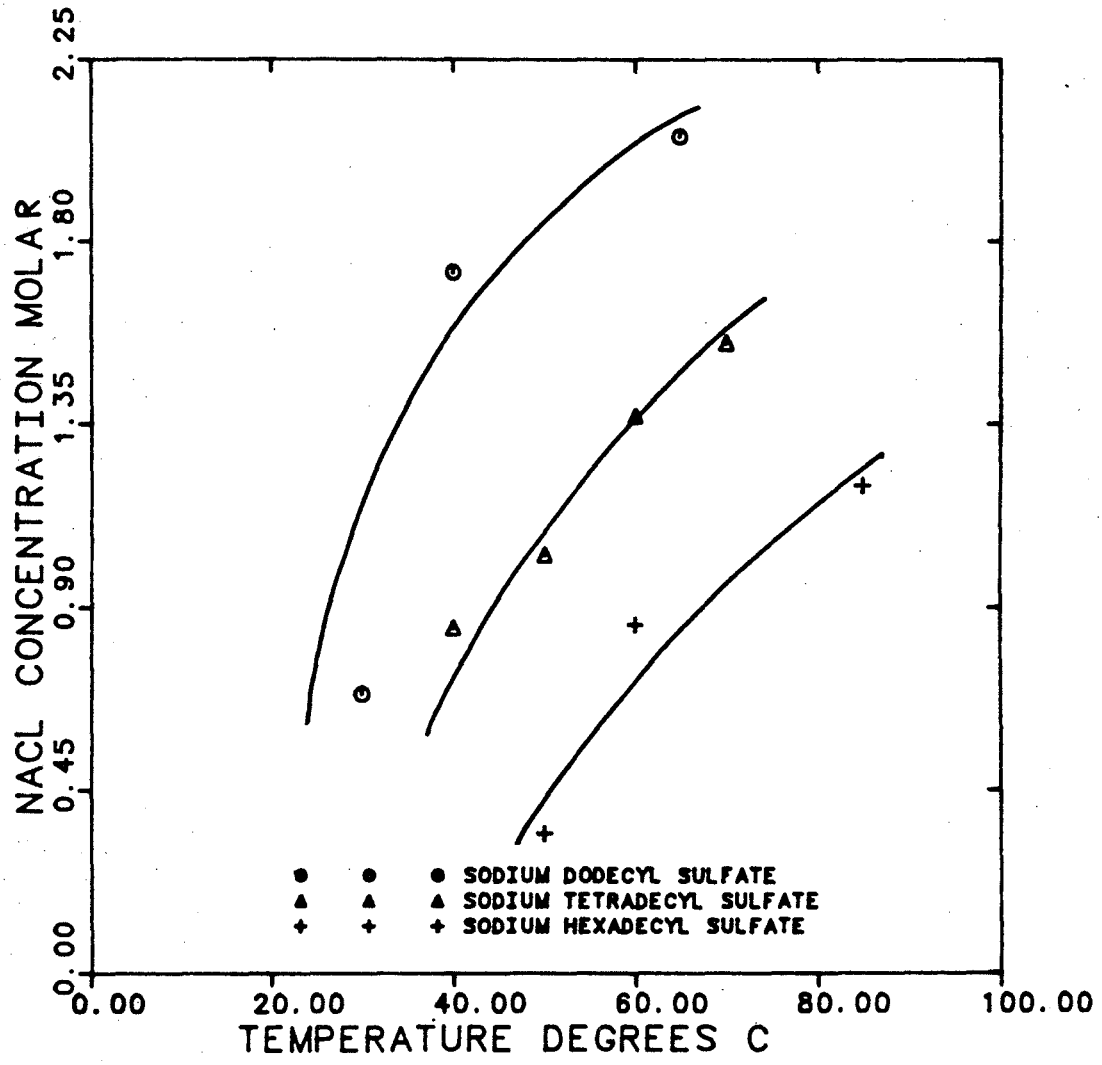

Figure 4.1 Phase Behavior of Sodium Dodecyl Sulfate, Sodium Tetradecyl Sulfate, and Sodium Hexadecyl Sulfate

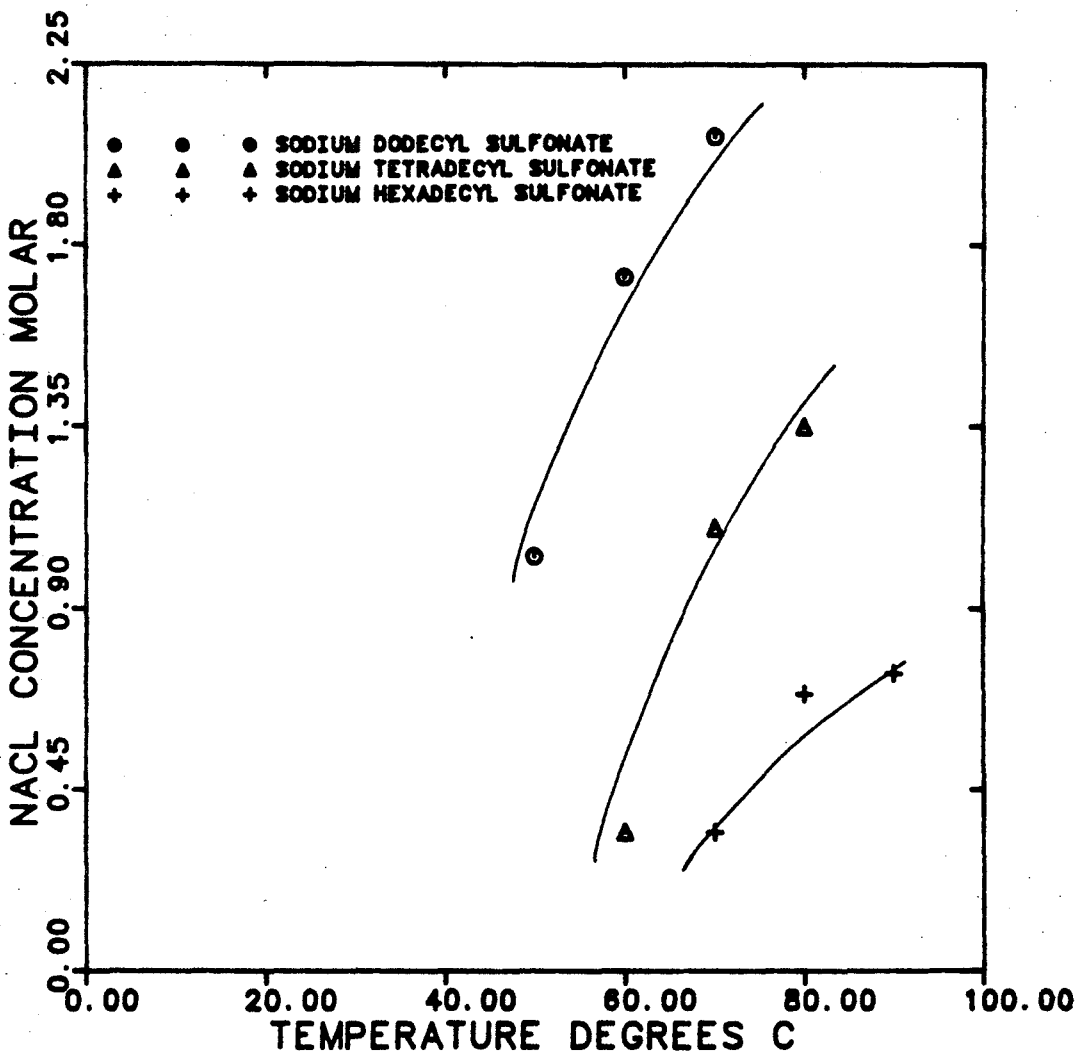

Figure 4.2 Phase Behavior of Sodium Dodecyl Sulfonate, Sodium Tetradecyl Sulfonate, and Sodium Hexadecyl Sulfonate

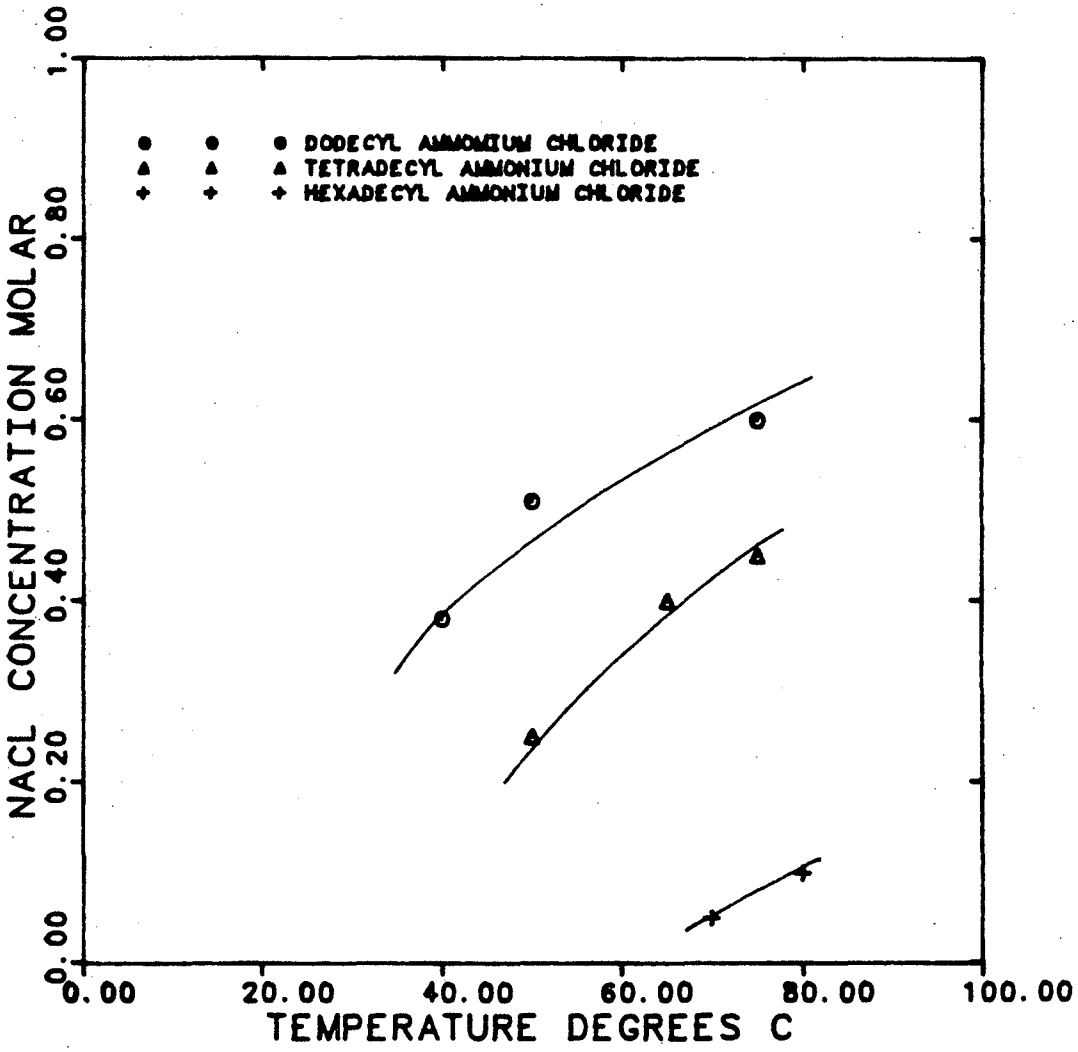

Figure 4.3 Phase Behavior of Dodecylammonium Chloride, Tetradecylammonium Chloride, and Hexadecylammonium Chloride

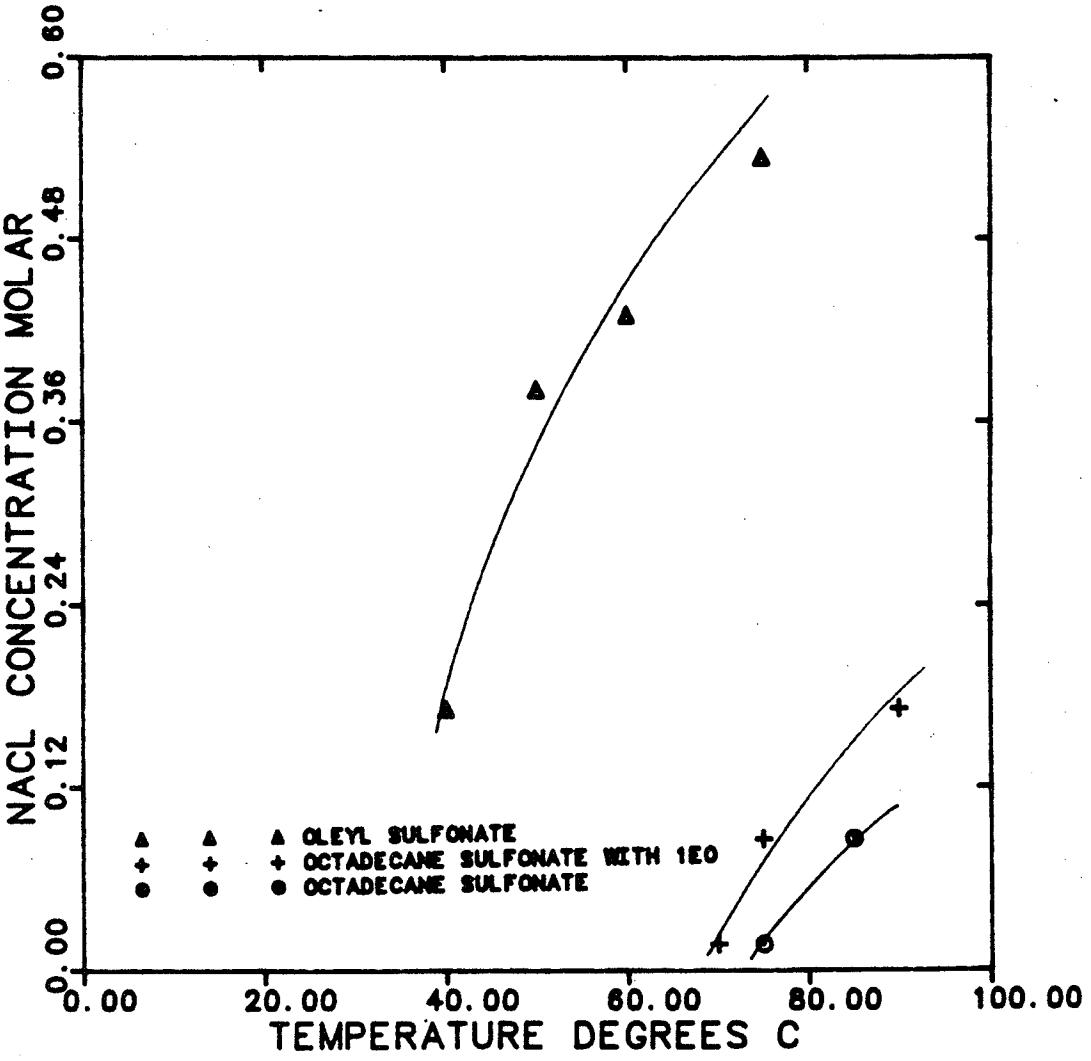

Figure 4.4 Phase Behavior of Oleyl Sulfonate, Octadecyl Sulfonate with $(EO)_1$ and Octadecyl Sulfonate

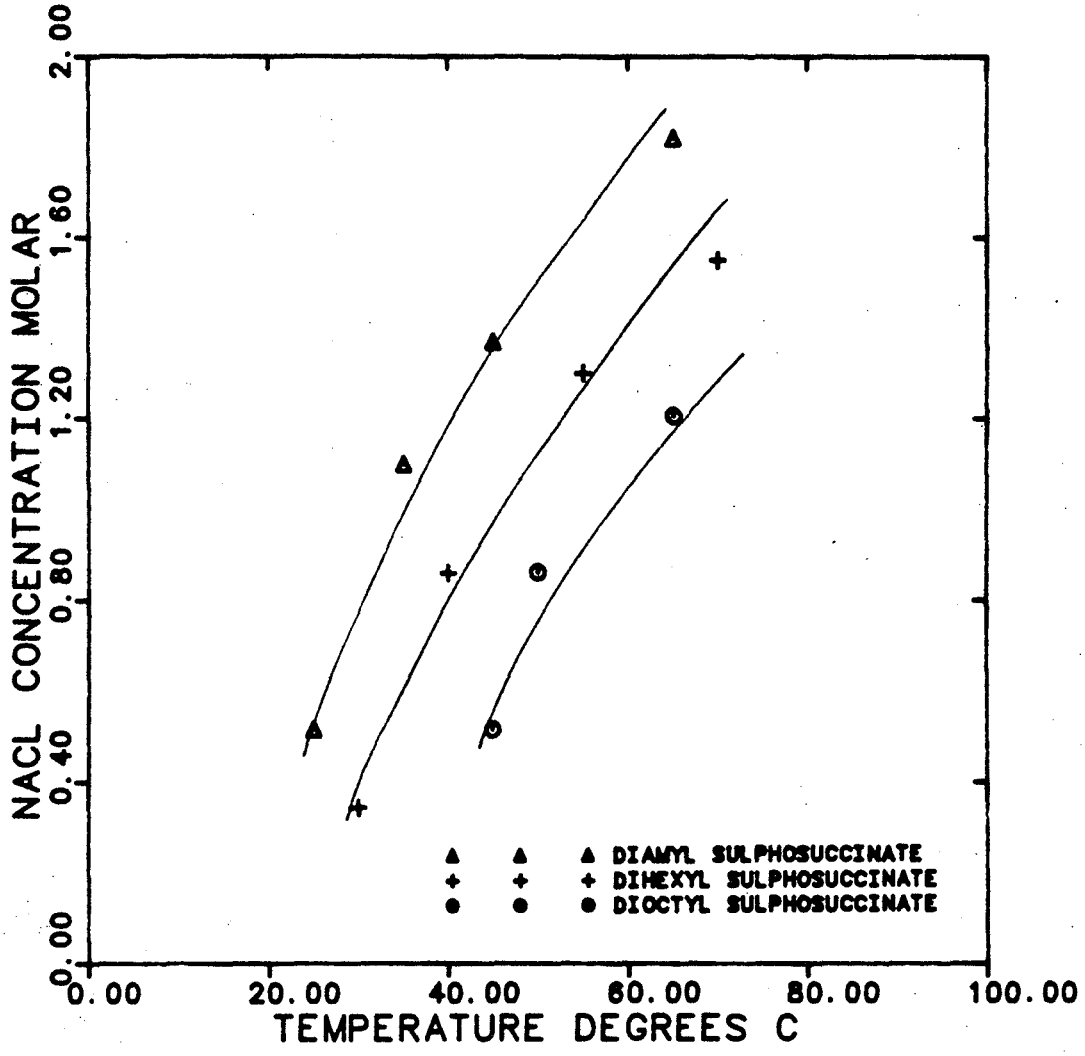

Figure 4.5 Phase Behavior of Sodium Diamylsulphosuccinate, Sodium Dihexylsulphosuccinate, and Sodium Dioctylsulphosuccinate

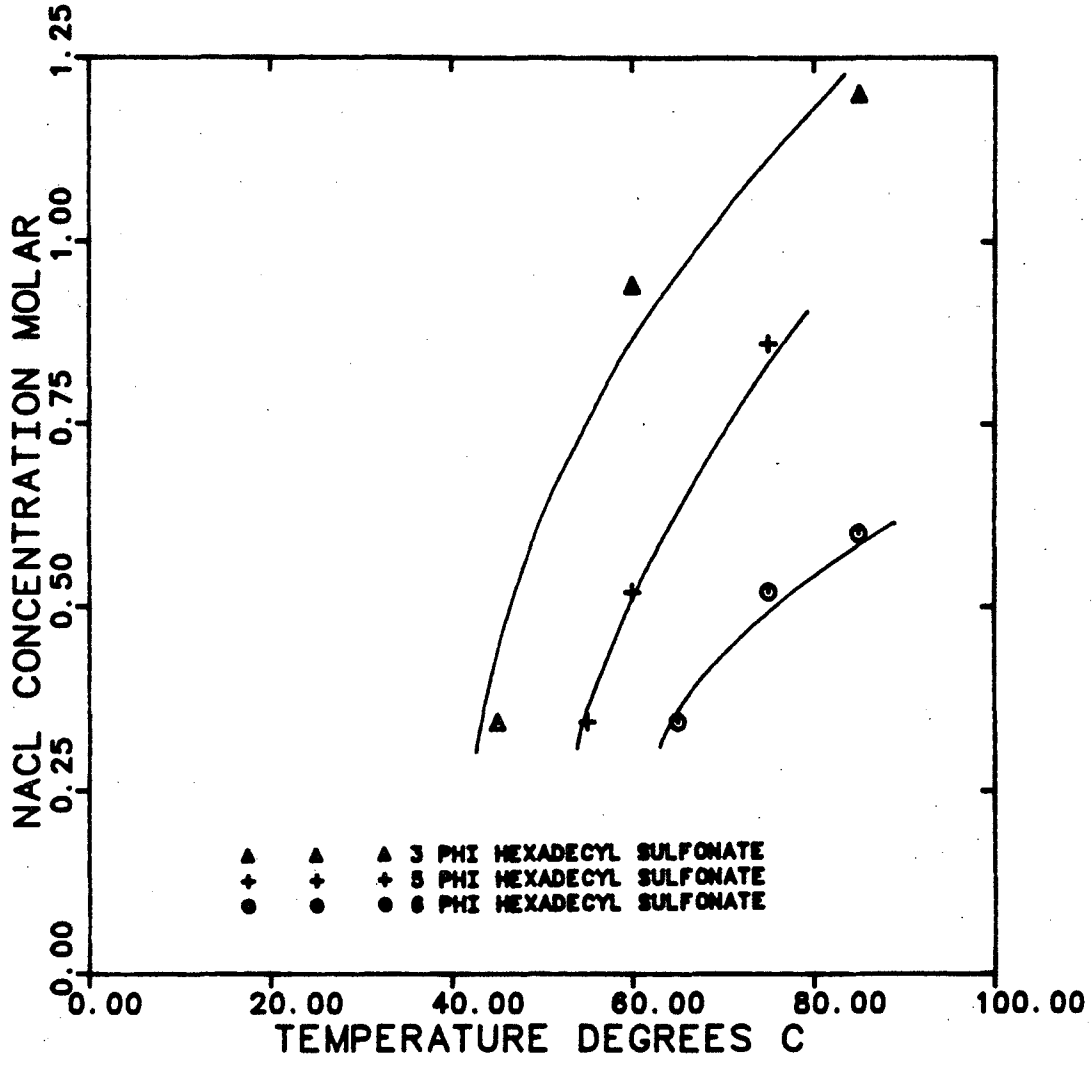

Figure 4.6 Phase Behavior of 3Ø-Hexadecyl Sulfonate, 5Ø-Hexadecyl Sulfonate, and 6Ø-Hexadecyl Sulfonate

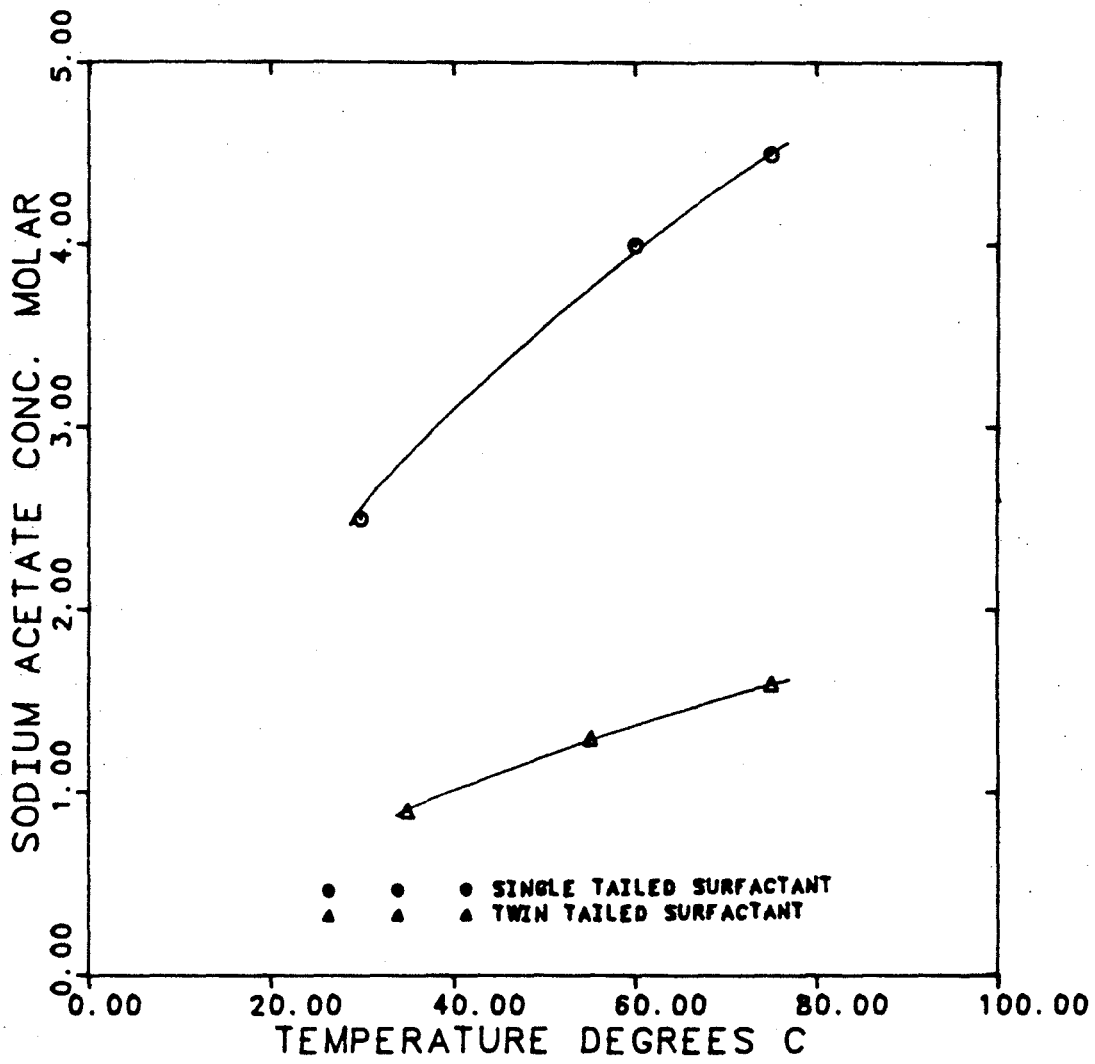

Figure 4.7 Phase Behavior of Hexadecyldimethylammonium Acetate and Dihexadecyldimethylammonium Acetate

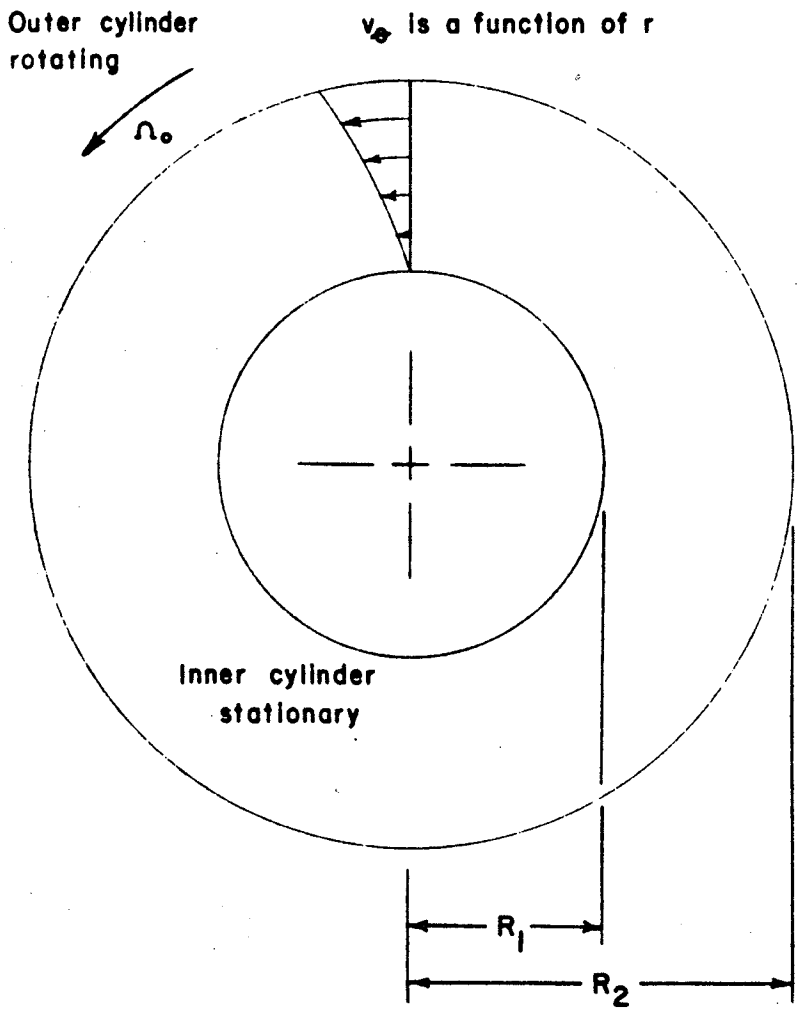

Figure 4.8 Velocity profile between cylinders of a Covette-Hatschek Viscometer.

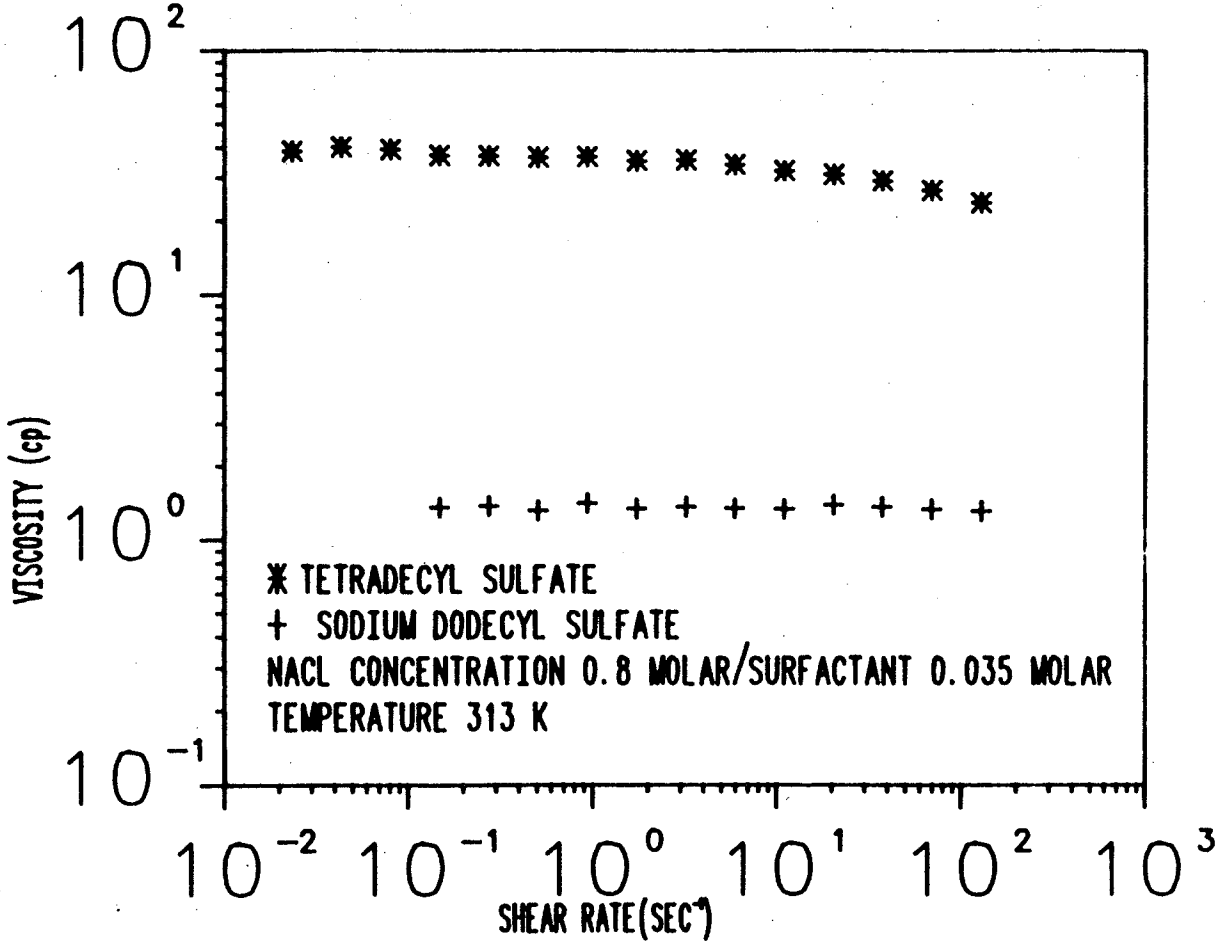

Figure 4.9 Viscosities as a Function of Shear Rate for Equal-Molar Sodium Dodecyl Sulfate and Sodium Tetradecyl Sulfate Solutions

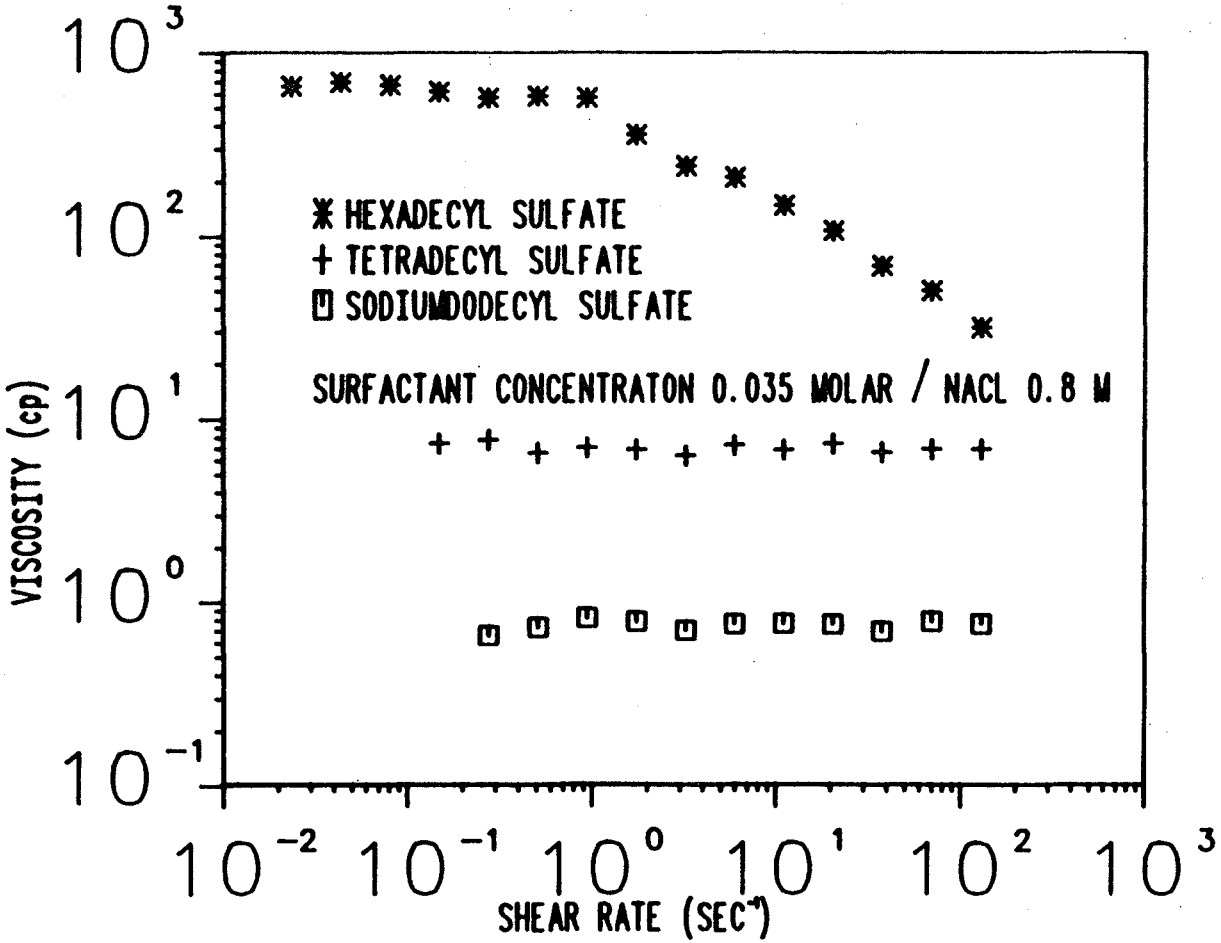

Figure 4.10 Viscosities as a Function of Shear Rate for Equal-Molar Sodium Dodecyl Sulfate, Sodium Tetradecyl Sulfate, and Sodium Hexadecyl Sulfate Solutions

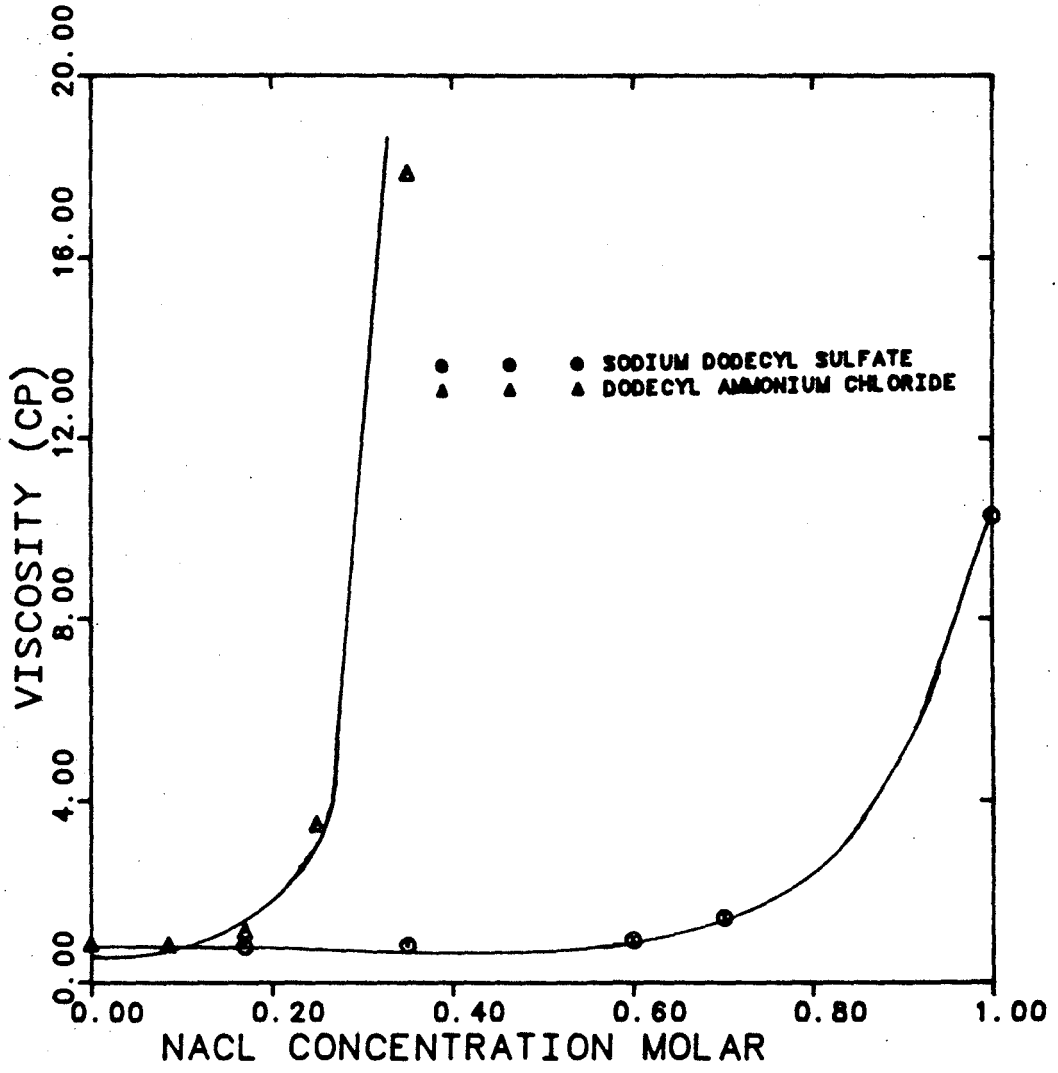

Figure 4.11 Viscosities of Equal-Molar Dodecylammonium Chloride and Sodium Dodecyl Sulfate Solutions as a Function of Salinity

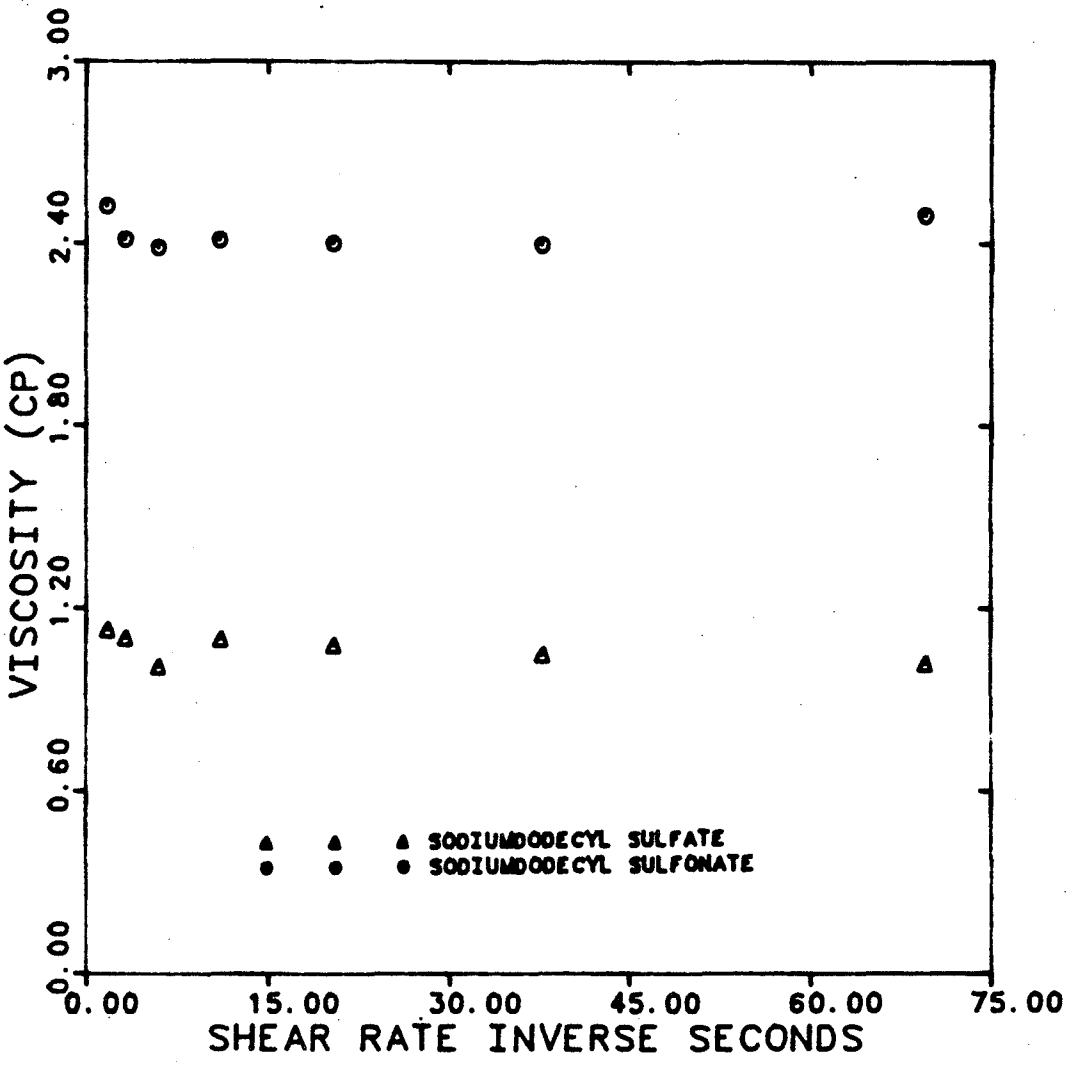

Figure 4.12 Viscosities of Equal-Molar Sodium Dodecyl Sulfate and Sodium Dodecyl Sulfonate Solutions

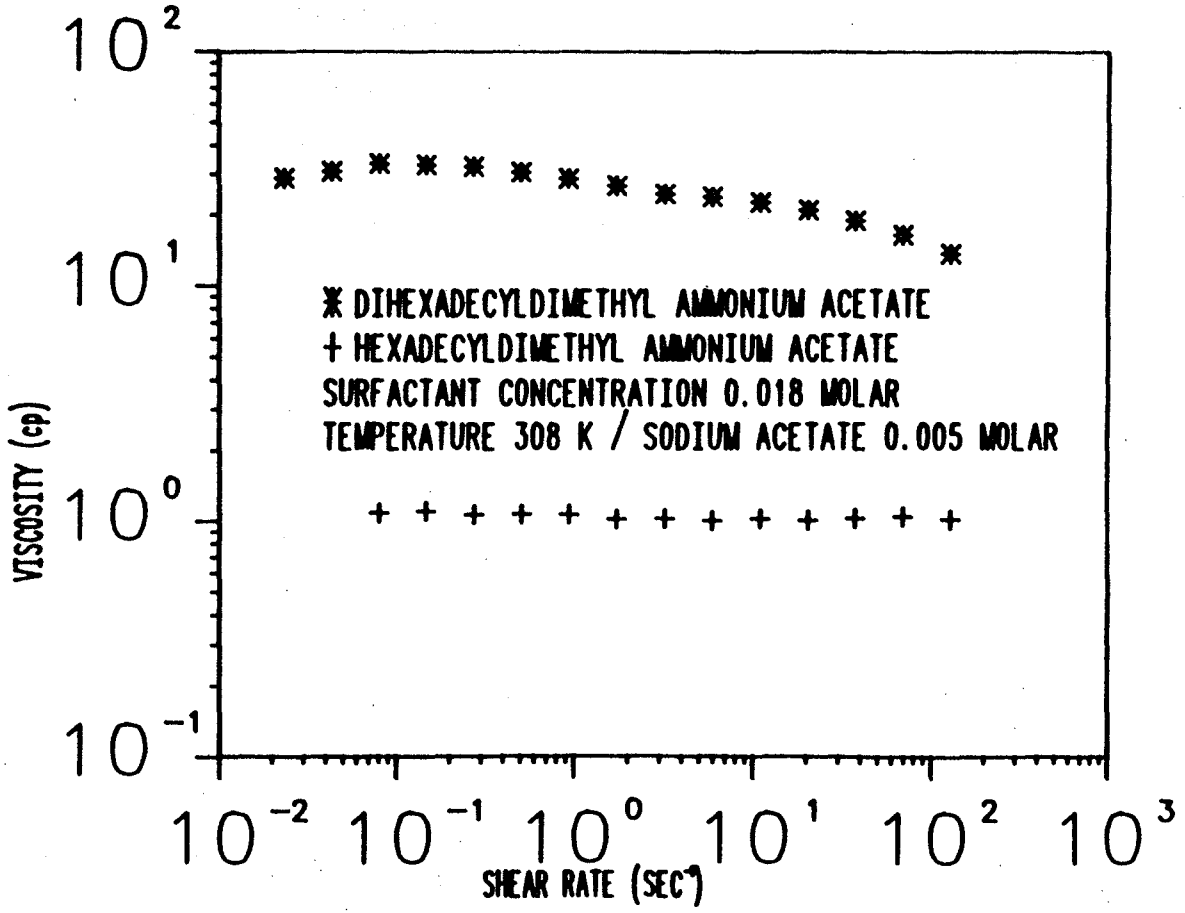

Figure 4.13 Viscosities of Equal-Molar Hexadecyldimethylammonium Acetate and Dihexadecyldimethylammonium Acetate

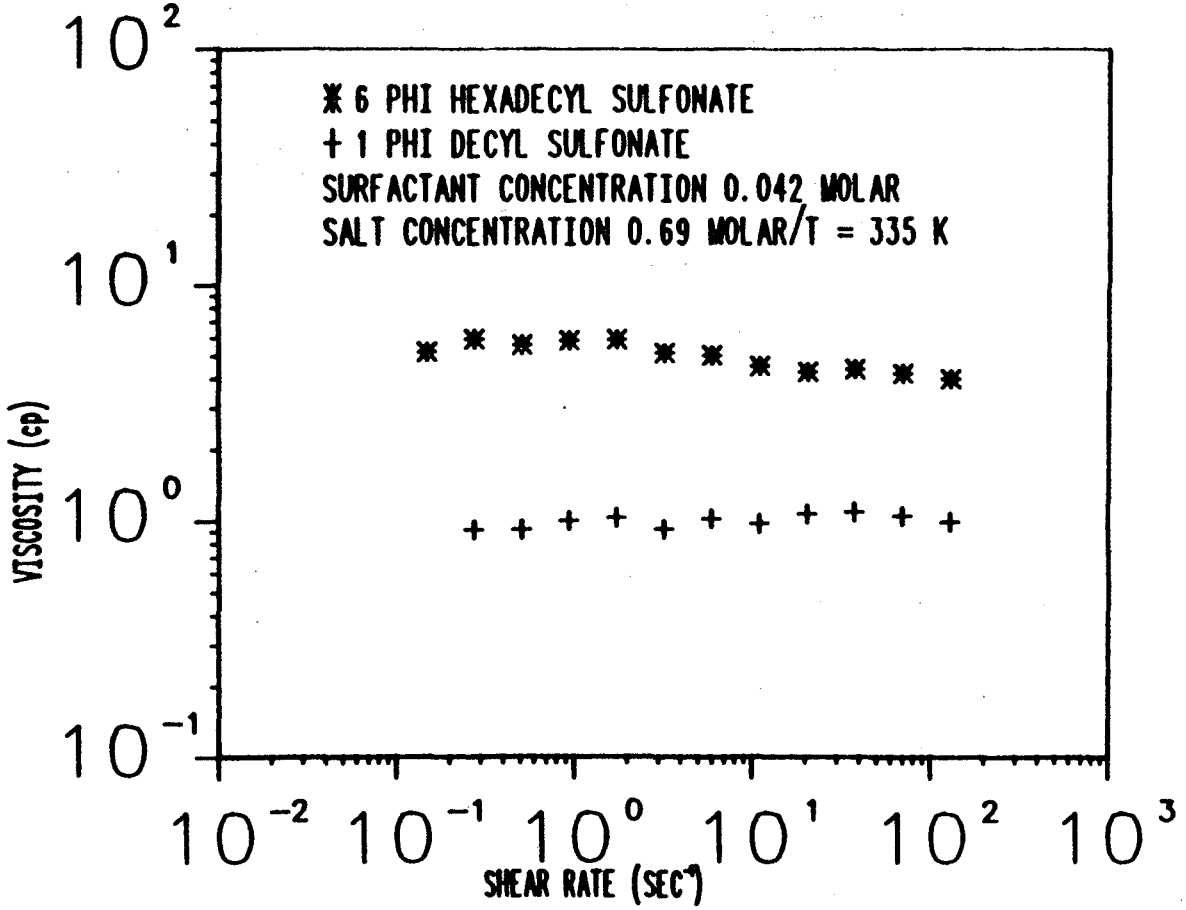

Figure 4.14 Viscosities of Equal-Molar 1Ø-Decyl Sulfonate and 6Ø-Hexadecyl Sulfonate

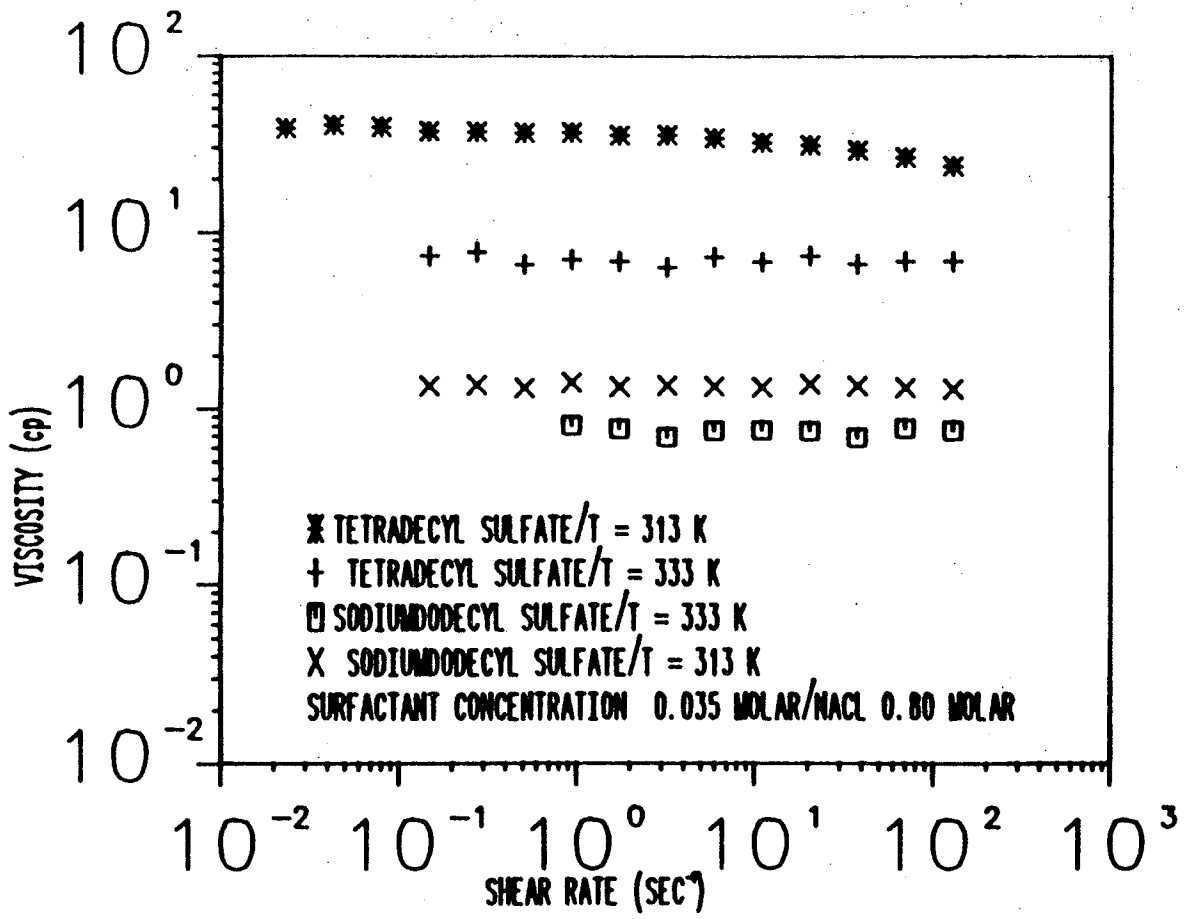

Figure 4.15 Viscosities of Equal-Molar Sodium Dodecyl Sulfate and Sodium Tetradecyl Sulfate Solutions at Two Different Temperatures

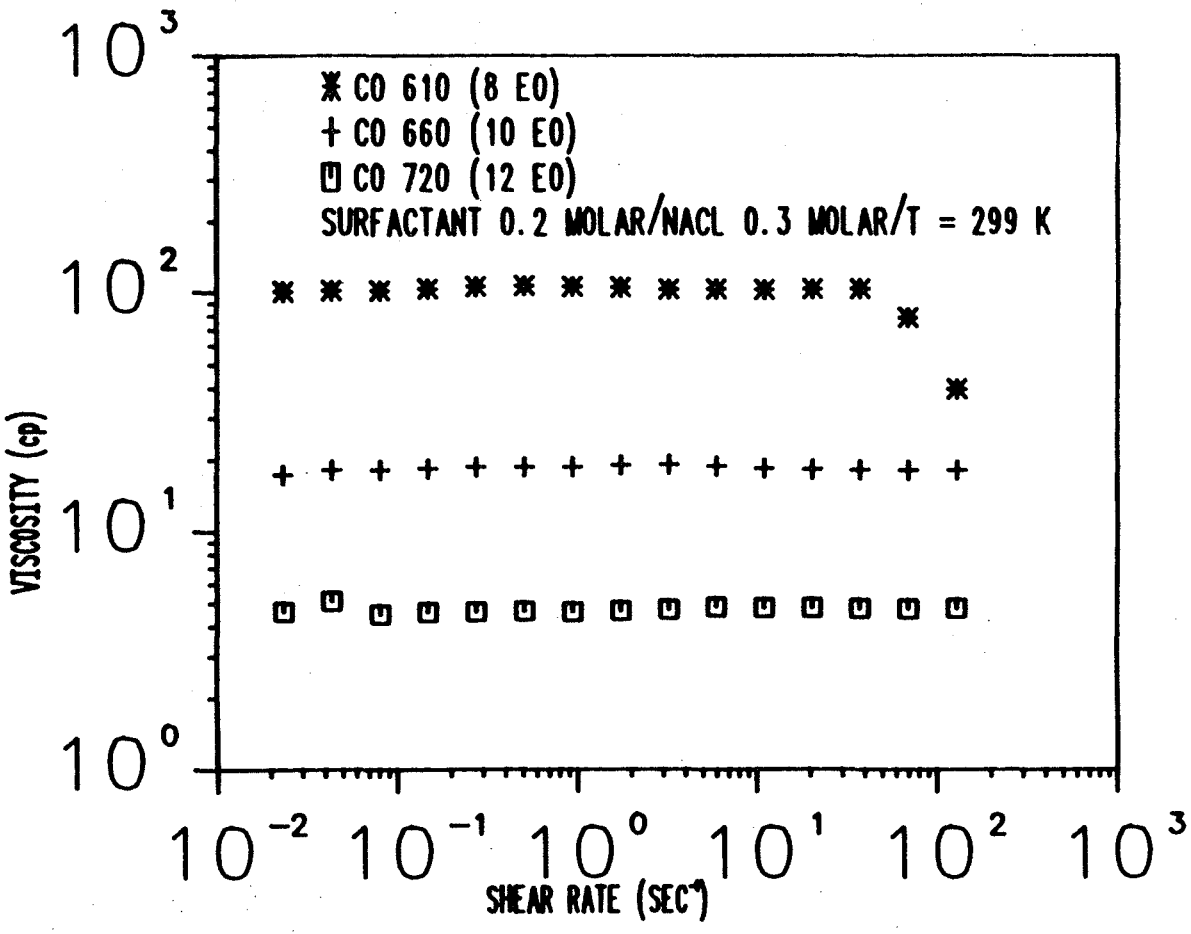

Figure 4.16 Viscosities of Equal-Molar Non-Ionic Surfactants with Different Numbers of Ethylene Oxide Groups.

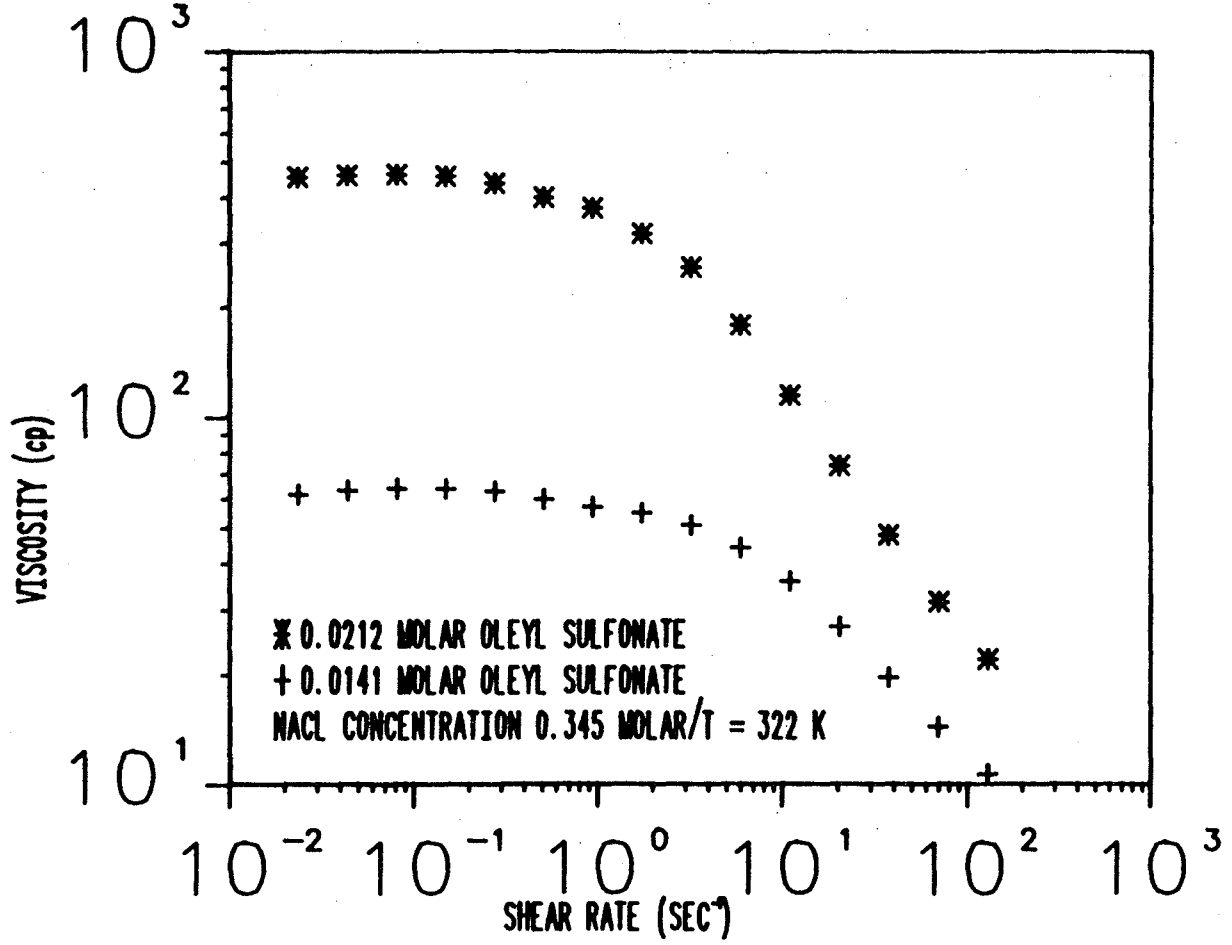

Figure 4.17 Viscosities of Oleyl Sulfonate at Two Concentrations (0.0141 M and 0.0212 M)

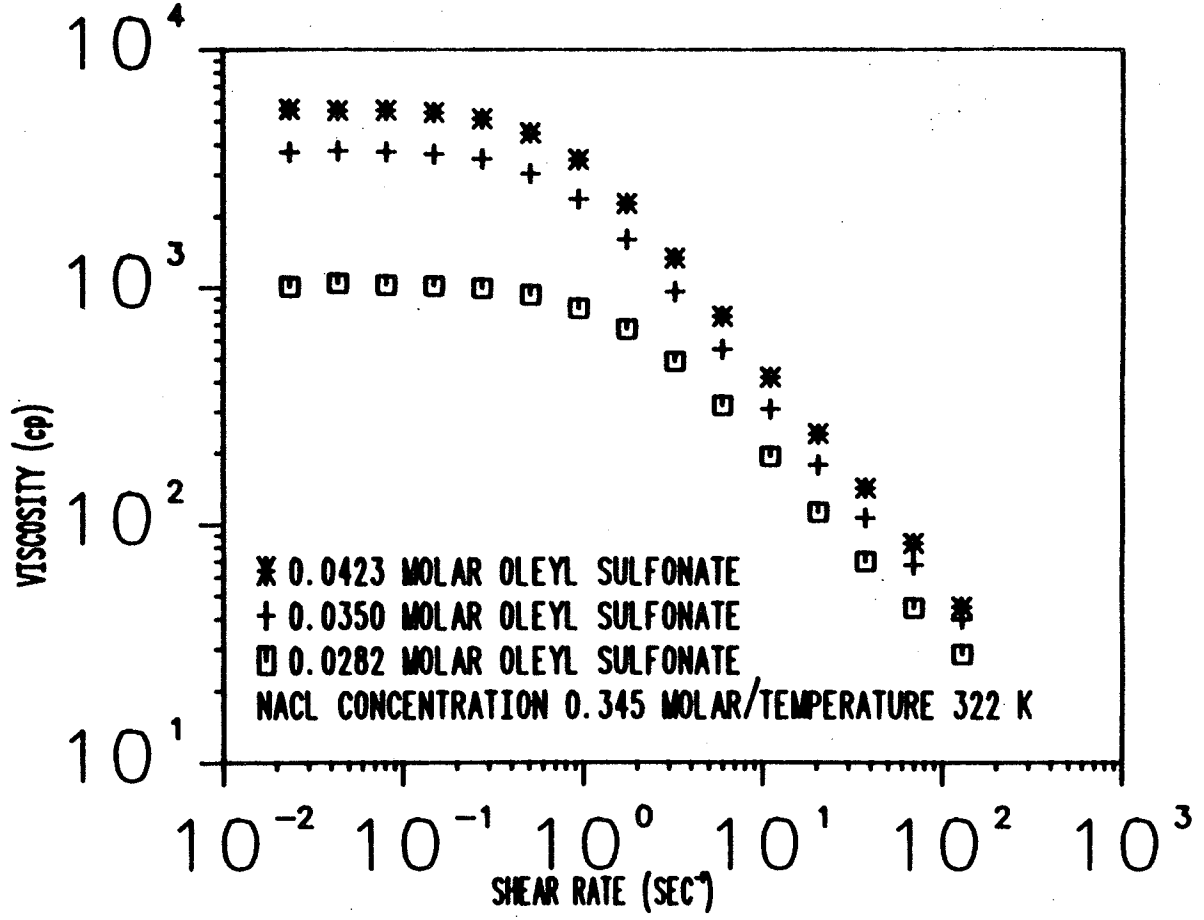

Figure 4.18 Viscosities of Oleyl Sulfonate for Three Surfactant Concentrations for Variable Shear Rates

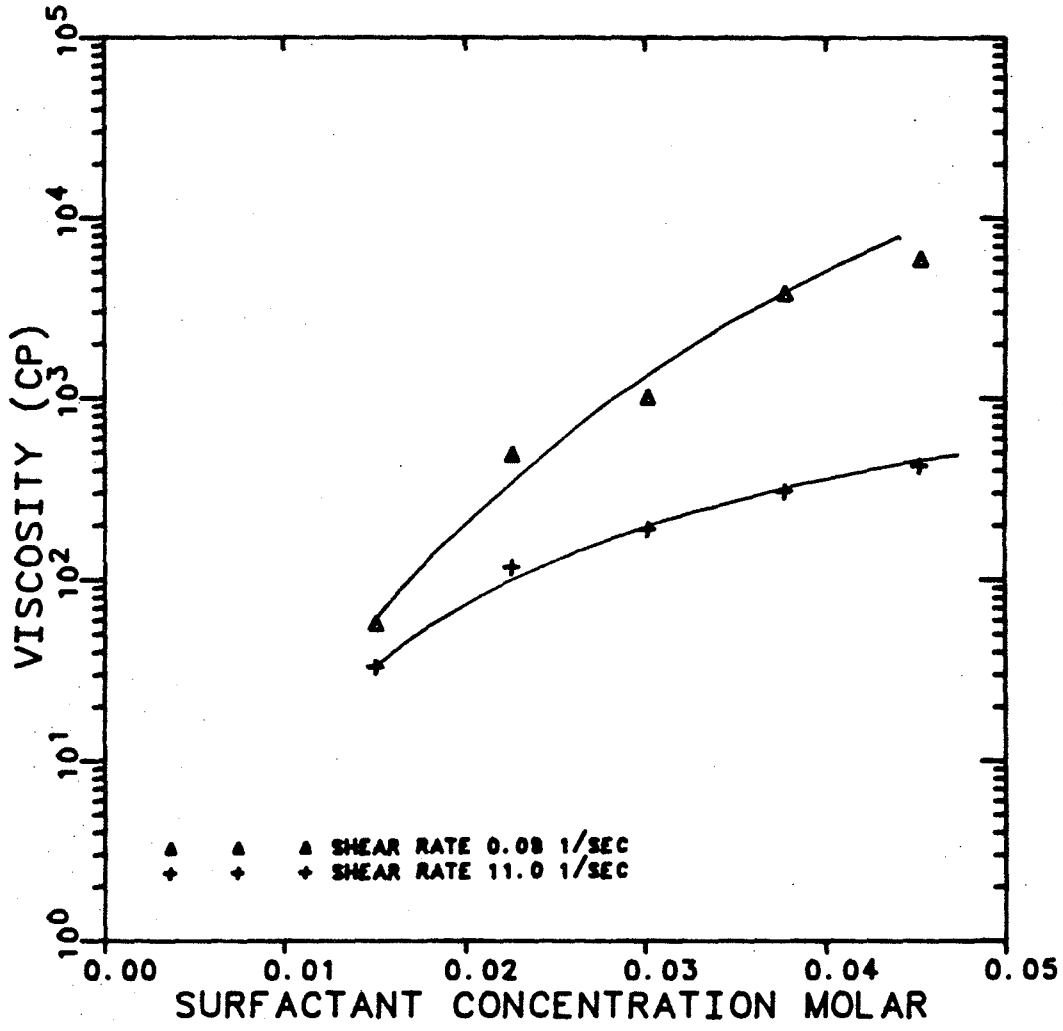

Figure 4.19 Viscosity of Oleyl Sulfonate for Two Shear Rates as a Function of Surfactant Concentration

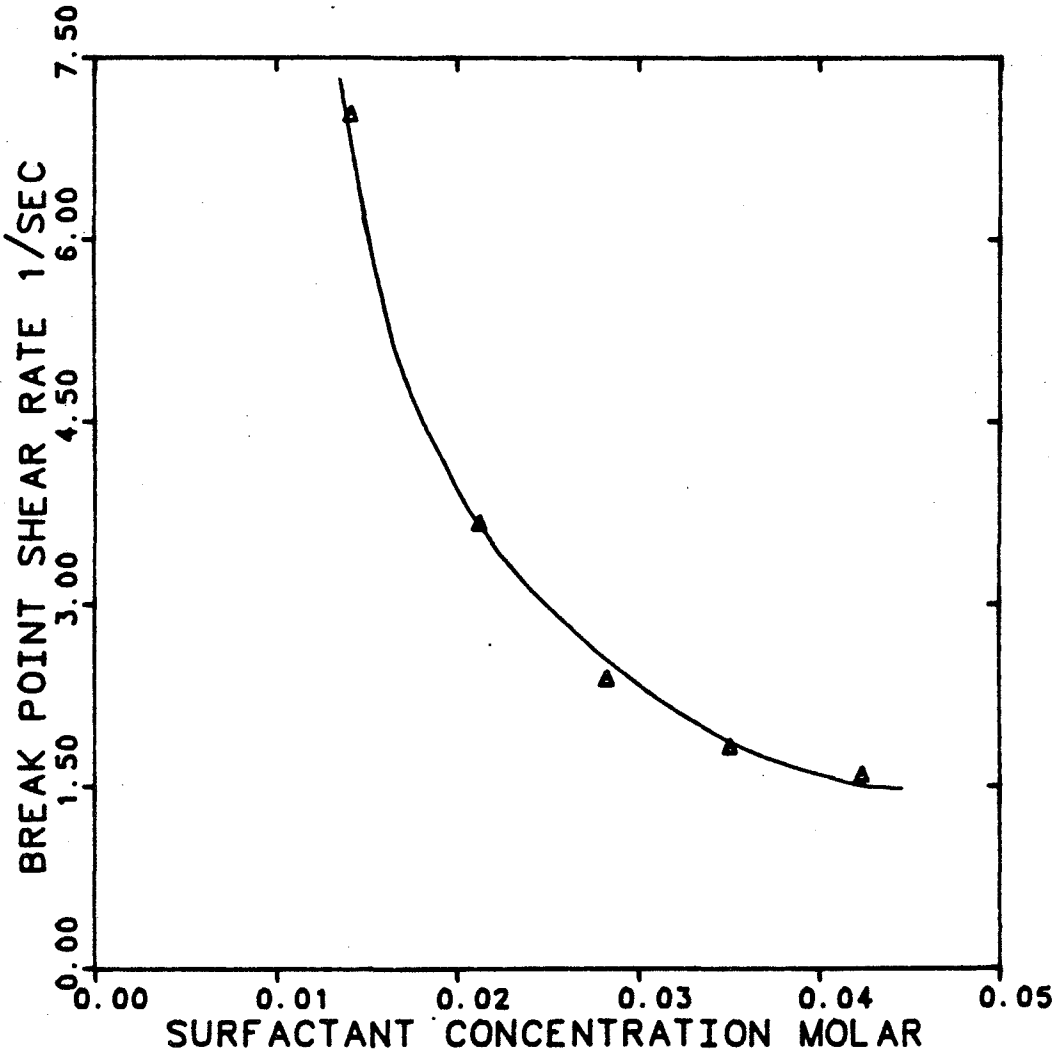

Figure 4.20 Break-point Viscosities of Oleyl Sulfonate as a Function of Surfactant Concentration for Two Shear Rates

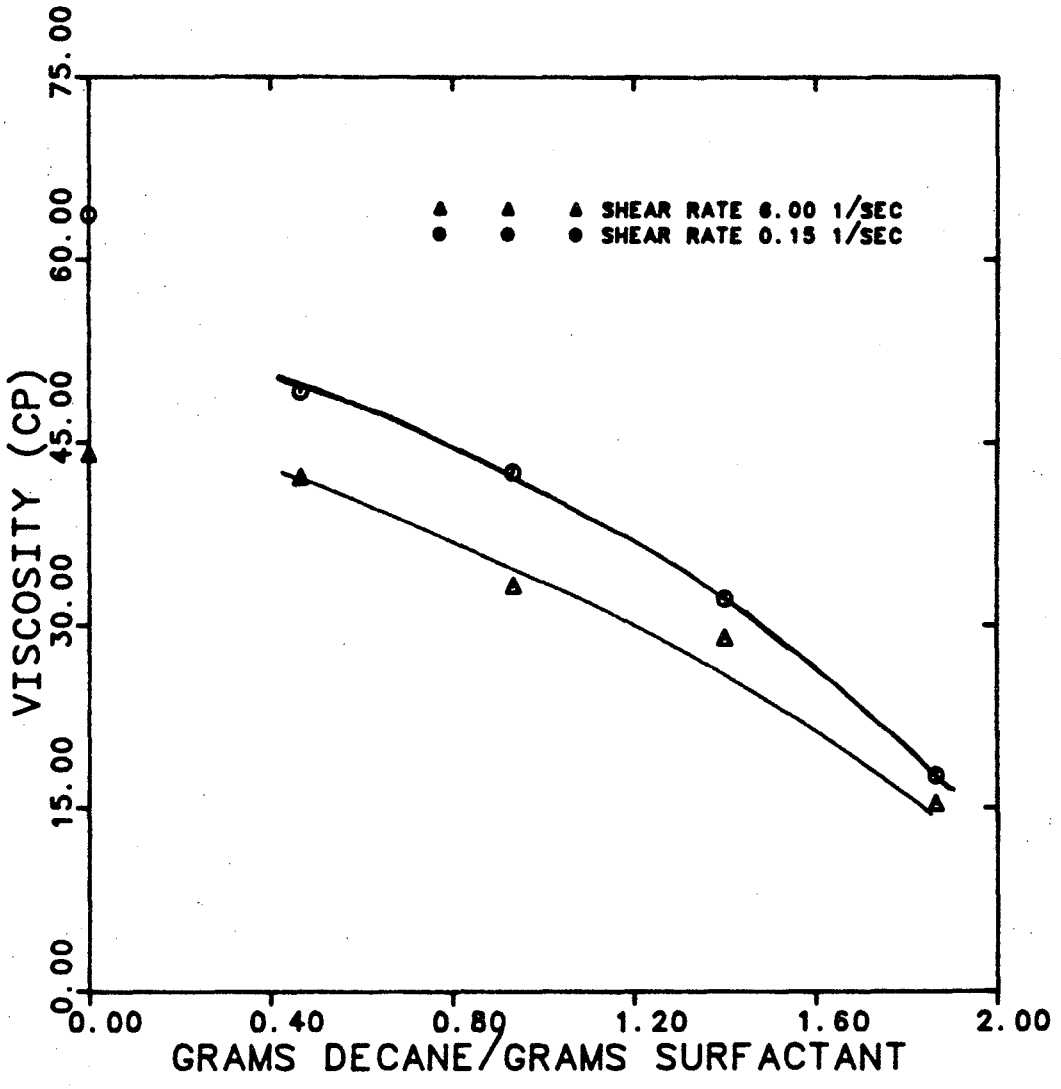

Figure 4.21 Effect of Decane Addition on the Viscosity of Oleyl Sulfonate for Constant Surfactant Concentration (0.5g/dl or 0.0141 M) and Two Shear Rates

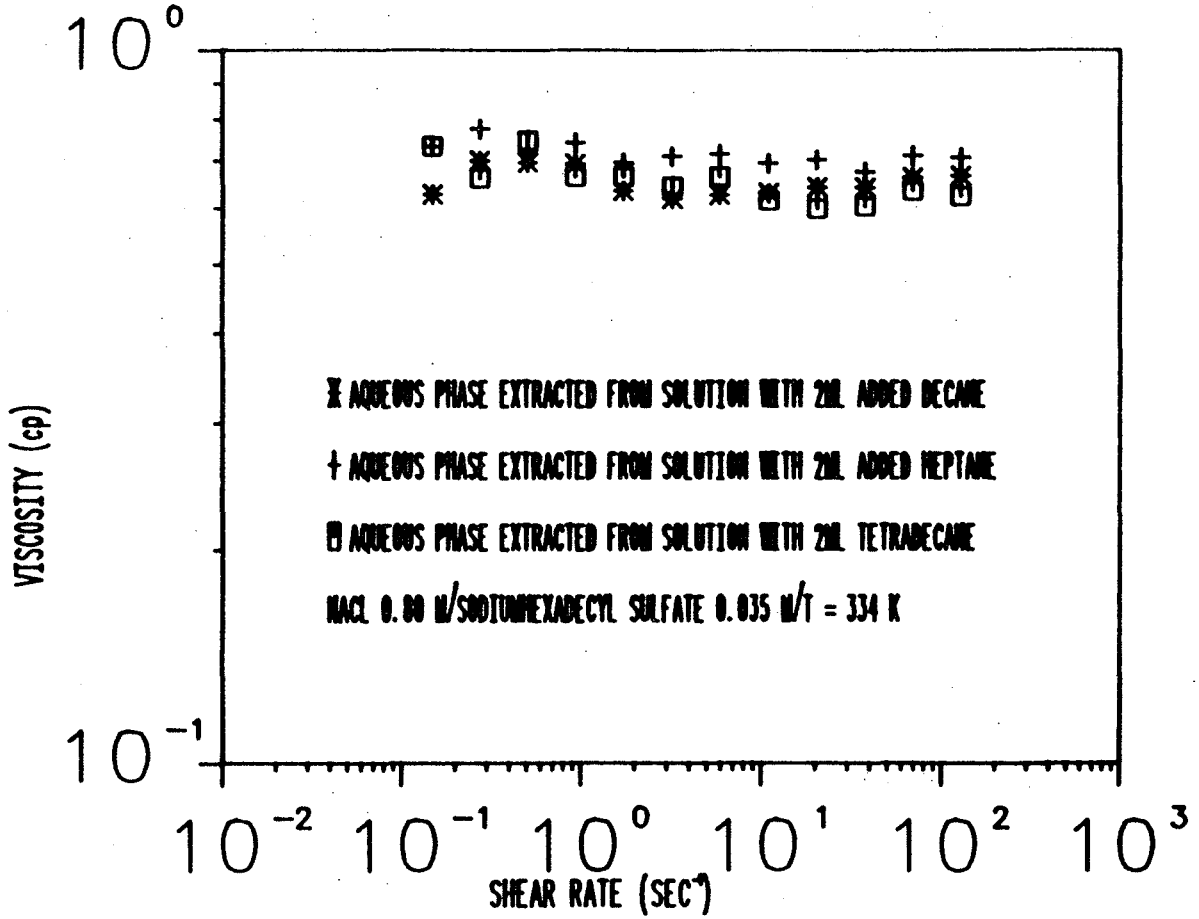

Figure 4.22 Effect of Various Oils on the Viscosity of Sodium Hexadecyl Sulfate

CHAPTER 5

Discussion of Results

5.1 Purpose

This Chapter will compare the predicted results of Chapter 3 with the experimentally observed data of Chapter 4. The significance of those viscosity measurements which reveal the feasibility of using surfactants for mobility control are also discussed.

5.2 Phase Behavior Trends

A few words concerning the phase plots of Chapter 4 are warranted since restrictions of phase stability are an important aspect of surfactant behavior. Knowledge of phase transitions is important in order to approximate the insitu behavior of an aqueous surfactant system. The presence of salinity and temperature gradients within all natural reservoirs necessitates this consideration.

The experimental trends with regard to phase boundaries are clear. Figures 4.1, 4.2, and 4.3 show that longer surfactant tail lengths experience a more restricted single phase region in temperature salinity space. The limit of practicality for purposes here is a tail length of 18 carbon atoms. Beyond this, the 1 phase region becomes too small to be considered acceptable. This limiting value of 18 carbon atoms is more definite, and important, than it may first appear. The reason being that head group structures which have $\Delta\alpha$-carbon distances less than the sulfates of Figure 4.1 show a progressively smaller single phase region. This is evident by comparing

Figures 4.1 and 4.2. For any given value of tail length, a sulfate is seen to be more soluble than a sulfonate. This difference in behavior can be accounted for in the $\Delta\alpha$-carbon values, where $\Delta\alpha$-carbon for a sulfate is approximately 3.2 Å and for a sulfonate 2.4 Å. Thus, while it is possible to realize significant solubility with normal sulfated and to a lesser degree sulfonated 18 carbon tail length surfactants, it is not possible to achieve such phase behavior using molecules with shorter $\Delta\alpha$-carbon lengths like normal ammonium compounds (ie where $\Delta\alpha$-carbon is about 1.8 Å).

Normal ammonium compounds have limited solubility when tail lengths are long. In fact, even short tailed ammonium surfactants have relatively small regions of phase stability. For example, at 313 K dodecylammonium chloride has a salt tolerance of only 0.38 M, while for the same temperature sodium dodecyl sulfate is single phase at salinities above 1 M. This can be seen by comparing Figures 4.1 and 4.3 which show the respective phase diagrams for sulfates and ammonium compounds. Evidently, smaller $\Delta\alpha$-carbon values or longer tail lengths both cause movement away from a single phase regime and toward precipitation. This prevents one from optimizing surfactant viscosities based solely on the relationships between viscosity and surfactant structural features. Phase stability must also be considered.

Figure 4.4 shows the phase diagram of three relatively long-tailed molecules. The interesting feature of this plot is the greatly improved solubility of oleyl sulfonate in comparison with either $C_{18}(EO_1)$ or normal C_{18} sulfonate. Futher consideration of this point is made in Section 5.4 where the oleyl sulfonate structure is discussed in more detail.

Sodium sulphosuccinates were studied as an example of an extreme class of surfactants which have high water solubility. Figure 4.5 shows that these molecules have substantial water solubility. The $\Delta\alpha$-carbon value for this surfactant is

somewhat larger than for a normal straight-chained alkane sulfonate. The double bonded arrangement of atoms near the head group of these molecules would seem to demand this. However, the short tail length of these molecules makes it difficult to determine how much of the increased salt tolerance results from an increased $\Delta\alpha$-carbon distance since the decreased hydrophobic tail obviously plays a major role. Nevertheless, both factors would favor increased phase stability and more than likely a combination of forces is the cause for the high solubilty of these molecules in water.

Figure 4.6 shows the phase diagram for a system of alkyl benzene sulfonates. These molecules show considerable sensitivity toward salt, more so than normal linear alkane sulfonates. It can also be noticed that as the position of the branch point is increased, the single phase region becomes larger. This would seem logical if one accepts that increased tail branching ($3\emptyset \rightarrow 5\emptyset \rightarrow 6\emptyset$) results in an effectively smaller tail length. The reason why these compounds do not have the solubility properties of straight chain sulfonates may be the result of a packing constraint which arises due to the presence of the benzene ring.

The last phase diagram, Figure 4.7, reveals the effect of increasing surfactant tail volume. The much larger tail volume of dihexadecyldimethylammonium acetate in comparison to hexadecyldimethylammonium acetate causes this twin tailed molecule to have a much more restricted single phase regime. The large tail volume must force formation of extended structures even at low salinities since the maximun allowable aggregation number for a spherical micelle is reduced by 1/2. Hence, like increased tail length and decreased $\Delta\alpha$-carbon distance, increased surfactant tail volume is seen to move toward the 2 phase region in temperature salinity space.

5.3 Viscosity - Trends

a) surfactant tail length

The relationship between surfactant structure and viscosity was examined theoretically in Chapter 3. The first prediction of the model indicated that increased surfactant tail lengths would be beneficial toward the formation of rod-like micelles. Specifically, the computer calculations of Table 3.3a indicated that for equal detergent concentrations, a comparison of sodium dodecyl sulfate (SDS) and sodium tetradecyl sulfate (STS) at 313 K and 0.8 molar salt would show viscous behavior is limited to the tetradecylsulfate molecule. The qualitative index which served to illustrate this was the change in the sign of the free energy difference ($\mu_{No}^{o} - N_o\mu^o$) . In Table 3.3a, the free energy difference increases from a negative number when the tail length is 16.7 Å and $\Delta\alpha$-carbon is 3.2 Å to a positive number when the tail length is 19.2 Å and the $\Delta\alpha$-carbon remains 3.2 Å. When the free energy is positive, rods can form and viscosities are expected to be high, whereas, a negative free energy change indicates spherical micelles and low viscosities.

Figure 4.9 of Chapter 4 is an experimental check of the predicted results given in Table 3.3a. It shows measured viscosities as a function of shear rate for 0.035 M SDS and TDS solutions. The temperature is 313 K and the salt concentration is 0.8 M which are the same conditions used in formulating Table 3.3a. Qualatative agreement betweeen theory and experiment is observed. Figure 4.9 shows what Table 3.3a predicted; viscous behavior at the prescribed conditions is limited to TDS, the SDS molecule shows no appreciable viscosity.

A second comparison of theory and experiment which looked at the effect of surfactant tail length considers the viscosity of equal molar SDS, TDS, and hexadecyl

sulfate (HDS) solutions at 333 K and 0.8 M salt. The theoretical results which are listed in Table 3.3b show that only HDS has a positive free energy difference. Therefore, if the theory were again qualitatively correct, of the three sulfate molecules, only HDS should show viscous behavior at the conditions of Table 3.3b. This is in fact true, and the experimental evidence supporting the theory is shown in Figure 4.10 which illustrates the viscosities of equal molar HDS, TDS, and SDS solutions for the temperature and salinity of Table 3.3b. The large viscosity of HDS in comparison to either TDS or SDS illustrates the importance of surfactant tail length for viscosity modification and agrees in a qualitative manner with theory.

b) Δα-carbon distance

The theoretical relationship between Δα-carbon and aggregation number showed a clear trend; as Δα-carbon is increased, there is a preference toward the formation of spherical aggregates. The fact that a spherical aggregate becomes the desired shape also implies a greater salt tolerance. Surfactants with larger Δα-carbon distances should be better able to accommodate monomer in a spherical structure, and hence, be less likely to form the very large extended structures which eventually precipitate. This is what is qualitatively predicted in Tables 3.3a and 3.3f. These tables show for example that SDS which has a large Δα-carbon value of approximately 3.2 Å should not form rod-like aggregates at a salinity of 0.8 M (Table 3.3a) but will for an increased salinity of 1.1 M as in Table 3.3f. In contrast, DAC with a much smaller Δα-carbon value of 1.8 Å, should easily form rod-like aggregates at the conditions of Table 3.3a. Thus, DAC should be viscous at a much lower salinities than SDS because it has a significantly smaller Δα-carbon distance.

One can check these predictions against the experimental results of Figure 4.11. This Figure shows the viscosities of equal molar SDS and DAC solutions as a function of salinity at constant temperature. The qualitative predictions of the theory are confirmed. SDS solutions show no appreciable viscosity until the salinity is raised to 1.0 M. Its viscosity at 0.8 M is low and this is in agreement with the negative free energy value in Table 3.3a. In comparison, DAC shows considerable viscosity at only 0.35 M salt, and it is not possible to increase the salinity much beyond 0.35 M with this molecule because it precipitates. These findings go along well with theory which indicated that DAC would be viscous at much lower salinities than SDS and have a smaller salinity tolerance. As a further test of the theory one can see if the free energy difference of DAC is positive at 0.35 M salt and 313 K. The experimental results in Figure 4.11 dictate that it should be. The output at these conditions is listed in Table 3.3c and the free energy for a 12 carbon tailed molecule with a $\Delta\alpha$-carbon value of 1.7 Å (recall DAC has $\Delta\alpha$-carbon of 1.8 Å) is notably non-negative. Additional experimental evidence which supports the observation that increased $\Delta\alpha$-carbon distances leads to lower viscosities is provided by Figure 4.12 which shows the viscosities of equal molar SDS and sodium dodecyl sulfonate soultions at a constant temperature. Sodium dodecyl sulfonate whcih has a smaller $\Delta\alpha$-carbon value than SDS is shown to be more viscous.

The theory seems qualitatively consistent with experiment for variations in surfactant $\Delta\alpha$-carbon distance. An increased $\Delta\alpha$-carbon value yields lower aggregation numbers, and as a result, lower viscosities. This is reflected in the sign of the free energy change which is negative for spherical micelles and positive when rod-like structures may form.

c) surfactant tail volume

Theoretically, an increase in surfactant tail volume leads to a large positive increase in the free energy difference (μ_{No}^{o} - $N_o\mu^o$). This is evidenced by Tables 3.3d and 3.3e. If theory agrees with experiment, an increase in tail volume should cause a corresponding viscosity increase. Experimentally, such a relationship is observed and illustrated in Figure 4.13. Thus, there is again agreement between the qualitative predictions of the theory and the experimentally determined values. In particular, we observe in Figure 4.13 that when the surfactant tail volume has been doubled (ie. hexadecyldimethylammonium acetate $\rightarrow$ dihexadecyldimethylammonium acetate) there is a significant increase in viscosity. Figure 4.14 provides futher evidence of this same relationship. In this diagram, $1ØC_{10}$ sulfonate is less viscous than $6ØC_{16}$ sulfonate. Since we assume that the effective tail lengths of these molecules are essentially the same, the larger tail volume of $6ØC_{16}$ sulfonate explains the difference in viscosities.

The relationship between tail volume and viscosity is theoretically predicted since the free energy for hexadecylammonium acetate is notably negative in Table 3.3d but positive in the case of dihexadecylammonium acetate represented in Table 3.3e. Recall that the ammonium head group is identified in the tables given here as having an alpha carbon value of 1.7 Å which is essentially the same as the literature value of 1.8 Å. In this case, the value of 1.7 Å is a convenience, it would not make any difference in the theoretical findings if 1.8 Å were used, as all trends with these molecules would be preserved. It is interesting to note that the tail volume of dihexadecylammounium acetate is large enough to produce significant viscosities at

very low salt concentrations. The large tail volume evidently makes it very difficult to pack monomer into a spherically shaped aggregate. At even low salinities, the preferred structure must become rod-like. Of course, one pays a price for the gain in viscosity and in this instance it is restricted salinity tolerance. The double tailed molecule has a much more restricted 1 phase region in temperature salinity space as noted previously in Section 5.2.

d) temperature and salt effects

The theory predicts that increases in salt or decreases in temperature will cause an increase in the free energy, and therefore, a larger aggregation number. If experiment confirms these predictions, one should see that salt increases or temperature decreases will be identified with increases in viscosities. Referring to Figures 4.15 and 4.11, it can be observed that the theoretical findings are correct. In Figure 4.11, greater salinities are unmistakably related to increased viscosities, and in Figure 4.15, higher temperatures are seen to cause a decrease in viscosity.

e) addition of ethylene oxide

The experimental relationship between viscosity and number of added (EO) groups is shown in Figure 4.16 where it is noticed that increased addition of (EO) is related to a decrease in viscosity. As mentioned previously, the theory does not specifically address the question of (EO) addditon. However, if one associates increases in the number of ethylene oxide groups with increases in the effective $\Delta\alpha$-carbon length, then the trends observed are in the expected direction.

5.4 Viscosities From Aggregation Numbers

In Chapter 3 it was observed that theoretically predicted aggregation numbers generally appeared inconsistent with physically acceptable values. One can make a more detailed study of the theory by calculating ϖ for the salinities and temperatures along the phase curves of Chapter 4. If very large aggregation numbers are considered to imply precipitation points, then one expects the values of ϖ along a phase boundary to be large, relatively constant, and independent of surfactant composition. However, upon performing the calculations for ϖ at points on the phase boundaries of DAC, TAC, and HAC, (recall Fig. 4.3), one finds that although ϖ is large, ($\approx 1.6 \times 10^8$), and relatively constant for DAC and TAC, it is very small, (≈ 107), for HAC. Thus, there does not exist the consistency in ϖ along the phase boundaries which one expects, and the calculations are not improved for other molecules.

For example, consider the sulfate molecules (recall Fig. 4.1). At points along phase boundaries, ϖ values are predicted to be small (i.e. essentially spherical aggregation numbers are calculated). This is not expected for the salinities and temperatures which define a phase boundary. At points near these curves, solid crystals will form for small changes in salinity or temperature; and therefore, aggregation numbers should be large. Furthermore, these predicted values of ϖ are in sharp contrast to the implications of viscosity measurements. For instance, one may remember that high viscosities were obtained near phase boundaries (i.e. recall Fig. 4.10 which showed very high viscosities for $C_{16}SO_4Na$ near its phase boundary). Since we generally expect high viscosities to be associated with the formation of long rod-like micelles, the theoretical aggregation numbers are not consistent with our viscosity values.

The central problem again appears to be that $\Delta\alpha$-carbon lengths provide for an inadequate calculation of the excluded micellar radius. More exact results will necessitate a rigorous theoretical treatment of this variable, one which considers the detailed effects of salt and temperature. A statistical mechanics approach may be warranted so that the arrangement of counterions about the micelle can also be considered.

Because the theoretically predicted aggregation numbers are not generally acceptable, it is not surprising that when these values of ϖ are used in the viscosity equations of Chapter 2, unacceptable viscosities are obtained. The viscosity equations depend strongly on reasonable estimates of ϖ. Yet, despite the inadequacies of viscosity calculations based on predicted aggregation numbers, it is worthwhile to arbitrarily choose a wide range of ϖ values and perform viscosity calculations using the procedure outlined in Chapter 2, Section 2.8. The results form these calculations will serve to main purposes:

1) They will determine whether or not the viscosity equations yield acceptable results for reasonable values of ϖ.
2) If the viscosity equations produce reasonable results, one will have an approximate, quantitative relationship between viscosity and aggregation number.

With these goals in mind, viscosities were calculated for assumed values of ϖ in accordance with the method of Section 2.8. The results are plotted in Figure 5.1. The curves of Figure 5.1 were calculated for a surfactant concentration of 0.035 M. CMC values for the three different tail lengths were assigned those quantities associated with SDS, TDS, and HDS, in the absence of added salt, respectively.[1] The volume of a water molecule which is a necessary input to Equation (2.3.2) was

taken as 30 $Å^3$. The value of $\Delta\alpha$-carbon was chosen as 3.0 Å. Selection of other $\Delta\alpha$-carbon values will change slightly the value of N_o, but not significantly effect viscosities.

Referring to Figure 5.1, it can be noticed that the viscosities for the 12 and 14 carbon molecules plotted virtually identical, and although the 16 tail length surfactant was not quite the same, its viscosities are relatively close. It may appear unexpected that the C_{16} molecule plotted below the shorter tailed surfactants, but it should be remembered that the values of ϖ in Figure 5.1 have been selected arbitrarily, and hence this Figure says nothing about the tendencey or likelihood for a particular molecule to actually form a micelle with a chosen aggregation number. The reason the C_{16} molecule lies below the shorter tailed surfactants in Figure 5.1 owes to the fact that this molecule has a significantly higher N_o value which contributes to a lower axial ratio, and ultimately to a lower viscosity.

The results in Figure 5.1 are encouraging. The viscosities seem reasonable based on the assumed aggregation numbers. For example, high viscosities (> 40 cp) are not observed until aggregation numbers are at least 20,000. The length of a rod-like micelle made of molecules with C_{16} tails and having an aggregation number of 20,000 would be approximately 0.5 μ. This number seems reasonable. Furthermore, Figure 4.10 showed that $C_{16}SO_4Na$ has a viscosity of nearly 700 cp at conditions near its phase boundary (refer to Figure 4.1 for the phase curve). One would expect rod-like micelles formed at these conditions to be very long; infact, being close to the phase boundary, and with such a high viscosity, they should almost be in the visible range. This is substanciated by Figure 5.1 which shows that for a viscosity of 700 cp, an aggregation number of 60,000 is needed. Such an aggregation number, assuming $C_{16}SO_4Na$ as the surfactant, implies a rod-like micelle

with a length of 1.5 μ. Thus, there is reason to expect that with a more accurate way of predicting aggregation numbers, one could make reasonable estimates of surfactant viscosities for dilute micellar solutions.

5.5 Oleyl Sulfonate Study

The net influence of all theoretical trends were reported in Chapter 3 to indicate that oleyl sulfonate would be an "ideal" molecule for mobility control purposes. Its structural features appear to represent an optimum design. The experiments of Chapter 4 evaluated those predictions and there is agreement between theory and experiment as oleyl sulfonate apparently demonstrates ideal behavior.

As evidence, consider first Figure 4.4 which shows a phase plot in temperature salinity space for oleyl sulfonate. This molecule has a very large 1 phase region especially in consideration of its long 18-carbon atom tail length. For instance, a straight tailed 18-carbon atom sulfonate, without any double bonds, has virtually no solubility at 2% salt even at relatively high temperatures. Thus, the unusual behavior of oleyl sulfonate appears to justify the theoretical prediction that incorporation of a double bond would effectively reduce surfactant tail length and thereby provide greater salt tolerance. Futhermore, it can be noticed in Figure 4.4 that oleyl sulfonate has substantially more solubility than C_{18}(1EO). If one considers that C_{18}(1EO) has a larger $\Delta\alpha$-carbon distance than a sulfonate in the absence of any added (EO) groups, then Figure 4.4 suggests that reduction of tail length is the most effective way to optimize phase stability. That is, the effect of tail length seems to be dominant to that of ethylene oxide addition with regard to influencing solubility character. In any

event, the oleyl sulfonate molecule, as illustrated by Figure 4.4, and qualitatively suggested by the theory, has ideal phase behavior in temperature-salinity space.

The second major characteristic predicted by theory to be optimized with the oleyl sulfonate molecule was solution viscosity. In particular, in Chapter 3 it was reasoned that a sulfonate would be an ideal head group because it has a reasonably small $\Delta\alpha$-carbon value and this should be very advantageous toward the formation of rod-like aggregates, and consequently, high viscosities. In addition, it was further thought that because of the angularity and rigid nature of double bonds as compared with single bonds, insertion of a carbon-carbon double bond into the surfactant tail would effectively "kink" the tail, and therefore, reduce the effective tail length while increasing its volume. Since the effect of increased tail volume moves strongly in the direction of increased viscosities, the net result should be favorable and yield increased viscosities.

Figures 4.17 through 4.19 lend support to this theoretical prediction. Oleyl sulfonate exhibits high viscosities even at dilute surfactant and salt concentrations. These figures also show that the viscosity is non-Newtonian and depends strongly on shear rate particularily at high concentrations. It is interesting to note that at high shear rates, the viscosities become independent of surfactant concentration and converge to a common value. This is best illustrated in Figure 4.18. In Figures 4.17 and 4.18 there is a precipitous drop in the viscosity at a particular shear rate which is apparently a function of surfactant concentration. Evidently, when the shear rate is increased enough, the viscosity breaks sharply. This may be the shear rate at which networks of rod-like micelles begin to shear faster than they can reform. Figure 4.20 shows the break point shear rates of the curves in Figures 4.17 and 4.18 as a function of surfactant concentration. As the surfactant concentration is decreased, the break

point shear rate is increased in a non-linear fashion. Apparently, the decrease in surfactant concentration promotes a movement toward newtonian behavior in which case one would anticipate that the break point shear rate will approach infinity for some small, but non-zero, value of surfactant concentration.

The tests of oleyl sulfonate thus far have shown that this molecule has "ideal" characteristics with respect to phase behavior and aqueous solution viscosity. Its viscosity at 0.5 g/dl (0.0141 M) is seen in Figure 4.17 to be approximately 60 cp at low to moderate shear rates. This is comfortably in the range of commerical interests. However, the final experimental test with this molecule, a viscosity study in the presence of oil, proved not to be as promising. In this experiment it may be remembered from Chapter 4 that small volumes of decane were added to a 0.5 g/dl solution of oleyl sulfonate at 322 K. For two values of shear rate, viscosity vs. mass fraction of added decane were plotted in figure 4.21.

An important result is illustrated in Figure 4.21, namely, even in the presence of very small decane fractions, the oleyl sulfonate viscosity is reduced considerably from its value in the absence of any added oil. Evidently, the very properties which force a surfactant molecule to be viscous in an aqueous solution, encourage solvation into an oil phase if it is present. To see if this behavior was specific to the oleyl molecule, a second oil study was conducted. In this case, a 0.035 molar solution of sodiumhexadecyl sulfate (HDS) was examined. All alkanes between normal heptane to normal tetradecane were considered with the hope that one might find an optimum oil solubility. Moving away from the optimum would then provide a narrow window in which the aqueous phase viscosity could be maintained even in the presence of an excess oil phase.

It is instructive before reviewing the results to recall that a 0.035 M (HDS) solution with 0.8 M NaCl at 333 K has a viscosity of several hundred centipoise in the absence of any added oil (refer to Figure 4.10). The results with oil present are plotted in Figure 4.22, and the results show that the viscosity is essentially destroyed. It should be remarked that for the sake of readability, only three curves are plotted in Figure 4.22. Since all viscosities were essentially identical, the choice of ACN was not critical. In addition, it should be remembered that the aqueous phases were extracted and it was with these phases that the viscosities of Figure 4.22 were obtained. Chapter 4 may be recalled for the experimental details.

Apparently, one finds that when a surfactant capably modifies viscosity in an aqueous solution, it does so to a certain degree because it has a preferred oil solubility. To decrease oil solubility, one would tend to move away from optimum viscosity increases in the aqueous phase. A summary of the results and conclusions follows.

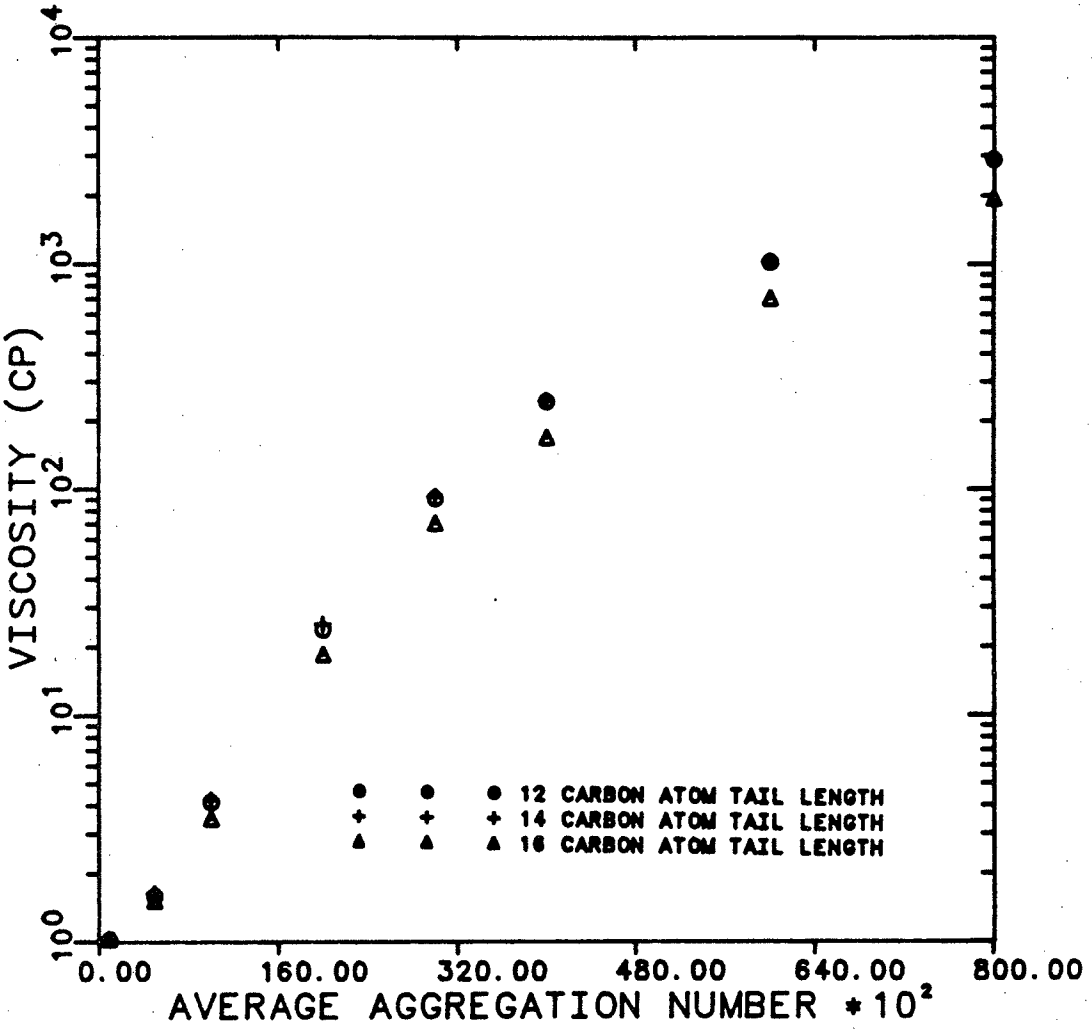

Figure 5.1 Predicted Viscosities From Assumed Aggregation Numbers

CHAPTER 6

Conclusions

The preceeding chapters address the feasibilty of using surfactants as mobility control agents in a chemical flood. It was noted in the introduction that high surfactant viscosities at dilute concentrations and low salinities would be among the essential requirements for successful application of surfactants as drive control fluids. Other important surfactant properties would be the formation of reasonable 1Ø regions in temperature-salinity space and the maintenance of viscosity in the presence of hydrocarbon.

Chapter 2 showed the theoretical equations which can be applied to help evaluate the potential viscosities of surfactant systems. It emphasized the relation between surfactant structural features and viscosity through electrostatic and thermodynamic considerations.

Chapter 3 listed the numerical results of a computer program which used the theoretical equations of Chapter 2. The important theoretical relations developed in Chapter 3 were the following:

1) Increasing the surfactant tail length is associated with increases in solution viscosity.
2) Considering that the surfactant head groups must occupy a finite volume in solution, and that the counterions will experience a distance of closest approach to the head group introduces the idea of an excluded micellar radius. This

distance should, in a strict sense, be a function of temperature, salinity, and surfactant head group structure. In the absence of such functional correlations, as a first approximation, the distance between the alpha carbon atom of the surfactant tail and the center of charge distribution was used to represent this distance. It was found that as the $\Delta\alpha$-carbon distance is increased the viscosity is decreased.

3) The relation between surfactant tail volume and viscosity showed that as the hydrocarbon tail volume is increased the viscosity is also increased.
4) Salt and temperature were found to have opposite effects on solution viscosity. Temperature increases show viscosity decreases, while salinity increases show viscosity increases.
5) The addition of ethylene oxide (EO) units was not specifically addressed in theoretical terms. It was reasoned, however, that increases in the number of (EO) groups could be viewed as an increase in the $\Delta\alpha$-carbon distance. Thus, increased (EO) addition is related to decreased viscosities.

Chapter 4 provided an experimental check of the theoretical predictions in Chapter 3. In all cases, experiments supported the theoretically predicted trends relating surfactant structural features to solution viscosity; however, quantitative predictions

of viscosities based on theoretically calculated aggregation numbers was not successful.

In Chapter 5, Section 5.4, viscosity equations were tested with aggregation numbers selected arbitrarily from a large range (i.e. 500 - 80,000). The predicted viscosities using these aggregation numbers appeared reasonable. This gives reason to expect that with a more accurate calcualtion of the average aggregation number, the viscosities of dilute micellar solutions could be approximated.

The structural features of oleyl sulfonate were compatible with good optimization of the relationships between surfactant structure and viscosity. Optimization of viscosity was considered in conjunction with surfactant phase behavior. The oleyl sulfonate molecule provided exceptionally high viscosities at commercially usable conditions, (i.e. 60 centipoise viscosity at 0.5 g/dl surfactant and 2g/dl NaCl). However, contact with hydrocarbon caused a significant reduction in viscosity. This problem was observed with a second viscous surfactant system and was found to be independent of oil composition.

APPENDICES

APPENDIX A

Chemical Manufacturers

	Surfactant	Manufacturer
1.	Dodecylammonium Chloride	Sigma Corporation
2.	Tetradecylammonium Chloride	Sigma Corporation
3.	Hexadecylammonium Chloride	Sigma Corporation
4.	Sodium Dodecyl Sulfate	Vista Corporation
5.	Sodium Tertadecyl Sulfate	Vista Corporation
6.	Sodium Hexadecyl Sulfate	Vista Corporation
7.	Sodium Dodecyl Sulfonate	Aldrich Chemical
8.	Sodium Tetradecyl Sulfonate	UT-Austin
9.	Sodium Hexadecyl Sulfonate	UT-Austin
10.	Hexadecyldimethylammonium Acetate	UT-Austin
11.	Dihexadecyldimethylammonium Acetate	U. Minnesota-St. Paul
12.	Oleyl Sulfonate	UT-Austin
13.	Octadecyl Sulfonate with $(EO)_1$	UT-Austin
14.	Octadecyl Sulfonate	UT-Austin
15.	3Ø-Sodiumhexadecyl Sulfonate	UT-Austin
16.	5Ø-Sodiumhexadecyl Sulfonate	UT-Austin
17.	6Ø-Sodiumhexadecyl Sulfonate	UT-Austin
18.	CO-610 (nonylphenol-$(EO)_8$)	GAF Corporation

19.	CO-660 (nonylphenol-$(EO)_{10}$)	GAF Corporation
20.	CO-720 (nonylphenol-$(EO)_{12}$)	GAF Corporation
21.	Diamylsodiumsulphosuccinate	GAF
22.	Dihexylsodiumsulphosuccinate	GAF
23.	Dioctylsodiumsulphosuccinate	GAF

APPENDIX B

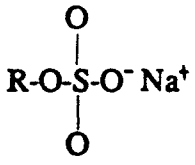

if R=12, Sodiumdodecyl Sulfate

if R=14, Sodiumtetradecyl Sulfate

if R=16, Sodiumhexadecyl Sulfate

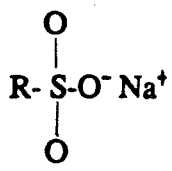

if R=12, Sodiumdodecyl Sulfonate

if R=14, Sodiumtetradecyl Sulfonate

if R=16, Sodiumhexadecyl Sulfonate

Alkylbenzene Sulfonates

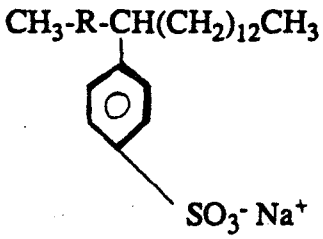

if R = 1, 3Ø-Sodiumhexadecyl Sulfonate

if R = 3, 5Ø-Sodiumhexadecyl Sulfonate

if R = 4, 6Ø-Sodiumhexadecyl Sulfonate

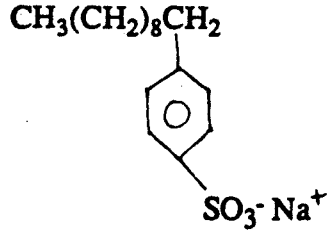

1Ø-Sodiumdecyl Sulfonate

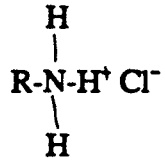

if R=12, Dodecylammonium Chloride

if R=14, Tetradecylammonium Chloride

if R=16, Hexadecylammonium Chloride

Hexadecyldimethylammonium Acetate

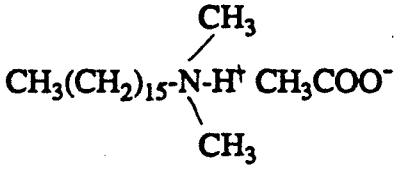

Dihexadecyldimethylammonium Acetate

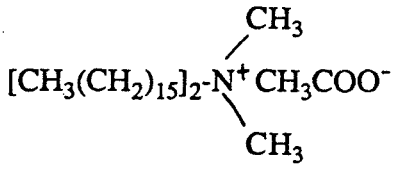

Oleyl Sulfonate

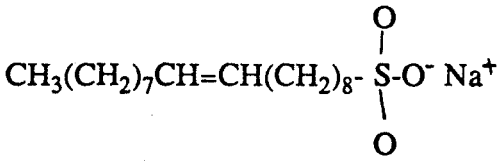

Octadecyl Sulfonate with $(EO)_1$

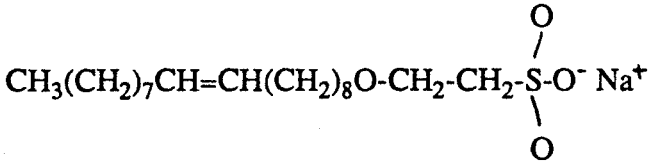

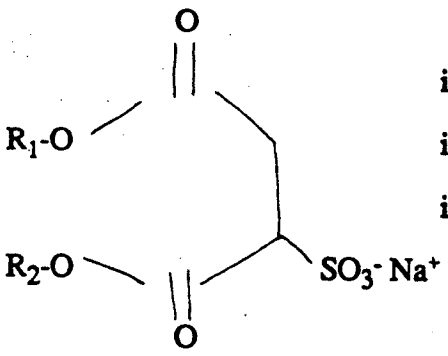

if $R_1=R_2=5$, Diamylsodiumsulphosuccinate

if $R_1=R_2=6$, Dihexylsodiumsulphosuccinate

if $R_1=R_2=8$, Dioctylsodiumsulphosuccinate

APPENDIX C

COMPUTER PROGRAM

```
1.  PROGRAM BESSEL (INPUT,OUTPUT,TAPE5=INPUT,TAPE6=OUTPUT)

C       THIS PROGRAM CALCULATES THE WEIGHTED AVERAGE AGGREGATION
C       NUMBER OF A MICELLE BASED ON ELECTROSTATIC AND SURFACE
C       CONTRIBUTIONS TO THE FREE ENERGY.  THE PROGRAM CONSIDERS
C       SPHERICAL AND ROD-LIKE MICELLES OF THE SAME AGGREGATION
C       NUMBERS AND COMPARES THE FREE ENERGY ADVANTANGE FOR
C       FORMING A CYLINDRICAL MICELLAR STATE VERSUS A SHPERICAL ONE

    2.  REAL A,T,I,K,MMBSK0,MMBSK1,R,KF,NBAR,SC,CMC

C       THE USER ASSIGNS VALUES TO BE READ IN FROM A DATA FILE
C       THE DATA IS READ IN AS FOLLOWS: INITIAL VALUE OF TAIL LENGTH
C       INPUTED AS THE NUMBER OF CARBON ATOMS IN THE SURFACTANT
C       TAIL,C, THE TEMPERATURE IN DEGREES KELVIN, T, THE MOLAR SALT
C       CONCENTRATION, I, THE NUMBER OF ITERATIONS FOR WHICH THE
C       PROGRAM IS TO INCREMENT, N, THE SURFACTANT TAIL VOLUME FACTOR
C       WHERE 1=SINGLE TAILED SURFACTANTS AND 2=DOUBLE MOLECULES,
C       THE SURFACTANT CONCENTRATION SC AS A MOLAR QUANITY, AND
C       LASTLY THE CRITICAL MICELLE CONCENTRATION, CMC

    3.  READ(5,*) C, T, I, N, V, SC, CMC
    4.  WRITE(6,55) T, I

C       CALCULATE THE RECIPROCAL DEBYE LENGTH IN METERS-1

    5.  K=SQRT( I / T ) * 56.79E9

C       PRINT OUT THE VALUES OF SURFACTANT CONCENTRATION AND CMC

    6.  WRITE(6,56) SC
    7.  WRITE(6,57) CMC

C       CHANGE SURFACTANT AND CMC CONCENTRATIONS TO
C       MOLE FRACTIONS

    8.  SC=SC/55.5
    9.  CMC=CMC/55.5

C       CALCULATE THE VALUE OF THE DIELECTRIC CONSTANT AT THE
        CHOOSEN TEMPERATURE
```

```
10.  E=305.6*EXP( -T / 219.)
11.  WRITE(6,88) E

C     BEGIN OUTSIDE DO LOOP WHICH WILL INCREMENT THE VALUE OF
C     THE TAIL LENGTH (DOES NOT CHANGE THE VALUE OF ALPHA
C     CARBON DISTANCE

12.       DO 30,L=1,3

C     CALCULATE THE TAIL VOLUME AND EXCLUDED MICELLAR RADIUS
C     BOTH ARE CONVERTED TO HAVE UNITS OF METERS3 AND METERS
C     RESPECTIVELY

13.            ALPHA=0.7E-10
14.            VT=(26.9*C + 27.4)*V*1.0E-30
15.            WRITE(6,44)
16.            WRITE(6,77) VT
17.            A=(1.265*C + 1.5)*1.0E-10

C     SET THE SURFACE RADIUS EQUAL TO EXCLUDED RADIUS BEFORE
C     ENTERING THE DO LOOP WHICH WILL INCREASE THE EXCLUDED
C     RADIUS, THIS INITIALIZES THE VALUE OF THE SURFACE RADIUS

18.            R=A
19.            WRITE(6,99) R
20.            WRITE(6,44)

C     INCREMENT THE TAIL LENGHT BY TWO CARBON ATOMS

21.            C=C + 2.0

C     BEGIN CALCULATION OF THE ELECTROSTATIC AND SURFACE
C     FREE ENERGY TERMS FOR THE NUMBER OF INCREMENTS
C     SPECIFIED BY THE USER

22.            DO 20,J=1,N

C     CALCULATE THE DEBYE PARAMETER

23.            ARG=A*K

C     CALCULATE THE RATIO OF THE BESSEL FUNCTIONS K_O TO K_1

24.            Z0=MMBSK0(1,ARG,IER)
25.            Z1=MMBSK1(1,ARG,IER)
26.            Z3=(Z0) / (ARG*Z1) + ALOG(A/R)
27.            Z4=(1+K*(A-R))/(1+ARG)
28.            Z5=0.5*Z4-0.75*Z3

C     ALL OF THE TERMS NECESSARY FOR THE EVALUATION OF
C     THE SURFACE AND ELECTROSTATIC ENERGIES ARE AVAILABLE
```

```
C       CALCULATION OF THE SURFACE TERM IN ERGS

   29.          SURF=5.2*1.0E5*(4./3.)*3.142*R**2

C       CALCULATION OF THE MAXIMUN SPHERICAL AGGREGATION
C       NUMBER VN

   30.          VN=(4.*3.142/3.)*A**3/VT

C       CALCULATION OF THE ELECTROSTATIC ENERGY IN ERGS

   31.          ELEC=2.31E-28*VN**2*Z5*/(E*R)*1.0E7

C       CALCULATION OF THE DIFFERENCE IN FREE ENERGIES BETWEEN
C       SPHERICAL AND CYLINDRICAL MICELLES OF THE SAME
C       AGGREGATION NUMBER VN

   32.          FGD=0.5*ELEC + SURF

C       CALCULATION OF THE K PARAMETER WHICH SHOWS THE
C       RELATIVE PREFERENCE FOR MICELLES TO BE IN THE SPHERICAL
C       VERSUS AGGREGATED STATES

   33.  KF=EXP(FGD/(1.38E-16*T))

C       CALCULATION OF THE AVERAGE AGGREGATION NUMBER NBAR

   34.          NBAR=VN + 2*SQRT( KF*(SC-CMC))
   35.          WRITE(6,66)ALPHA,A,ARG,VN,FGD,KF,NBAR

C       INCREMENT THE VALUE OF ALPHA BY 0.5 ANGSTROMS

   36.          ALPHA=ALPHA + 0.5E-10

C       INCREASE THE EXCLUDED MICELLAR RADIUS BY ALPHA

   37.          A=A + 0.5E-10
   38   20     CONTINUE
   39.  30    CONTINUE
   40.  44  FORMAT('0','**************************************************')
   41.  55  FORMAT('0','TEMPERATURE = ',F5.1,' K',3X,'SALT =',F4.2,1X,'MOLAR')
   42.  56  FORMAT('0','THE SURFACTANT CONCENTRATION = ',E10.4,1X,'MOLAR')
   43.  57  FORMAT('O','THE ASSUMED VALUE OF THE CMC = ',E10.4,1X,'MOLAR')
   44.  66  FORMAT('0',7(E10.4,2X)
   45.  77  FORMAT('0','SURFACTANT TAIL VOLUME = ',E10.4,1X,'CUBIC METERS')
   46.  88  FORMAT('0','THE DIELECTRIC CONSTANT FOR THIS RUN IS ',F6.2)
   47.  99  FORMAT('0','THE SURFACTANT TAIL LENGTH = ',E10.4,1X,'METERS')
   48.  STOP
   49.  END
```

BIBLIOGRAPHY

Chapter 1

1. Lake, L.W., "A Technical Survey Of Micellar-Polymer Flooding", Symposium On Enhanced Oil Recovery For The Independent Producer, presented by Institute For The Study Of Earth And Man at Southern Methodist University, Dallas, Texas, November 9-10, (1983).

2. Kuuskraa, V. A., "Current and Future Economics of Enhanced Oil Recovery", Symposium On Enhanced Oil Recovery For The Independent Producer, presented by Institute For The Study Of Earth And Man at Southern Methodist University, Dallas, Texas, November 9-10, (1983).

Chapter 2

1. Guth, E. and Simha, R., "Untersuchungen uber die Viskositat von Suspensionen und Losungen", Kolloid-Z ,74, 266, (1936).

2. Parkinson, C., Matsumoto, S., and Sherman, P., "The Influence of Particle-Size Distribution of the Apparent Viscosity of Non-Newtonian Dispersed Systems", Journal of Colloid and Interface Science, Vol. 33, no. 1, 150, (May 1970).

3. Tanford, C., Physical Chemistry of Macromolecules, John Wiely, New York, (1961).

4. Nagarajan, R., "Are Large Micelles Rigid or Flexible? A Representation of Viscosity Data for Micellar Solutions", Journal of Colloid and Interface Science, Vol. 90, no. 2, 477, (Dec. 1982).

5. Wennerstrom, H. and Lindman, B., "Physical Chemistry of Surfactant Association", Physics Reports, 52, (1), 1, (1979).

6. Matheson, R. R., "Viscosity of Solutions of Rigid Rodlike Macromolecules", Macromolecules, 13, 643, (1980).

7. Mukerjee, P., "The Hydration of Micelles of Association Colloidal Electrolytes", Journal Colloid Sci., 19, 722, (1964). "Counterion Specificity in the Formation of Ionic Micelles: Size, Hydration, and Hydrophobic Bonding Effects", Journal of Physical Chemistry, 71, 4166, (1967).

8. Stigter, D., "Micelle Formation by Ionic Surfactants II. Specificity of Head Groups, Micelle Structure", Journal of Physical Chemistry, Vol. 78. no. 24, (1974).

9. Tanford, C., The Hydrophobie Effect, John Wiley and Sons, New York, (1973).

10. Israelachvili, J. N., Mitchell, J. D., and Ninham, B. W., "Theory of Self-Assembly of Hydrocarbon Amphiphiles into Micelles and Bilayers", Journal of Chemical Soc. Faraday Trans. II, 72, 1525, (1976).

11. Frank, H. S. and Evans, M. W., "Free Volume and Entropy in Condensed Systems III. Entropy in Binary Liquid Mixtures; Partial Molal Entropy in Dilute Solutions; Structure and Thermodynamics in Aqueous Electrolytes", Journal Chemical Physics, 13, 507, (1945).

12. Nemethy, G. and Scheraga, H.,"Structure of Water and Hydrophobic Bonding in Proteins. I. A Model for the Thermodynamic Properties of Liquid Water", Journal Chemical Physics, 36, 3382, (1962).

13. Tanford, C., "Theory of Micelle Formation in Aqueous Solutions", Journal Physical Chemistry, 78, 2469, (1974).

14. Herman, R. B., "Theory of Hydrophobic Bonding. II The Correlation of Hydrocarbon Solubility in Water with Solvent Cavity Surface Area", Journal Physical Chemistry, 76, 2754, (1972).

15. Portis, A. M., Electromagnetic Fields Sources and Media, John Wiley and Sons, (1978).

16. Verwey, E. J. W. and Overbeek, J. Th. G., Theroy of the Stability of Lyophobic Colloids, Elsevier Pub. Co., (1948).

17. Philip, J.R. and Wooding, R. A., "Solution of the Poisson-Boltzmann Equation About a Cylindrical Particle", Journal Chemical Physics, 52, No. 2, (1970).

18. Stigter, D., "On the Adsorption of Counterions at the Surface of Detergent Micelles", Journal Physical Chemistry, 68, 3603, (1964).

19. Stigter, D., "Micelle Formation by Ionic Surfactants. III. Model of Stern Layer, Ion Distribution, and Potential Fluctuations", Journal of Physical Chemistry, 79,(10), 1008, (1975a)

20. Hoffmann, H., Platz, G., Rehege, H., Schorr, W., and Ulbricht, W., Ber. Bunsenges. Phys. Chem., 85, 255, (1981).

21. Hoffmann, H., Platz, G., Rehege, H. and Schorr, W., "The Influence of Counter-Ion Concentration on the Aggregation Behavior of Viscoelastic Detergents", Ber. Bunsenges. Phys. Chem., 85, 877-882, (1981).

22. Stigter, D., "On the Thermodynamics of Micellar Solutions", Recueil des Travaux Chimiques des Pays-Bas, 73, 593, (1954).

23. Hill, T.L., "Approximate Solution of the Free Energy of Nucleic Acids and Other Cylindrical Macromolecules", Arch. Biochem. Biophysics, 57, 229, (1955).

24. Tanford, C., The Hydrophobie Effect, John Wiley and Sons, New York, (1973).

25. Padday, J. F. and Uffindell, N. D., "The Calculation of Cohesive and Adhesive Energies From Intermolecular Forces at a Surface", Journal Physical Chemistry, 72, No. 6, (May 1968).

26. Missel, P. J., Mazer, N. A., Benedek, G. B., Young, C. Y., and Carey, M. C., "Thermodynamic Analysis of the Growth of Sodium Dodecyl Sulfate Micelles", Journal of Physical Chemistry, 84, 1044, (1980).

Chapter 3

1. Tatar, H. V., "A Theory of the Structure of Micelles of Normal Paraffin Chain Salts in Auqeous Solutions", Journal of Physical Chemistry, 62, 1195, (1955).

2. Stigter, D., "Micelle Formation by Ionic Surfactants II. Specificity of Head Groups, Micelle Structure", Journal of Physical Chemistry, Vol. 78. no. 24, (1974).

Chapter 4

1. Rosen, Milton J., Surfactants And Interfacial Phenomena, A Wiley-Intersicence Publication, John Wiley and Sons, Inc. N.Y. (1978).

2. Bird, R. B., Stewart, W. E., and Lightfoot, E. N., Transport Phenomena, John Wiley and Sons, Inc., New York, (1960).

3. Salager, J. L., Bourrel, M., Schechter, R. S., and Wade, W. H.,"Mixing Rules for Optimum Phase-Behavior Formulations of Surfactant/Oil/Water Systems", Soc. Pet. Eng. J., 271, (Oct. 1979).

Chapter 5

1. Mukerjee, P. and Mycels, K. J., "Critical Micelle Concentrations of Aqueous Surfactant Systems", National Bureau of Stnadards, Washington, (1971).